2-1981

Continental Shelf Processes Affecting the Oceanography of the South Atlantic Bight. Progress Report, 1 June 1980-1 June 1981

Larry P. Atkinson
latkinso@odu.edu

Original Publication Citation
Atkinson, L P. (1981). *Continental shelf processes affecting the oceanography of the South Atlantic Bight. Progress report, 1 June 1980-1 June 1981*. United States. doi:10.2172/6549027.

DOE/EV/00889-7
VOL. 1

MASTER

PROGRESS REPORT
CONTRACT DE-AS09-76EV00889

Larry P. Atkinson
-SKIO-

VOLUME 1

[redacted]

CONTINENTAL SHELF PROCESSES AFFECTING THE OCEANOGRAPHY OF THE SOUTH ATLANTIC BIGHT

PROGRESS REPORT

BY

Larry P. Atkinson

Skidaway Institute of Oceanography
Post Office Box 13687
Savannah, Georgia 31406

June 1, 1980 to June 1, 1981

Report Date - February 1981

Prepared for the U.S. Department of Energy

Under Contract No. DE-AS09-76EV0089.

TABLE OF CONTENTS

INTRODUCTION

In the past year we executed our largest field effort to date, GABEX-1. The vast amount of data gathered has now been reduced to workable form and we report on some of the first results in this report. The GABEX-1 measurements combined with other observations in the last year have greatly increased our understanding of the South Atlantic Bight during the spring transition period when the shelf goes from horizontal to vertical stratification.

This progress report contains selected reprints, drafts and parts of technical reports that represent our work over the past three years.

INDEX VOLUME 1

Note: Blue sheets have been inserted between articles to separate them.

INDEX VOLUME 2

First Preliminary Report of the GABEX-I Cruises:

Station Logs, Standard Sections and Maps and Time Series Transects.

INDEX VOLUME 3

Note: The technical reports are in order according to their tech report series numbers. In a case where data has been excluded, a yellow blank sheet has been inserted. The reports included are as follows:

Series #	Title
80-1	Hydrographic Observations off Savannah and Brunswick, Georgia (March, May and September, 1977 and January, 1978).
79-5	Hydrographic Observations in the Georgia Bight (April 1978).
79-3	Hydrographic Observations in the Georgia Bight (July 1977).
79-1	Hydrographic Observations in the Georgia Bight (December 1976).
78-7	ACTD System: Description, Operation, Data Acquisition and Processing.
78-5	Hydrographic Observations in the Georgia Bight (April 1977).
78-1	The Results of Four Oceanographic Cruises in the Georgia Bight.

PUBLICATIONS AND MEETINGS

During the past year the following papers and technical/data reports were published or accepted for publication.

Papers Published or in Press in Reviewed Journals or Books

Atkinson, L.P. and L.J. Pietrafesa. 1980. A flushing model of Onslow Bay, North Carolina, based on intrusion volumes. J. Phys. Ocean., 10: 472-474.

Atkinson, L.P., J.J. Singer and L.J. Pietrafesa. 1980. The volume of summer subsurface intrusions of Gulf Stream water into Onslow Bay, North Carolina. Deep-Sea Res., 27: 421-434.

Hofmann, E.E., L.J. Pietrafesa and L.P. Atkinson. Description of a bottom intrusion in Onslow Bay, North Carolina. Deep-Sea Res., in press.

Blanton, J.O., L.P. Atkinson, L.J. Pietrafesa and T.N. Lee. The intrusion of Gulf Stream water across the continental shelf due to topographically induced upwelling. Deep-Sea Res., in press.

Yoder, J.A., L.P. Atkinson, T.N. Lee, H. Kim and C. McClain. Role of Gulf Stream frontal eddies in forming phytoplankton patches on the outer southeastern U.S. shelf. Limnol. Oceanog., in press.

Cordes, C., L.P. Atkinson, R. Lee and J.O. Blanton. 1980. Pelagic tar off Georgia and Florida in relation to physical processes. Marine Pollution Bull., 11: 315-317.

Hofmann, E.E., L.J. Pietrafesa, J.M. Klinck and L.P. Atkinson. 1980. A time dependent model of nutrient distribution in continental shelf waters. Ecological Modelling, 10: 193-214.

Kim, H.H., C.R. McClain, L.R. Blaine, W.D. Hart, L.P. Atkinson and J.A. Yoder. 1980. Ocean chlorophyll studies from a U-2 aircraft platform. J. Geophys. Res., 85: 3982-3990.

Paffenhöfer, G.-A., D. Deibel, L.P. Atkinson and W.M. Dunstan. 1980. The relation of concentration and size distribution of suspended particulate matter to hydrography in Onslow Bay, N.C., Deep-Sea Res., 27: 435-447.

Singer, J.J., L.P. Atkinson and L.J. Pietrafesa. 1980. Summertime advection of low salinity surface water into Onslow Bay, N.C. Estuarine and Coastal Mar. Sci., 11: 73-82.

Papers in Final Preparation

Atkinson, L.P., L.J. Pietrafesa and E.E. Hofmann. On nutrient sources to Onslow Bay, North Carolina.

Atkinson, L.P. and T.E. Targett. A synoptic observation of upwelling along the 60 m isobath from Cape Canaveral to Cape Hatteras with reference to fish distribution.

Papers Submitted

Natural fluorescence as a tracer for distinguishing between piedmont and coastal plain river water in the nearshore waters of Georgia and North Carolina. Coastal Estuarine Marine Science.

Technical Data Reports

1980 Singer, J.J., L.P. Atkinson and W.S. Chandler. Onslow Bay XBT Data: 1975 (OBIS I, II, III and IV). Georgia Marine Science Center Technical Report 80-2.

1980 Singer, J.J., L.P. Atkinson, W.S. Chandler and S.S. Bishop. Hydrographic observations off Savannah and Brunswick, Georgia (March, May and September 1977 and January 1978). Georgia Marine Science Center Technical Report 80-1.

1981 Lasley, S.R., L.P. Atkinson, J.J. Singer and W.S. Chandler. Hydrographic observations in the Georgia Bight (April 1979). Georgia Marine Science Center Technical Report (in press).

1980 Atkinson, L.P., J.J. Singer and W.S. Chandler. First preliminary report of the Gabex-1 cruises: station logs, standard sections and maps and time series transects. Informal Report.

1981 Singer, J.J. R/V ISELIN Hydrographic data. 200 pp.

1981 Singer, J.J. R/V EASTWARD Hydrographic data. 200 pp.

Oral and Poster Presentations

Results of DOE sponsored oceanographic research have been given at the following meetings:

June 1980. Hydrographic observations of the Charleston Bump. Singer, Atkinson, Yoder and Lee. 43rd Annual Meeting of ASLO. Knoxville.

June 1980. The nitrogen pool of a mid-shelf intrusion. O'Malley, Atkinson and Yoder. 43rd Annual Meeting of ASLO. Knoxville.

June 1980. Effect of eddy-forced upwelling on nutrient and phytoplankton distributio near the shelfbreak in the South Atlantic Bight. Bishop, Lasley, Atkinson and Yoder. 43rd Annual Meeting of ASLO. Knoxville.

December 1980. Oceanographic climatology of the southeastern U.S. Continental Shelf Waters. Atkinson, Blanton and Chandler. AGU Fall Meeting, San Francisco.

December 1980. Thermal and visible color expressions of an upwelling off the Gulf Stream. Kim, McClain, Hart, Atkinson and Yoder. AGU Fall Meeting, San Francisco.

January 1981. Nutrient sources to the southeastern United States Shelf Waters: rivers, recycling and the Gulf Stream. Winter Meeting of ASLO. Seattle.

January 1981. Effect of upwelling on primary productivity of the outer southeastern shelf. Winter Meeting of ASLO. Seattle.

Other talks not listed, have been given to regional and governmental groups.

The P.I. attended the DOE workshop on the environmental effects of future OTEC plants in Upton, New York on 22-24 January 1980.

FIELD OBSERVATIONS

Cruises under this contract or cooperatively with other contracts are summarized in Table 1.

TABLE 1. Department of Energy funded cruises 1975 to 1981.

Date	Cruise #	Data	Comment
6-7 Aug 1975	AD-75-01	14BC	Onslow Bay Mooring Cruise (P)
4-14 Sept 1975	E-9-75	212BC/112XBT	Onslow Bay Intrusion Study (P)
13-14 Oct 1975	AD-75-2	20BC/15XBT	Onslow Bay Mooring Cruise (P)
8-11 Dec 1975	AD-75-3	99C/59XBT	Onslow Bay mooring Cruise (P)
13 Feb 1976	BF-76-2	4BC	Georgia Bight (NP)
26 Feb 1976	BF-76-3	21BC	Georgia Bight (P)
10 Mar 1976	BF-76-6	6BC/5XBT	Georgia Bight (P)
29 Mar 1976	BF-76-9	7BC/4XBT	Georgia Bight (P)
29 Apr 1976	BF-76-13		Test (NP)
5-6 May 1976	BF-76-15	16BC	Georgia Bight (P)
19 May 1976	BF-76-17		Test (NP)
26 May 1976	BF-76-18	2BC	Georgia Bight (aborted), (P)
7 June 1976	BF-76-23		Test (NP)
17 June 1976	BF-76-24		Test (NP)
14-18 July 1976	BF-76-085	42CTD/11XBT	Onslow Bay Study (P)
21-23 July 1976	BF-76-086	45CTD	Onslow Bay Study (P)
26 July-6 Aug 1976	BF-76-087	30CTD/32XBT	Onslow Bay Study (P)
14-16 Aug 1976	BF-76-088	42CTD	Onslow Bay Study (P)
18 Aug 1976	BF-76-089	4CTD	Onslow Bay Study (P)
8 Oct 1976	BF-76-30	42CTD	Georgia Bight, Front Hunt 1 (P)
14 Oct 1976	BF-76-32	49CTD	Georgia Bight, Front Hunt 2 (P)
15 Oct 1976	BF-76-33	34CTD	Georgia Bight, Front Hunt 3 (P)
17-18 Oct 1976	BF-76-39	88CTD	Georgia Bight, Front Hunt 4 (P)
9-15 Dec 1976	CI-76-12	37CTD/38XBT	Georgia Bight (P)
6-9 Mar 1977	BF-77-14	35XBT	Georgia Bight (P)
6-16 Apr 1977	AD-77-4	86CTD/30XBT	Georgia Bight (P)
19 Apr 1977	BF-77-29	14XBT	Georgia Bight (P)
21 Apr 1977	BF-77-30	14RSS	Georgia Bight, Front Hunt 5 (P)
26-27 May 1977	BF-77-38	15CTD/1XBT	Georgia Bight (P)
4-10 July 1977	CI-77-03	61CTD/30XBT	Georgia Bight (P)
10-11 Aug 1977	BF-77-54	22XBT	Georgia Bight Intrusion Study I (Paffenhofer)
12-15 Aug 1977	BF-77-54	34XBT	Georgia Bight Intrusion Study II
17-21 Aug 1977	BF-77-54	42XBT	Georgia Bight Intrusion Study III
22-23 Aug 1977	BF-77-54		Georgia Bight Intrusion Study IV
26-27 Aug 1977	BF-77-54	23XBT	Georgia Bight Intrusion Study V
13-14 Sept 1977	BF-77-57	14CTD/12XBT	Georgia Bight (P)
5-9 Nov 1977	CI-77-07	55CTD	Georgia Bight (IP)
23-27 Jan 1978	CI-78-01	24BC/24XBT	Georgia Bight (P)
17-21 Feb 1978	BF-78-07	13CTD	Tests (NP)
12-23 Apr 1978	CI-78-04*	59CTD/19XBT	Georgia Bight (P)
9-12 May 1978	BF-78-21	28CTD/12RSS	Georgia Bight, Front Flux (P)
9-12 May 1978	KJ-78-01	26 RSS	Georgia Bight, Front Flux (P)
3-10 August 1978	CI-78-06(L3)	36CTD/59XBT	Georgia Bight (IP)
8-14 Nov. 1978	CI-78-09**	50CTD/4XBT	South Atlantic Bight (P)
13-19 March 1979	PP-79-01**	43CTD/16XBT	South Atlantic Bight (P)
27 May-2 June 1979	PP-79-02**	52 CTD	South Atlantic Bight (P)
5 July-17 Aug. 1979	BF-79-34	28CTD/194XBT	Georgia Bight Instrusion Study (IP)
22-29 Aug. 1979	PP-79-03**	52CTD	South Atlantic Bight (P)
3-4 Oct. 1979	BF-79-51	8XBT	Georgia Bight (IP)
15-17 Oct. 1979	BF-79-55	4XBT	Georgia Bight (IP)
26 Oct.-3 Nov. 1979	CI-79-02**	55CTD/53XBT	South Atlantic Bight (P)
6-10 Nov. 1979	CI-79-02(L3)	72 CTD	Georgia Bight, Front Flux (IP)
6-10 Nov. 1979	BF-79-59	69RSS	Georgia Bight, Front Flux (IP)
5 Dec. 1979	BF-79-65		Georgia Bight (IP)
7-8 Jan 1980	KJ-80-1		Georgia Bight (IP)
10-27 April 1980	E-80-02	107CTD/140XBT	GABEX I (P)
10-27 April, 1980	CI-80-03	60CTD/98XBT	GABEX I (P)
29 Aug.-14 Sept.	PP-80-01**	68CTD/57XBT	Blake Plateau (P)

Ships: BF=Blue Fin; CI=Columbus Iselin; E=Eastward; AD=Advance II; KJ=Kit Jones; PP=Pierce

Abbreviations: NP=not publishable, P=published, IP=in preparation

*DOE/BLM funded

** Principally BLM funded

PAPERS AND REPORTS PUBLISHED UNDER THIS CONTRACT

1975 Atkinson, L.P. and D. Wallace. The source of unusually low surface salinities in the Gulf Stream off Georgia. Deep-Sea Research 22: 913-916.

1976 Atkinson, L.P. and J. Hall. The distribution and production of methane in the Georgia salt marsh. Estuarine and Coastal Marine Science 4: 677-68

1976 Dunstan, W.M. and L.P. Atkinson. Sources of new nitrogen for the South Atlantic Bight. pp. 69-78 in M. Wiley, ed. Proceedings of 3rd International Estuarine Research Conference, Galveston, Texas.

1977 Atkinson, L.P. Modes of Gulf Stream intrusion into the South Atlantic Bight shelf waters. Geophysical Research Letters 4(12): 583-586.

1978 Atkinson, L.P., J.O. Blanton, and E. Haines. Shelf flushing rates based on the distribution of salinity and freshwater in the Georgia Bight. Coastal and Estuarine Marine Science 7(5): 464-472.

1978 Atkinson, L.P., G.-A. Paffenhöfer and W.M. Dunstan. The chemical and biological effect of a Gulf Stream intrusion off St. Augustine, Florida. Bulleting of Marine Science 28(4): 667-679.

1978 Blanton, J.O. and L.P. Atkinson. Physical transfer processes between Georgia tidal inlets and nearshore waters. pp. 515-532 in J. Wiley, ed. Estuarine Interactions. Academic Press.

1978 Pietrafesa, L.J., J.O. Blanton and L.P. Atkinson. Evidence for deflection of the Gulf Stream at the Charleston Rise. Gulf Stream 4(9): 3, 6-7.

1979 Atkinson, L.P., J.J. Singer and W.S. Chandler. The 9400 CTD Systems reliability, calibrated and data acquisition. in Proceedings of Fifth STD/Ocean Systems Conference and Workshop. Grundy Enviornmental Systems, San Diego. In Press.

1980 Atkinson, L.P., J.J. Singer and L.J. Pietrafesa. The volume of summer subsurface intrusions of Gulf Stream water in Onslow Bay, North Carolina. Deep-Sea Research 27(6A): 421-424.

1980 Singer, J.J., L.P. Atkinson and L.J. Pietrafesa. Summertime advection of low salinity surface water into Onslow Bay, North Carolina. Estuarine and Coastal Marine Science 11: 73-82.

1980 Atkinson, L.P. and L.J. Pietrafesa. A flushing model of Onslow Bay, North Carolina, based on intrusion volumes. Journal of Physical Oceanography. 10(3): 472-474.

1980 Paffenhöfer, G.-A., D. Deibel, L.P. Atkinson and W.M. Dunstan. The relation of concentration and size distribution of suspended particulate matter to hydrography in Onslow Bay, North Carolina. Deep-Sea Research 27(6A): 435-447.

1980 Kim, H.H., C.R. McClain, L.R. Blaine, W.D. Hart, L.P. Atkinson and J.A. Yoder. Ocean chlorophyll studies from a U-2 aircraft platform. Journal of Geophysical Research 85(C7): 3982-3990.

1980 Hofmann, E.L., L.J. Pietrafesa, J.M. Klinck and L.P. Atkinson. A time dependent model of nutrient distribution in continental shelf waters. Ecological Modelling 10: 193-214.

1980 Cordes, C., L.P. Atkinson, R. Lee and J. Blanton. Pelagic tar off Georgia and Florida in relation to physical processes. Marine Pollution Bulletin 11: 315-317.

1980 Lee, T.N., L.P. Atkinson and R. Legeckis. Detailed observations of a Gulf Stream frontal eddy on the Georgia continental shelf, April 1977. Deep-Sea Research. In Press.

1980 Yoder, J.A., L.P. Atkinson, T.N. Lee, H. Kim and C. McClain. Role of Gulf Stream frontal eddies in forming phytoplankton patches on the outer southeastern U.S. shelf. Limnology and Oceanography. In press.

1981 Blanton, J.O., L.P. Atkinson, L.J. Pietrafesa and T.N. Lee. The intrusion of Gulf Stream water across the continental shelf due to topographically-induced upwelling. Deep-Sea Research. In press.

1981 Hofmann, E.E., L.J. Pietrafesa and L.P. Atkinson. Description of a bottom intrusion in Onslow Bay, North Carolina. Deep-Sea Research. In press.

Technical Reports

1967 Stefansson, U. and L.P. Atkinson. Physical and chemical properties of the shelf and slope waters off North Carolina. Duke University Marine Laboratory Technical Report. 230 pp.

1975 Atkinson, L.P. Oceanographic observations in the Georgia Bight. R.V. EASTWARD Cruise E-13-73 and E-19-73. Georgia Marine Science Center Technical Report 75-6.

1976 Atkinson, L.P. Oceanographic observations in the Georgia Bight. R.V. EASTWARD Cruise E-3-74 and E-12-74. Georgia Marine Science Center Technical Report 76-1.

1976 Atkinson, L.P., J.J. Singer, W.M. Dunstan and L.J. Pietrafesa. Hydrography of Onslow Bay: September 1975 (OBIS II). Georgia Marine Science Center Technical Report 76-2.

1976 Atkinson, L.P., J.J. Singer and L.J. Pietrafesa. Onslow Bay intrusion study. Hydrographic observations during current meter servicing cruises in August, October and December 1975 (OBIS I, III and IV). Georgia Marine Science Center Technical Report 76-4.

1977 Hofmann, E.E., L.J. Pietrafesa, L.P. Atkinson, G.-A. Paffenhöfer and W.M. Dunstan. A mathematical model of nutrient distribution in coastal waters. Center for Marine and Coastal Studies, North Carolina State University, Technical Report No. 77-2.

1977 Pietrafesa, L.J., D.A. Brooks, R. D'Amato and L.P. Atkinson. Preliminary data report, physical/dynamical observations made in Onslow Bay; summer, fall and winter, 1975. Center for Marine and Coastal Studies, North Carolina State University, Technical Report No. 77-05.

1977 Atkinson, L.P., G.-A. Paffenhöfer and W.M. Dunstan. Hydrographic and biological observations at an anchor station off St. Augustine, Florida, 9-14 April 1975 (R.V. EASTWARD Cruise E-1G-76). Georgia Marine Science Center Technical Report 77-4.

1977 Singer, J.J., L.P. Atkinson, W.S. Chandler and P.G. O'Malley. Hydrographic observations in Onslow Bay, North Carolina: July-August 1976 (OBIS V), Data Graphics. Georgia Marine Science Center Technical Report 77-6.

1978 Chandler, W.S., L.P. Atkinson, J.J. Singer, P.G. O'Malley and C.V. Baker. A. CTD System: Description, operation, data acquisition and processing. Georgia Marine Science Center Technical Report 78-7.

1978 O'Malley, P., L.P. Atkinson, J.J. Singer, W.S. Chandler and T.N. Lee. Hydrographic observations in the Georgia Bight (April 1977). Georgia Marine Science Center Technical Report 78-5.

1979 Deschamps, J.R., L.P. Atkinson, J.J. Singer, W.S. Chandler and T.N. Lee. Hydrographic observations in the Georgia Bight (December 1976). Georgia Marine Science Center Technical Report 79-1. 97 pp.

1979 Atkinson, L.P., A.L. Edwards, J.J. Singer, W.S. Chandler and G.-A. Paffenhöfer. Hydrographic observations in the Georgia Bight (July 1977). Georgia Marine Science Center Technical Report 79-3. 126 pp.

1979 McCarthy, J.E., L.P. Atkinson, J.J. Singer and W.S. Chandler. Hydrographic observations off Savannah, Georgia (winter/spring 1976). Georgia Marine Science Center Technical Report 79-2. 41 pp.

1979 Lasley, S.R., L.P. Atkinson, J.J. Singer and W.S. Chandler. Hydrographic observations in the Georgia Bight (April 1978). Georgia Marine Science Center Technical Report 79-5.

1979 Kim, H.H., C.R. McClain, L.R. Blaine, W.D. Hart, L.P. Atkinson and J.A. Yoder. Ocean chlorophyll studies from a U-2 aircraft platform. NASA Technical Memorandum 80574. 27 pp.

1980 Singer, J.J., L.P. Atkinson and W.S. Chandler. Onslow Bay XBT Data: 1975 (OBIS I, II, III and IV). Georgia Marine Science Center Technical Report 80-2. 114 pp.

1980 Singer, J.J., L.P. Atkinson, W.S. Chandler and S.S. Bishop. Hydrographic observations off Savannah and Brunswick, Georgia (March, May and September 1977 and January 1978). Georgia Marine Science Center Technical Report 80-1. 105 pp.

1980 Atkinson, L.P., J.J. Singer and W.S. Chandler. First preliminary report of the GABEX-1 Cruises: station log, standard sections and maps and time series transects. Informal Report.

1981 Singer, J.J. R/V ISELIN Hydrographic Data. GABEX-1. 200 pp.

1981 Singer, J.J. R/V EASTWARD Hydrographic Data. GABEX-1. 200 pp.

RECENT RESULTS AND REPORTS

In this section we will present recent results some of which are brief reports others pre-prints or re-prints and others technical reports or data reports. Items are separated by blue pages. Yellow pages represent large blocks of data that were not reproduced for this report.

Field observations in 1980-81 included the large field experiment GABEX-1, a smaller experiment during the summer of 1979 and 1980 to acquire data relevant to the proposed GABEX-2 experiment. Results of the summer 1979 cruise can be found in the proposal.

Gabex-1 Preliminary Results

Gabex-1 was a large scale observational effort involving three ships (ISELIN, EASTWARD, BLUE FIN), three airplanes (Coast Guard P-3, NASA U-2 and C-130), several satellites for communication and remote sensing and a large array of current meter/temperature/pressure moorings. This particular contract was responsible for much of the coordination and in particular the CTD/XBT/O_2/nutrient measurements on the ISELIN and EASTWARD.

The observational schedule of GABEX-1 is given in detail in the document "First Preliminary Report of the GABEX-1 Cruises: station logs, standard sections, maps and time series transects" which can be found in the Progress Report. During the cruises the EASTWARD mapped the shelf with transhelf sections corresponding to principal current meter sections (Figure 1). Meanwhile, the ISELIN repeatedly mapped events at the shelf break where springtime upwelling is usually restricted (Figure 2).

For this proposal, we will discuss one facet of the results which is directly related to this proposal and do not require data from other contracts which has not yet been merged. We will present observations from the St. Augustine Time Series which demonstrate the rapidity with which Gulf Stream associated upwelling can change the character of adjacent shelf waters.

Over a period of 13 days in April, the St. Augustine transect was occupied 11 times. We will specifically discuss the temperature, density and nitrate data which are shown in Figure 3.

At the onset it must be said that throughout the observation period active upwelling occurred as indicated by the cold nutrient-rich waters over the middle and outer shelf and even occasionally in nearshore waters (EASTWARD section 5 and 7).

Prior to April 12, a mass of 17°C water was advected onto and across the shelf at St. Augustine. Because of the high nitrate concentrations, this event probably occurred within a few days prior to the 12th. Through the 13th (ISELIN Section 4) the situation inshore of the shelfbreak apparently changed very little. Over the upper slope, however, there was a definite doming, probably associated with frontal eddy formation. This conjecture is supported by the presence of a surface filament of relatively warm water (21°C) over the shelfbreak. During this period (12-13 April) nitrate concentrations were uniformly high and penetrated well across the shelf (EASTWARD Section 2).

Between 13 April (ISELIN Section 4) and 15-16 April, the situation changed. The surface mixed layer over the upper slope deepened, dome structure over the upper slope disappeared and the warm surface filament was missing. Isotherms over the shelfbreak and upper slope descended ca. 50 m and the 17°C water mass on the shelf was stranded at mid-shelf. Thus between 13 and 15 April, the dynamics at the shelfbreak appear to have gone through a transition from frontal eddy dominated to Gulf Stream domination. During this period the shelf was vertically stratified with strong horizontal gradients occurring only at the shelfbreak.

Between 15 April and 23 April hydrographic structure changed relatively little. The lower layer shelf temperature persisted at 18°C and nitrate concentrations slowly decreased, probably due to assimilation by phytoplankton. The 18°C shelf water mass appeared to move offshore between 15 and 23 April. On 24 and 25 April, the Stream appeared to move farther west (onshore) causing upper shelf isotherms to deepen and shelfbreak bottom temperatures to rise from 18°C to 21°C. The high nitrate water mass that persisted over the shelf throughout the observations was stranded on 24 April (EASTWARD Section 15). The lower layer at mid-shelf was mixing into the surface layer, reducing surface salinities.

The most dramatic change in shelf hydrography occurred between 24 April and 25-26 April. Freshly upwelled (high nitrate) water penetrated at least half way across the shelf. The 18°C isotherm ascended from 140 m to less than 40 m. A warm filament appeared (stations 403-406, EASTWARD, Section 18) over the shelf-break accompanied by a dome structure both of which are indicative of frontal eddy activity.

The sequence of events leading to the 25-26 April upwelling can be examined in more detail via the other alongshore and transhelf measurements made during the period.

On the 23rd prior to ISELIN, Section 18, we made an 60 m isobath XBT run from 28 to 30°N (Figure 4). The thermal structure indicated an upwelling event at ca. 29°50'N, just south of St. Augustine, with minimum temperatures of 17.9°C. A second event extending from Cape Canaveral to New Smyrna (29°N) was much larger in the alongshore and more intense with minimum observed temperatures of 15.5°C.

Immediately after the 60 m isobath run a section was run at 30°N (St. Augustine) (ISELIN, Section 18) where at 60 m the near bottom temperatures were still between 18°C and 19°C. Apparently the < 18 C water mass observed in the northern part of the 60 m run was past or had not yet reached 30°N. On the 24th, the 30°N section was occupied again (EASTWARD, Section 15) and at 60 m temperatures had increased to ca. 20°C and surface temperatures approached 25°C. Clearly at this time the Stream had moved onshore and we were observing a part of the event previously seen at 29°10'N at 1400 on 22 April during the 60 m run. This translates to a phase speed of ca. 161 cm sec^{-1}. On 25-26 April the section was again repeated and 60 m bottom temperatures had decreased to < 16°C indicating the event seen during the 60 m run between 28 and 29°N was now at 30°N. The absence of 16°C water at 60 m at 29°N was confirmed by a CTD section (EASTWARD, Section 17) run on 25 April. At that time 60 m bottom water had increased to 17.5°, the event had clearly passed 29°N and was in the 30°N area.

These observations are an excellent example of the upwelling process in the SAB demonstrating that the events propagate north, cause significant displacement of shelf waters and advect significant amounts of nutrients into shelf waters. In the next year the results of this cruise will be synthesized with other data sets to further elucidate the process of shelf water/Gulf Stream interaction.

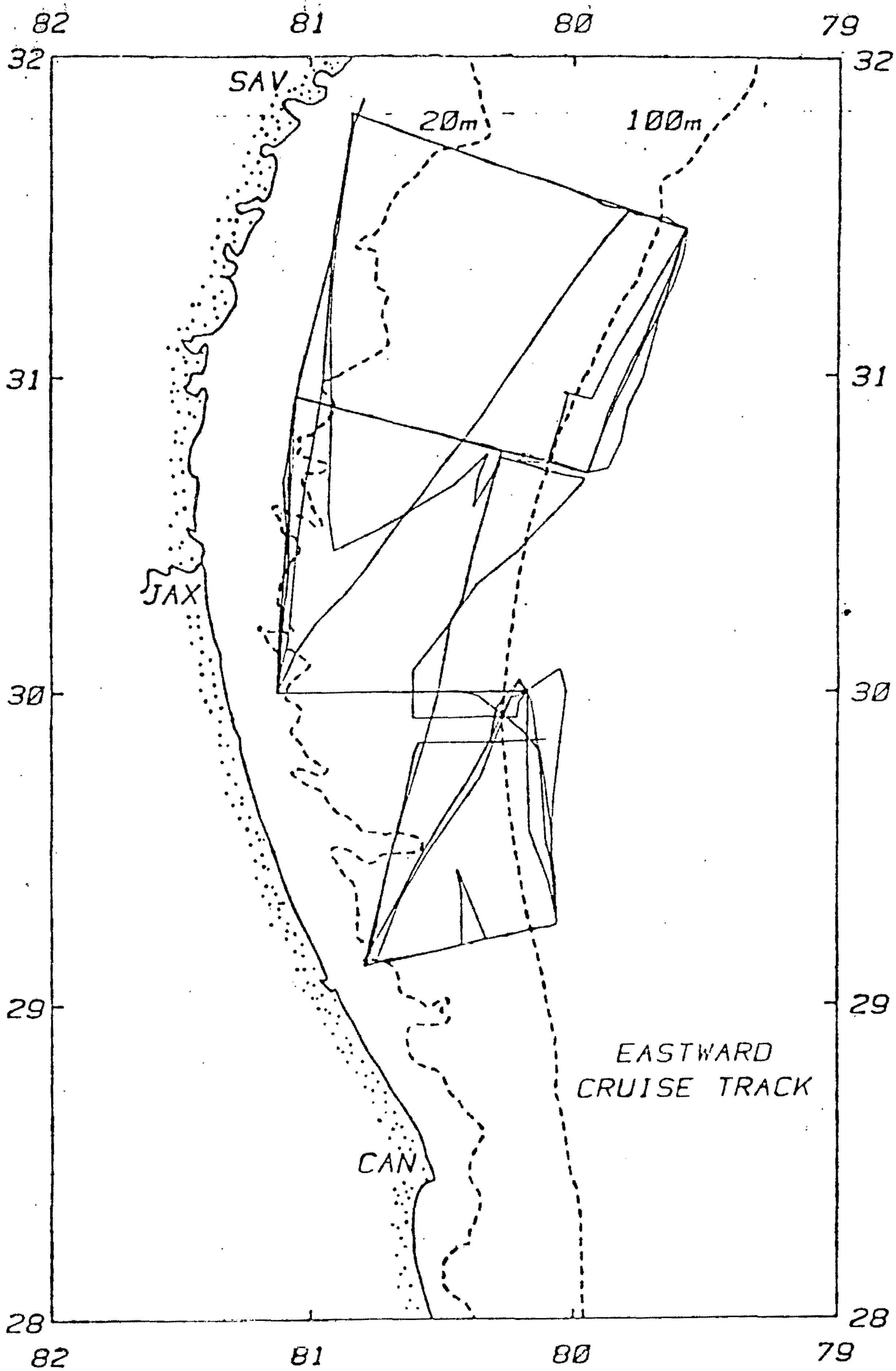

Figure 1a. EASTWARD cruise track

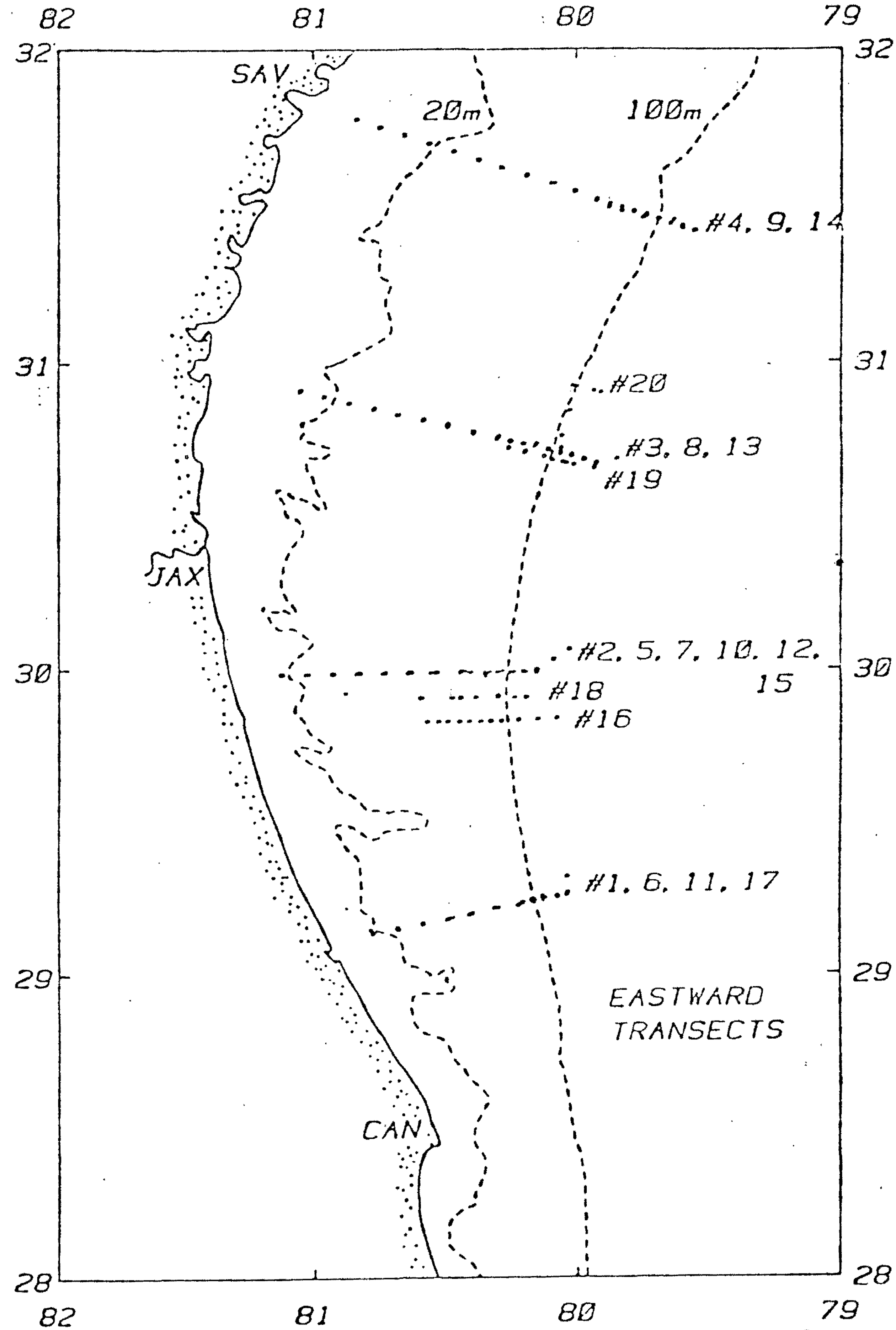

Figure 1b. EASTWARD sections. Section numbers indicated. Refer to Table 3 for stations, etc.

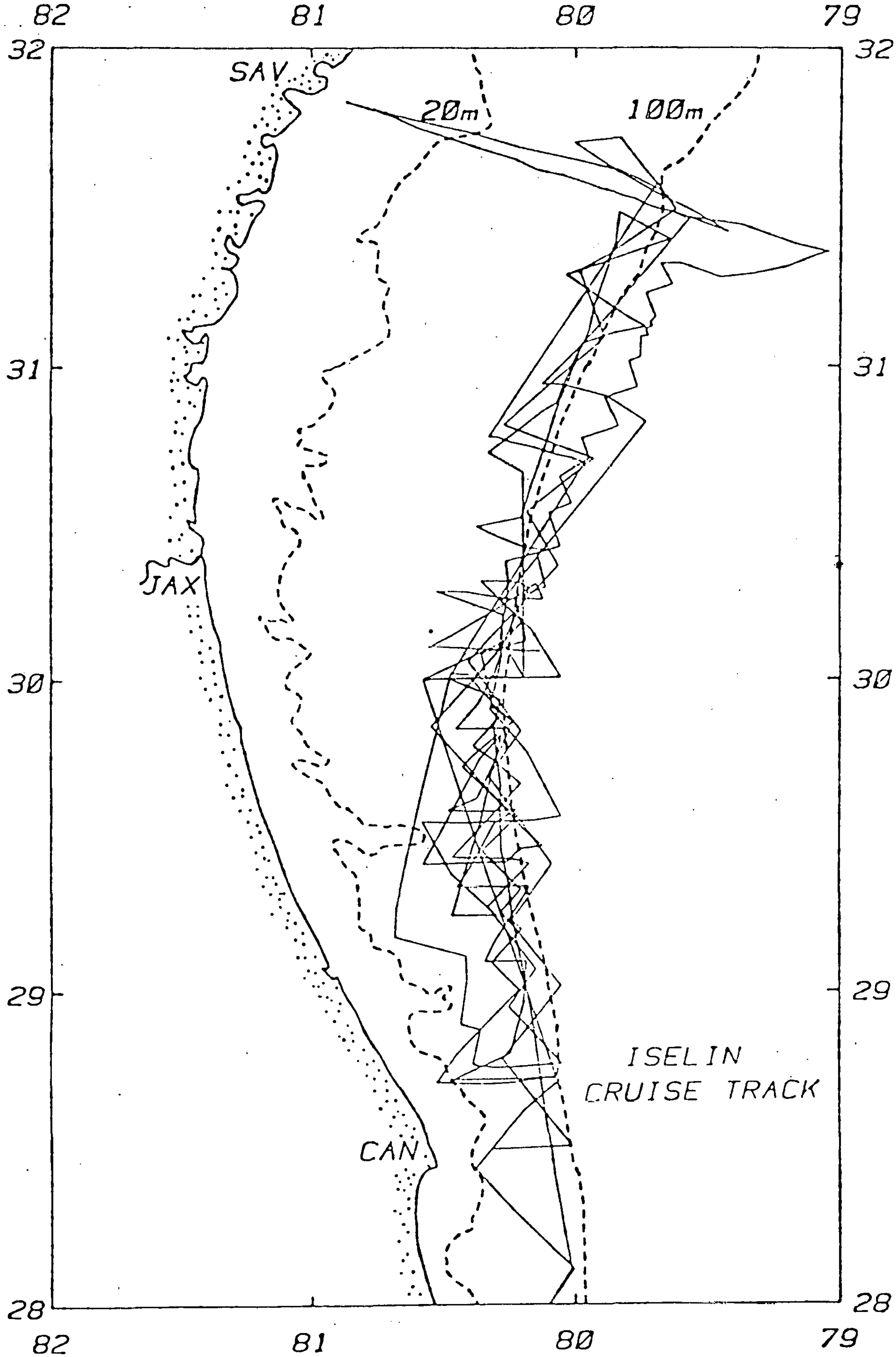

Figure 2a. ISELIN cruise track

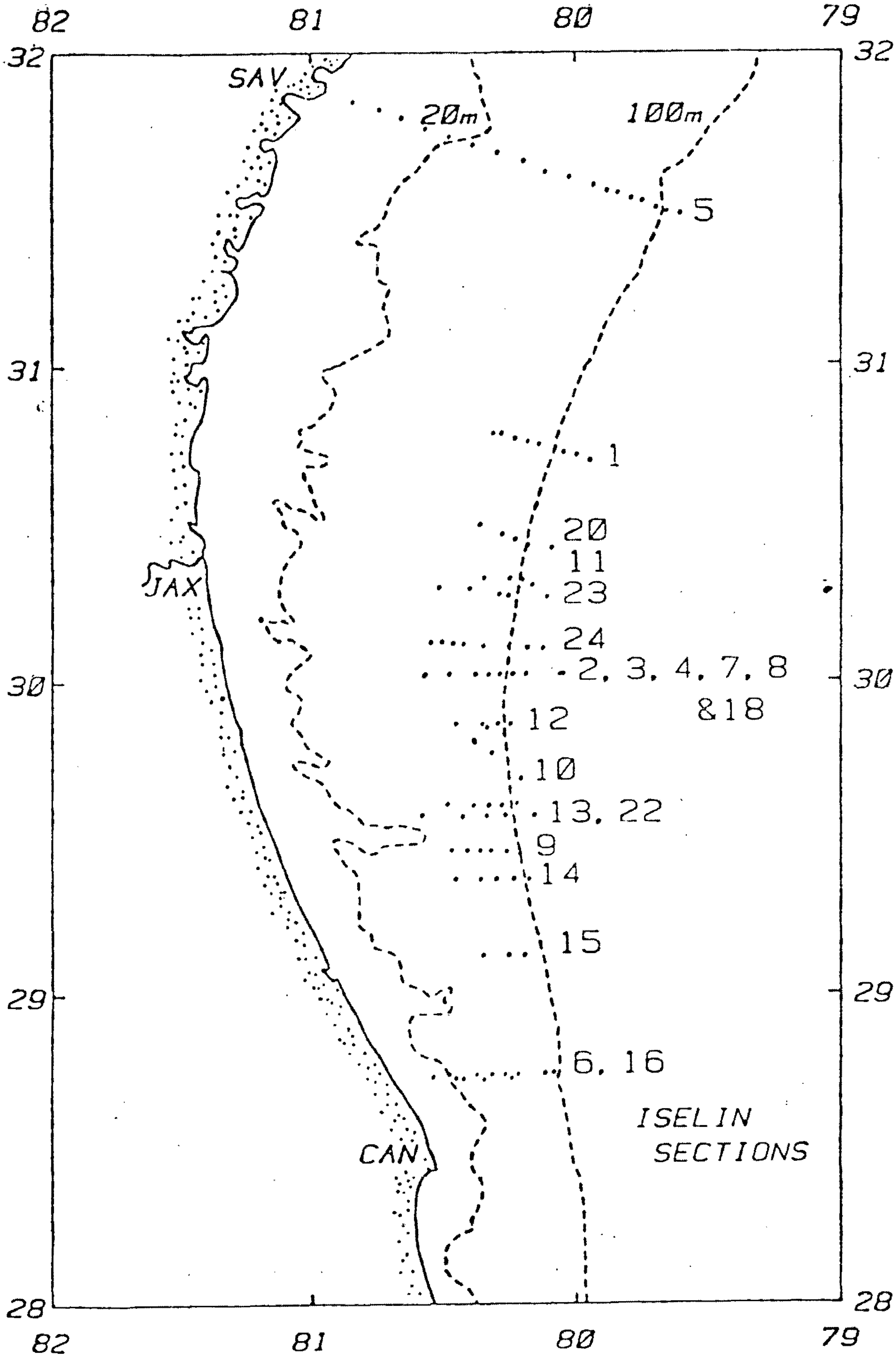

Figure 2b. ISELIN sections. Section number indicated. Refer to Table 1 for stations, etc.

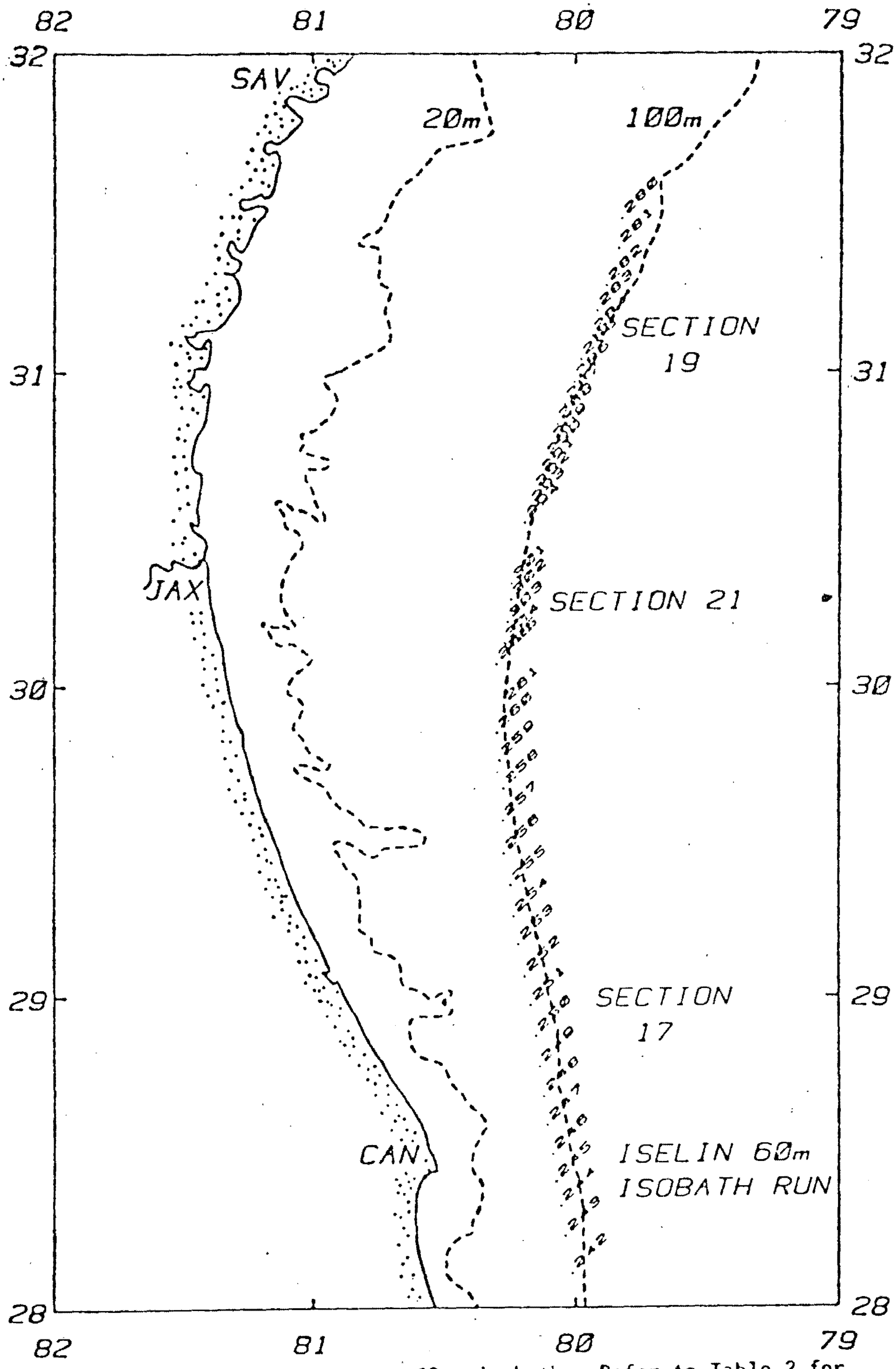

Figure 2c. ISELIN stations on 60 m isobath. Refer to Table 2 for stations, etc.

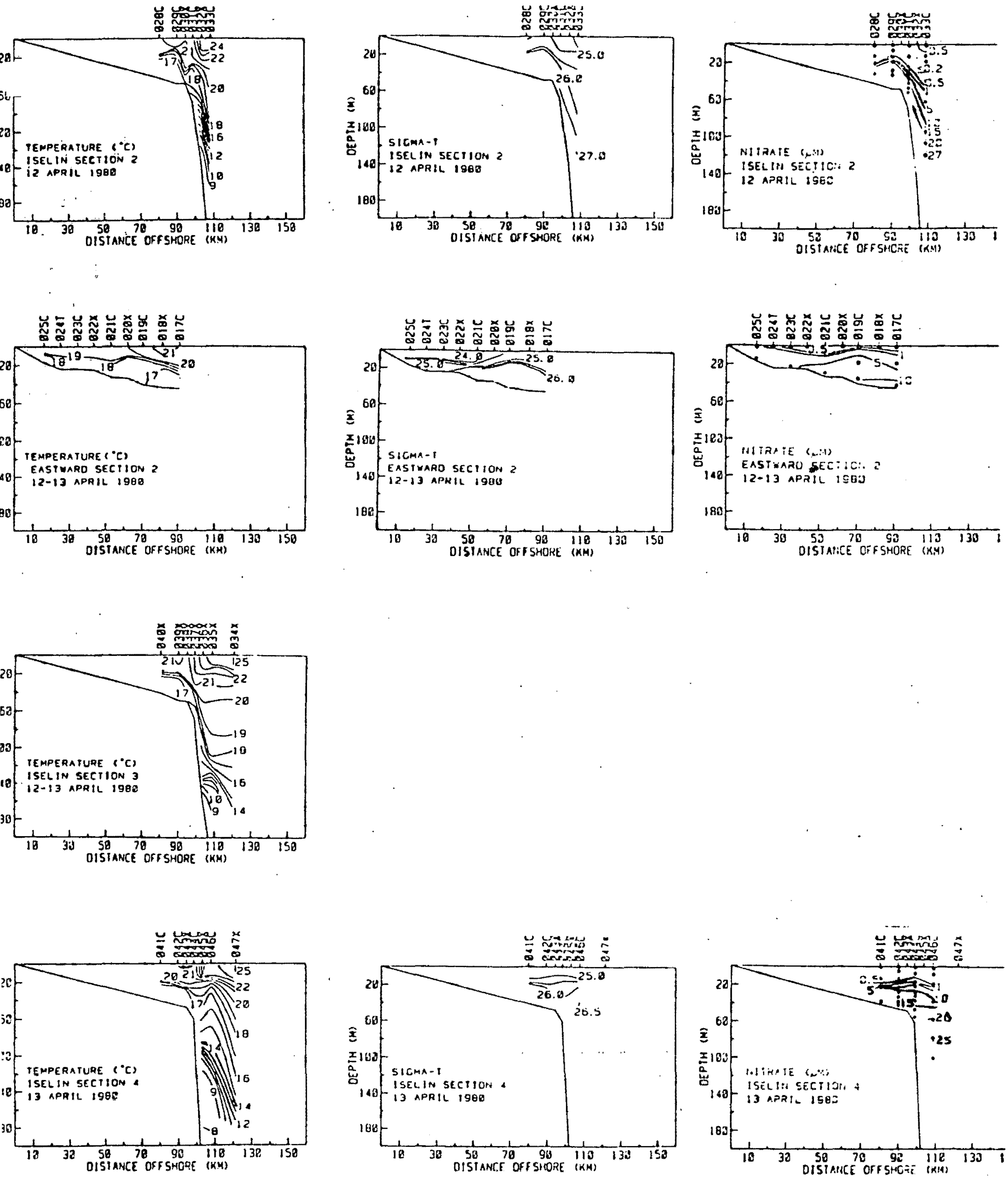

Figure 3. St. Augustine time series during Gabex-1

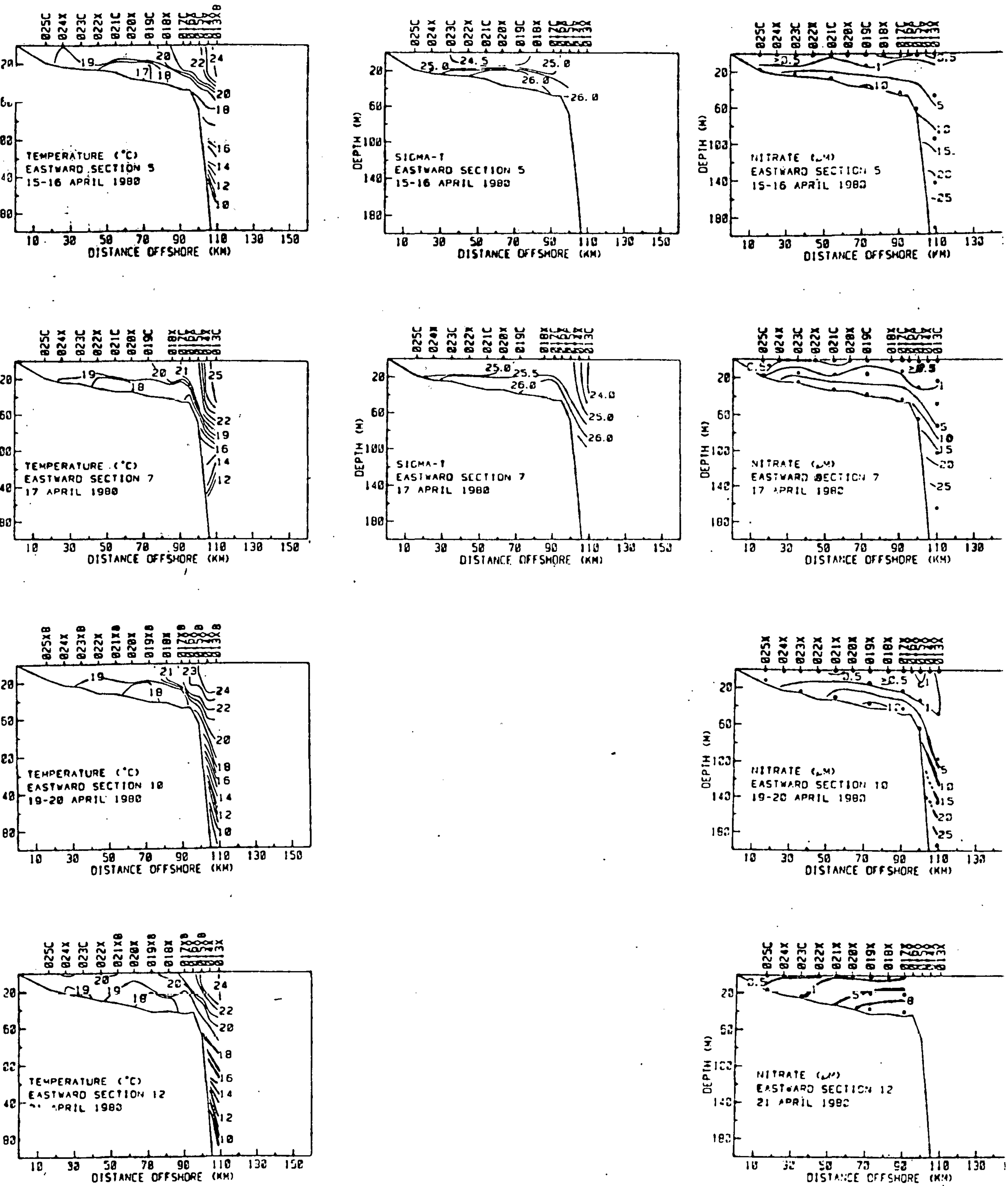

Figure 3. St. Augustine time series during GABEX-1 (cont.).

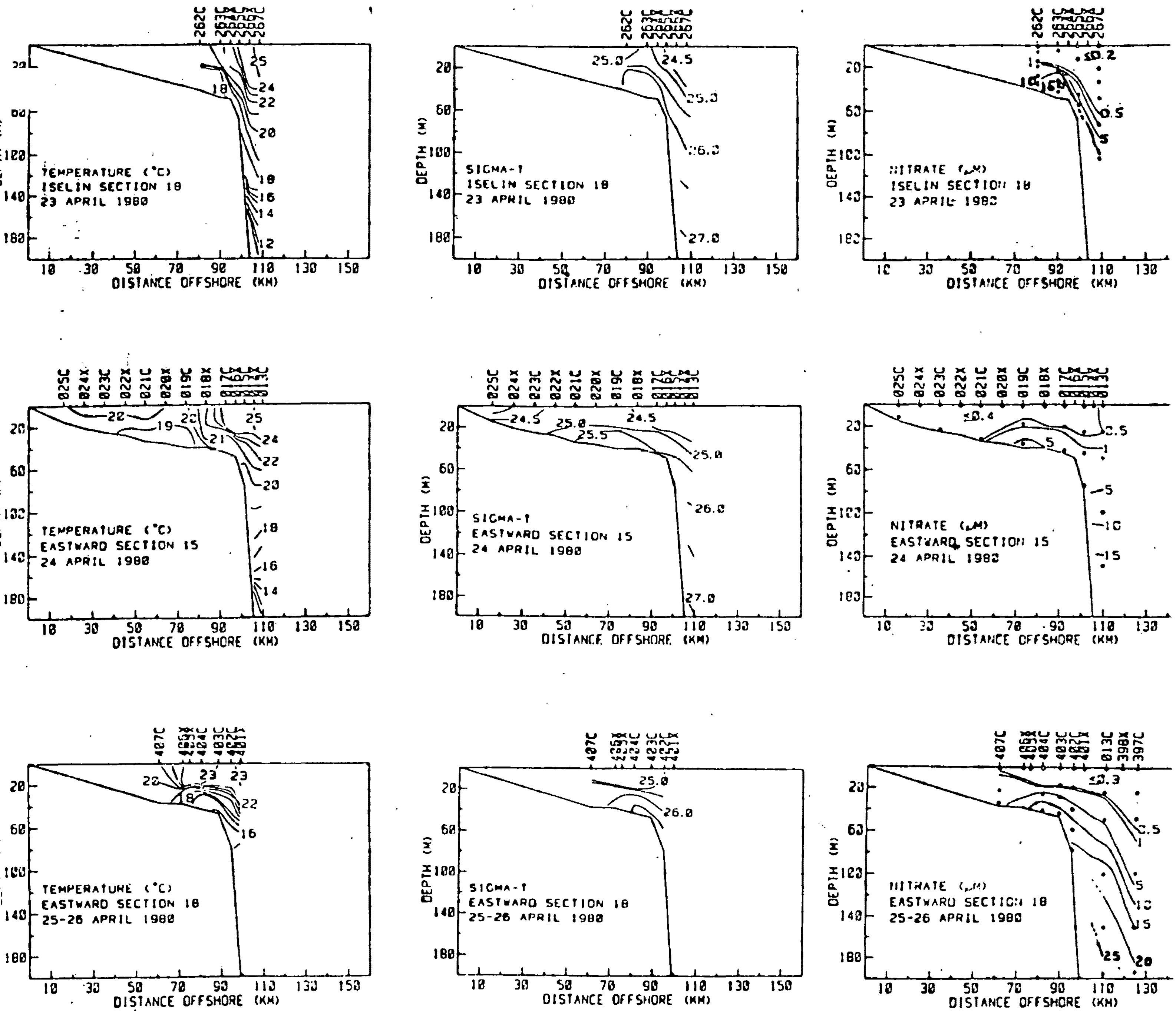

Figure 3. St. Augustine time series during GABEX-1 (cont.).

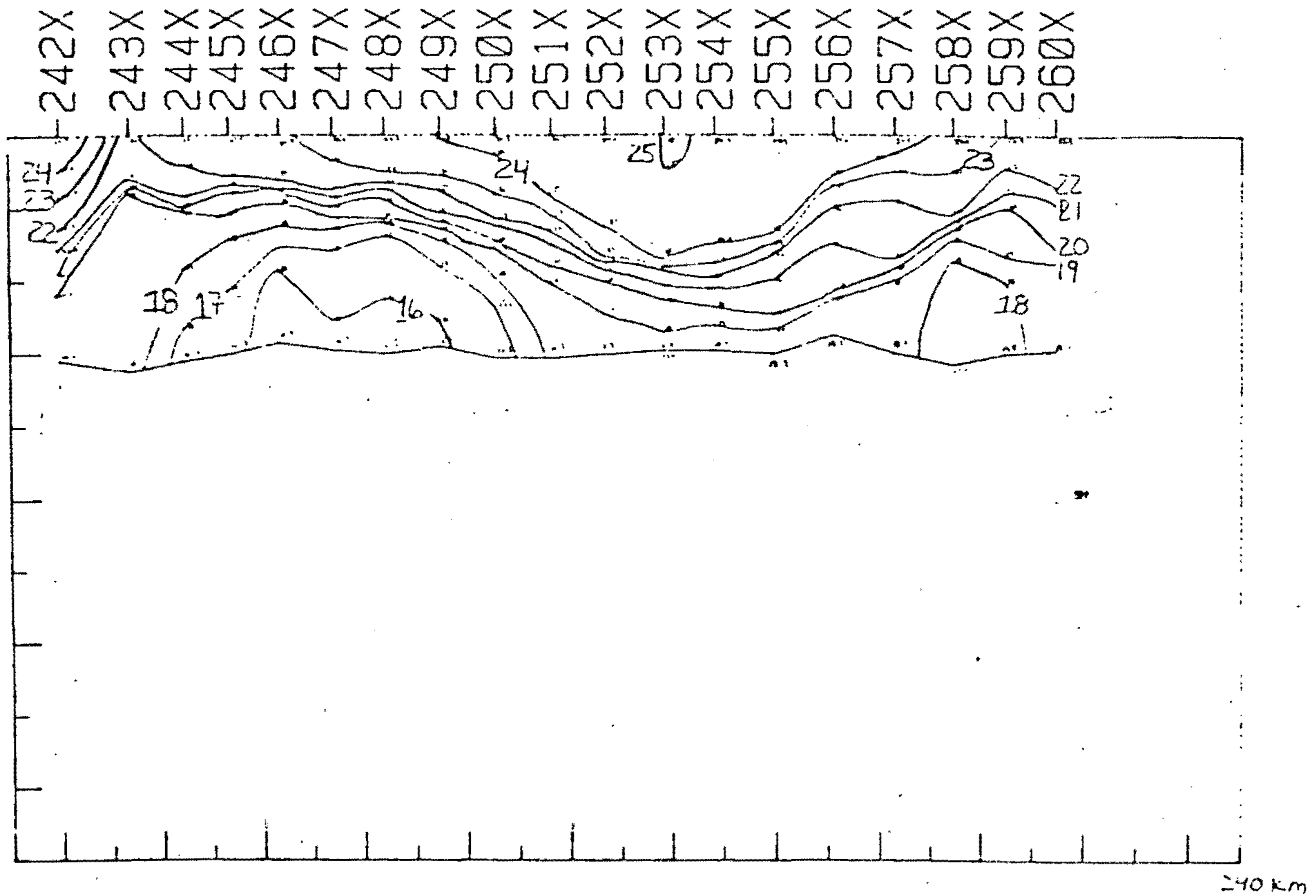

Figure 4. Thermal structure at 60 m from Cape Canaveral (242) to St. Augustine (260).

A SPATIAL LOOK AT THE 20-23 APRIL PERIOD DURING GABEX-1

In the previous section we examined the St. Augustine Time Series and noted the presence of an upwelling event in that area. In this section we will present data showing the north/south extent of the upwelling area. Figure 1 shows bottom nitrate concentrations from an EASTWARD map made on 20-23 April. Between 29 and 31°N nitrate appears to be advecting shoreward which agrees with data from the April 22 60 m isobath run (Figure 2) which placed an upwelling event at 29°45'N (Station 258, in Figure 2). The upwelling center at 28°20' thru 28°50'N (Station 244-250 in Figure 2) was south of the area mapped by the EASTWARD on 20-23 April (Figure 1).

During the time period the ISELIN made several transects between 28°43'N and 30°19'N. The Southern most ISELIN section (Section 16, Figure 3) shows the strong upwelling occurring in that area. This section was at the location of station 246 in the 60 m isobath run (Figure 2) which was in a definite zone of upwelling. At this location nitrate concentrations where above 15 μM inshore of the 60 m isobath. At the next section north (Section 15, 29°06'N) upwelling was much less in evidence with 20°C water restricted to the upper slope and nitrate concentrations below 0.5 μM above 30 m. This section agrees with the observations at 29°N in the bottom nitrate map and the distribution of upwelling centers observed in the 60 m run. Section 15 intersects the 60 m isobath run (Figure 2) at station 253 where upwelling is less prevalent.

Further north at ISELIN sections 14-11 upwelling is obvious with the 18°C isotherm extending across the outer shelf and high nitrate concentrations at all depths below the shallow surface layer. The 60 m isobath run on 22 April indicated the upwelling area was north of 29°30'N. This is further north than indicated in the sections. This is probably because the sections were run on

20-22 April with the northern sections run on 20 April which was 2-3 days before the 60 m isobath run. No doubt the northward advection of the upwelling center accounts for this difference.

The onshore extent of the intrusion appears to extend well across the shelf and possibly to the nearshore zone (EASTWARD Section 12 (Figure 4) at 30°N (Station 260 in Figure 2)). Although nitrate concentrations are low they are normally less than 0.5 μM but in this case concentrations above 1 μM cover 2/3 of the shelf and concentrations above 0.5 μM cover nearly all of the shelf; clearly a case of massive upwelling.

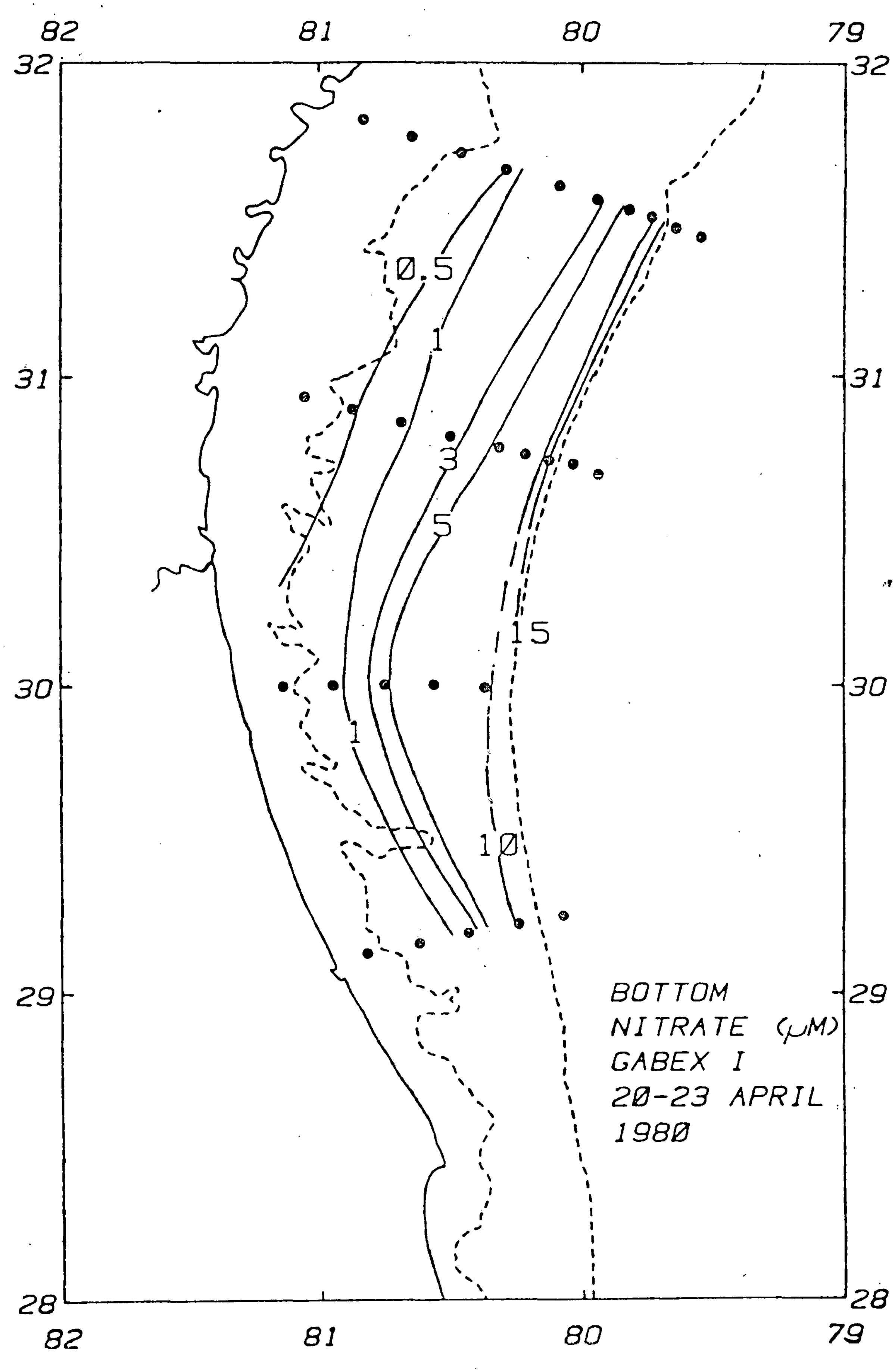

Figure 1. Near bottom nitrate concentrations during 20-23 April, 1980.

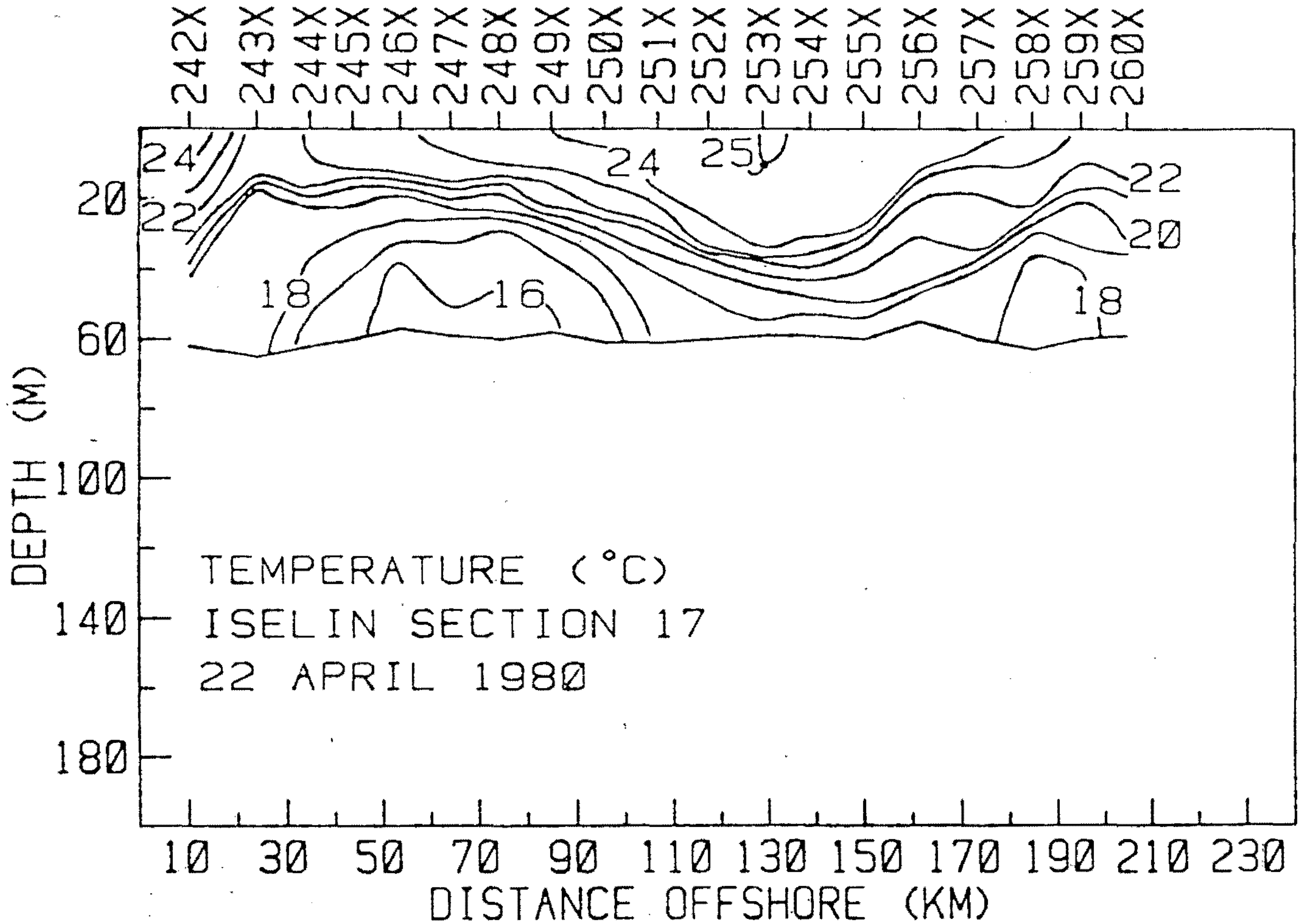

Figure 2. Thermal structure along 60 m isobath from Cape Canaveral (242X) to St. Augustine (260X).

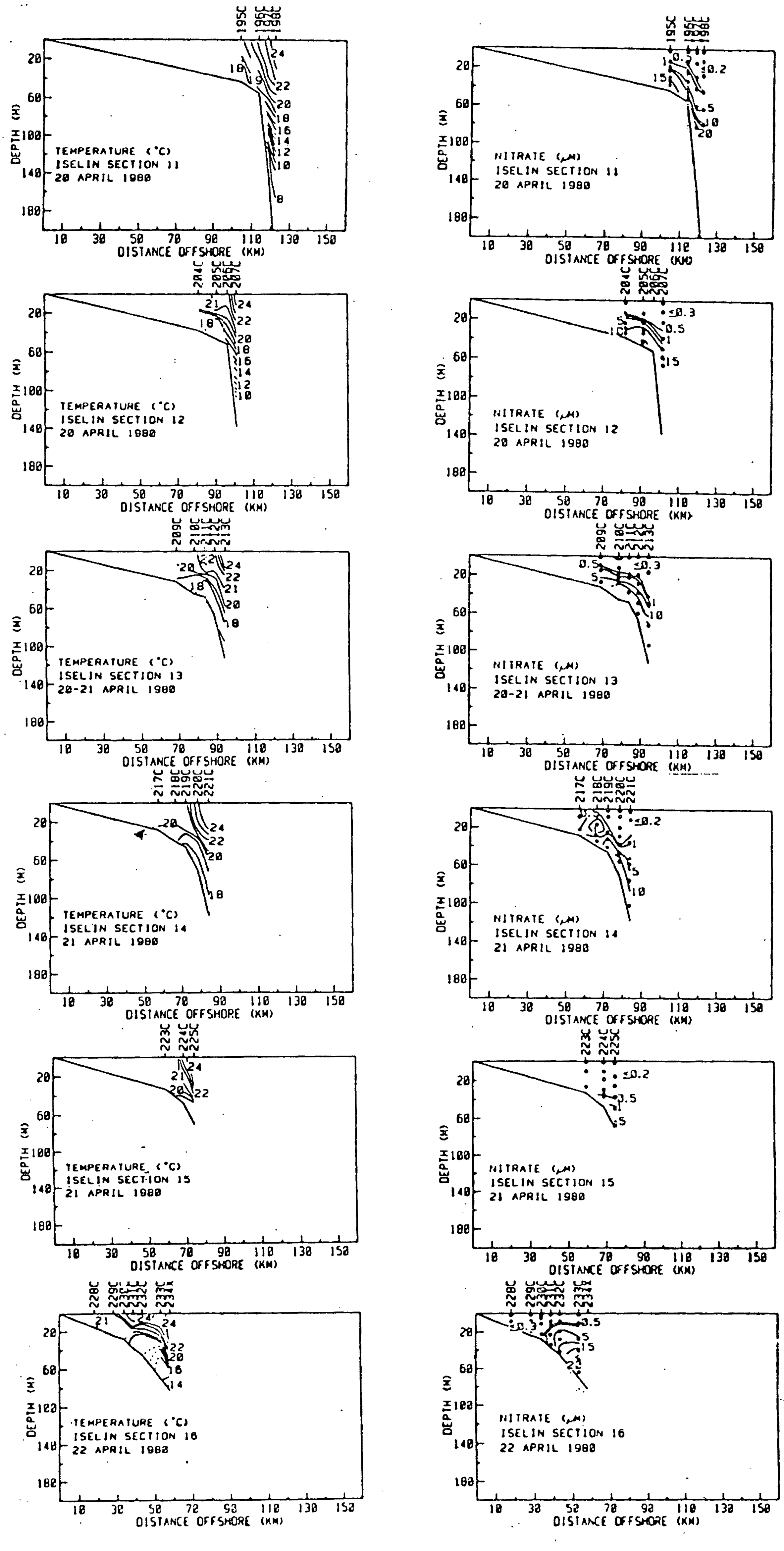

Figure 3. Cross shelf sections between 28°43' and 30°19'N.

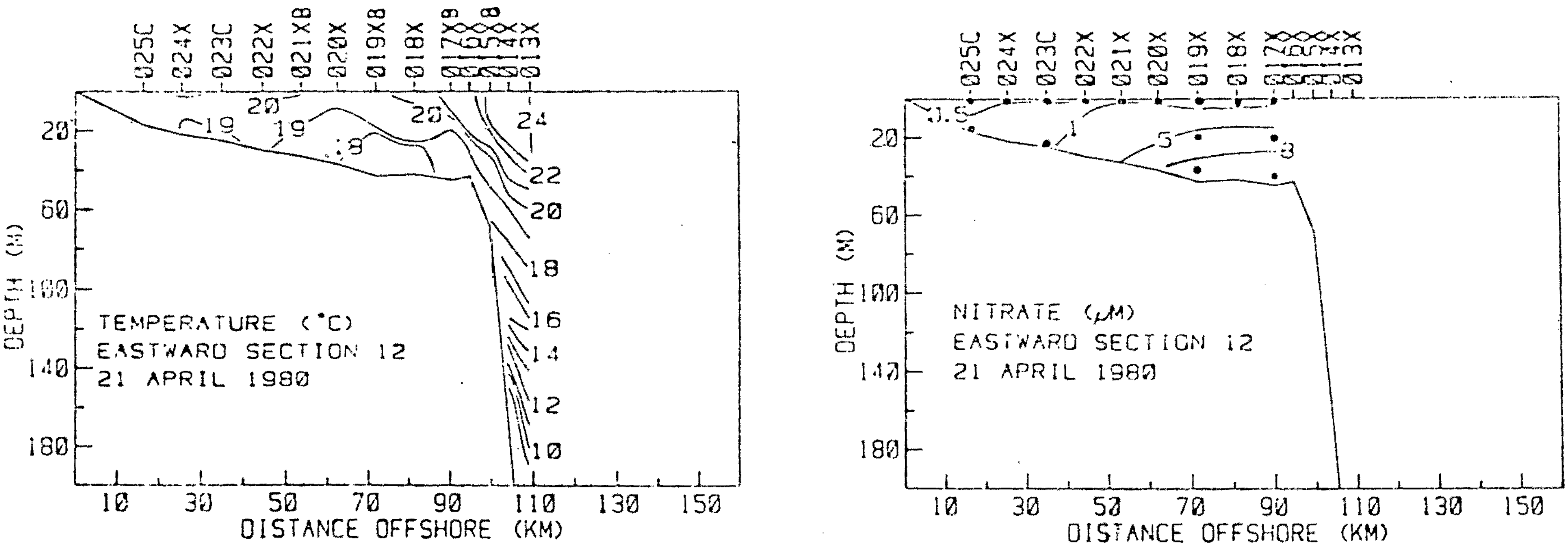

Figure 4. Trans-shelf section at St. Augustine. High nutrient concentrations indicate intruded water is reaching the beach.

Larry Atkinson

THE INTRUSION OF GULF STREAM WATER ACROSS THE CONTINENTAL SHELF DUE TO TOPOGRAPHICALLY - INDUCED UPWELLING

J.O. BLANTON*

L.P. ATKINSON*

L.J. PIETRAFESA**

T.N LEE***

*Skidaway Institute of Oceanography, Savannah, Georgia 31406

**Department of Marine Science and Engineering, North Carolina State University, Raleigh, North Carolina 27650

***Rosenstiel School of Marine and Atmospheric Science, University of Miami, Miami Florida 33149

ABSTRACT

Summer bottom temperatures along the continental shelf between Cape Hatteras and Cape Canaveral are abnormally cold in regions where isobaths diverge. These regions are located north of capes and shoals which force the flow of shelf water to change vorticity whereby upwelling is induced. The Gulf Stream intrudes across bottom during summer to replace the upwelled water and accounts for the colder and more stratified water found over the northern Florida continental shelf and the North Carolina shelf.

INTRODUCTION

Wave-like perturbations on the western (cyclonic) edge of the Gulf Stream are advected northward by the strong flow of the Gulf Stream along the southeastern U.S. continental shelf (the South Atlantic Bight). Certain mainfestations of these waves have been described as shingles (Von Arx, Bumpus and Richardson, 1955), meanders (Webster, 1961), and spin-off eddies (Lee, 1975; Lee and Mayer, 1977). Some confusion presently exists in the scientific community as to the exact process meant by the use of these terms. There is general agreement that the waves occur each 5-10 days and propagate northward between Cape Canaveral and Cape Hatteras at about 30 km/day (Legeckis, 1975; Legeckis, 1979) under a variety of stable and unstable configurations. The waves induce upwelling of colder North Atlantic Central Water, hereafter called Gulf Stream Water of slightly lower salinity at the edge of the shelf (Lee, Atkinson, and Legeckis, 1980). Under certain hydrographic conditions found in summer, the upwelled water can intrude along the bottom displacing large amounts of shelf water (Blanton, 1971; Blanton and Pieterfesa, 1978; Atkinson and Pietrafesa, 1980).

Intrusions of Gulf Stream Water onto the shelf occur most dramatically during summer months when the shelf water has its lowest density (Atkinson, 1977) and Gulf Stream transport is maximum (Niiler and Richardson 1973). Consistent with high transport, the horizontal density gradient through the Gulf Stream frontal zone is highest during summer and the Gulf Stream Water at the depth of the shelf break (ca. 50m) is usually of higher density than the adjacent shelf water. Thus the Gulf

Stream Water intrudes shoreward underneath the shelf water (Blanton, 1971; Atkinson, 1977) and appears to be the dominant process that maintains the vertical density stratification of the ocean during summer on the continental shelf of the South Atlantic Bight.

Detailed studies of thermal structure, winds and currents in the vicinity of Cape Canaveral (Leming, 1979) suggested that frequent intrusions of colder Gulf Stream Water could occasionally produce a narrow zone (< 20 km) of low surface temperatures north of Cape Canaveral. Anomalously cold water temperatures in this region were first reported by Green (1944) during July and August, and the prevailing northeast wind stress north of Cape Canaveral was thought to induce upwelling across the continental shelf. The cold coastal temperatures extend from Cape Canaveral north to Jacksonville in summer (Taylor and Stewart, 1959). Periods of cold water are accompanied by a lowering of sea level and by wind stresses most conducive to upwelling. Leming (1979) demonstrated that the changing vorticity of streamlines following the curved isobaths north of Cape Canaveral could induce upwelling on the north side of the Cape, which is downstream under prevailing flow conditions in summer.

It is the purpose of this paper to present further evidence that Gulf Stream intrusions prevail and perhaps are strengthened in regions where capes and shoals change the vorticity of the flow on the shelf. This process can account for cold bottom temperatures and strong vertical stratification of the shelf water observed north of Cape Canaveral and in the region of the Carolina Capes (Fig. 1).

TOPOGRAPHICALLY - INDUCED UPWELLING

Upwelling in the vicinity of capes and other topographic irregularities has been studied since the 1930's by Japanese oceanographers (see Uda, 1959 for a list of references). Arthur (1965) noted from Reid, Roden and Wyllie (1958) that there appeared to be an intensification of upwelling south of capes and points that extend out into coastal currents on the U.S. West Coast. Arthur (1965) demonstrated that changes in the relative vorticity along a streamline could enhance upwelling south of capes for southward flow. The equation for conservation of vorticity is (Arthur, 1965)

$$f \frac{dw}{dz} = \frac{D\xi}{Dt} + \beta v$$

where $\xi = \frac{v}{R} - \frac{dv}{dn}$ = the vorticity (ξ) in local coordinates of the horizontal flow velocity (v) along a stream line of radius of curvature (R). The term $\frac{dv}{dn}$ is the shear normal to the streamline (n-direction); $\beta = 2 \times 10^{-11} m^{-1} s^{-1}$ = change of the planetary vorticity (f) with latitude; w is the vertical velocity along z (positive upward). For the estimates below, we neglect $\frac{dv}{dn}$ so that the vorticity is calculated by $\xi = v/R$.

The prevailing winds in July and August along the South Atlantic Bight exert a northeastward wind stress (Weber and Blanton, 1980). This induces a northeastward flow on the shelf and places the north side of capes and shoals on the downstream side of this flow. Leming (1979) showed that north of Cape Canaveral, the term βv and $D\xi/Dt$ cause upwelling for northward flow.

Experimental data do not presently exist to evaluate the theory quantitatively. However, some regions in the South Atlantic Bight have favorable bathymetry to induce upwelling (Fig. 1). North of Cape Canaveral and north of the Carolina Capes, the isobaths between 20-30 m have radii of curvature as large as 50 - 100 km with the small value associated with the Carolina Capes. The isobaths downstream (north) of the curving portions diverge for several tens of kilometers. Since low frequency currents tend to follow isobaths, the divergent flow induces upwelling to preserve continuity. Thus upwelling occurs over a large region of diverging bathymetry. We can estimate w near bottom associated with the curving flow and apply the estimates to the entire region of diverging bathymetry. For these estimates (Table 1) we assume $v = 0.3$ m/s.

The assumption on R and isobath areas required to compute $D\xi/Dt$ and volume fluxes (Table 1) at each cape can have a wide range within one-half of an order of magnitude. Thus the differences between capes are not significant but the orders of magnitude are indicative. Specifically, the upwelling velocities are slightly smaller than "typical" values of 10^{-5} m/s often quoted for upwelling.

The intent of Table 1 is to indicate the potential significance of topographically induced upwelling to the hydrography of the continental shelf. We will present data to support the hypothesis that cold bottom temperatures and strong vertical stratification are observed downstream of the same regions where there occurs upwelling produced by the changing vorticity of the flow.

Table 1. Estimates of volume fluxes due to upwelling in areas of curving isobaths north of Cape Canaveral, Florida, and Cape Lookout, North Carolina. Estimates are based on the curvatures of the 30-m isobath, $V = 0.3$ m/s, and W is estimated at a depth of 30 m.

	CAPE CANAVERAL	CAPE LOOKOUT
f (s^{-1})	6.6×10^{-5}	7.7×10^{-5}
R (km)	100	50
$D\xi/Dt$ (S^{-2})	-1.8×10^{-11}	-2.4×10^{-11}
βv (S^{-2})	6×10^{-12}	6×10^{-12}
W_{30} (m/s)	5×10^{-6}	7×10^{-6}
Area of diverging isobaths (km^2)	80 x 40	100 x 50
Volume flux (M^3/s)	1.7×10^4	3.5×10^4

DATA PRESENTATION

We suspected upwelling to occur in areas where the flow follows curving isobaths. The areas north of Cape Canaveral, Cape Fear and Cape Lookout are thus prime areas of interest (Fig. 1). Our data files (recent data) and those of the National Oceanographic Data Center (archived data since 1953) were used to compute surface and bottom temperatures. Three depth intervals (1-20m, 21-40m, 41-60m) were averaged over one-degree squares from 28° N to 36° N. The region 28° - 30° N is called North Florida shelf; region 31° - 33° N is called Georgia-South Carolina shelf; and 34° - 35° N is called Carolina Capes. The data for July and August are summarized for bottom temperature and surface-bottom temperature differences (Fig. 2).

Coldest bottom temperatures are found between 41 - 60 m in the region 29° - 30° n. Bottom temperature increases rapidly with increasing latitude through 31° - 32° N. A sharp decrease is noted again between 33° - 35° N. In the mid-shelf regions (21-40 m) coldest bottom temperatures are found between 30° - 31° N. Bottom temperatures near the coast (1-20 m) are also the coldest in the region 29° - 31° N and 34° - 35° N. In summary, coldest bottom temperatures are found on the north Florida shelf. While the gradients are most dramatic along the outer shelf, colder temperatures also exist in the region closest to shore.

Similar patterns are reflected in the mean differences between surface and bottom temperatures. The difference is greater along the north Florida shelf, an effect that shows up even in the 1-20 m depth range, but most strongly exists along the 41-60 m depth range. The difference is minimum off Georgia and South Carolina and increases again off the Carolina Cape region. Thus, the thermal stratification of the shelf waters is greatest on the north Florida shelf and the Carolina Capes.

Mean surface temperature (Fig. 3) close to shore has a maximum between 31° - 33° N, off Georgia and South Carolina. In August, there is a minimum region that extends across the shelf off northern Florida.

Two quasi-synoptic surveys of the Georgia and north Florida shelf were conducted over a ten-day period in July - August 1978 (Fig. 4 and 5). They illustrate colder bottom temperatures off north Florida. Downstream from New Smyrna Beach to Savannah (Fig. 4), isotherms were sloped parallel to the continental slope. Near the shelf break, 18° - 24°C isotherms shoaled upward, then downward farther inshore. The 18° - 24°C isotherms pentrated into shallower water off New Smyrna Beach and St. Augustine than in areas farther north (Fig. 5). These isotherms formed a bottom temperature front strongest in the south along the 40-m isobath. The front weakened and extended farther offshore with distance northward.

The same region was resurveyed about ten days later, and significant changes were found. Off St. St. Augustine, near bottom temperatures <20°C were present (Fig. 6). Surface water temperatures had decreased slightly between 50-100 km offshore. Conditions off Brunswick had remained essentially unchanged. Bottom temperatures from 18° - 20° (Fig. 7) south of Brunswick had moved onshore and bottom temperatures <16°C were found in a small region along the outer shelf. The cold bottom water originated from the Gulf Stream according to its temperature-salinity correlation.

Other surveys have shown the presence of Gulf Stream water near bottom extending into shallower water on the north Florida shelf (Fig. 8). Some features in bottom temperatures were common to those described above. The bottom waters at water depths less than 30 - 40 m were consistantly cooler off Florida than off Georgia. Warmer bottom temperatures off Georgia were separated from the cooler water farther south by a sharp temperature gradient. The vertical distribution of temperature and salinity (not shown) indicated that this gradient separated Gulf Stream Water from less saline modified shelf water.

A quasi-synoptic survey was conducted off Cape Lookout, North Carolina, in August 1968 (Fig. 9). This survey was completed in less than 48 hours during moderate northeast wind stress. Near bottom water east (downstream) of the shoal area south of the cape was 1° - 2° colder than that to the west.

DISCUSSION

We hypothesize that the areas on the downstream side of capes and shoals induce upwelling (Arthur, 1965) and that this upwelling induces Gulf Stream Water present at the shelf break farther offshore to intrude across the shelf bottom during summer months. The prevailing northeast wind stress during summer (Weber and Blanton, 1980) induces northeast flow in the inner and mid-shelf regions. Thus we expect intrusions to be more prevalent north of Cape Canaveral(north Florida shelf) than off Georgia and South Carolina.

Statistical data (Fig. 2) support this hypothesis. Regions of cold bottom water are found off north Florida. Similar regions off the Carolina Capes are suggested but the manner in which the data were sorted (by latitude) may not have sufficient spatial resolution for that region since the shoals associated with the capes cut across lines of equal latitude.

The surface-bottom temperature differences are also consistent with the hypothesis (Fig. 2). Intrusions are the primary process responsible for maintaining this difference which is clearly greater off the north Florida shelf than off Georgia and South Carolina. During summer, Gulf Stream Water is generally found along the bottom in shallower depths off Florida than off Georgia (Fig. 5, 7 and 8). Even an April survey depicted this situation. The temperature differences would not clearly show the effect in seasons other than summer because surface temperatures are colder off Georgia than off north Florida except in summer. However, the upwelling process for flow along curving isobaths would occur regardless of season.

A small amount of data off Cape Lookout (Fig. 9) suggests that upwelling occurs on the downstream side. Evidence shows that intrusions in Onslow Bay enter the embayment just east of the Cape Fear shoals then spread throughout the embayment (Blanton and Pietrafesa, 1978; Atkinson and Pietrafesa, 1980). This is consistent with the hypothesis that cape induced upwelling induces the Gulf Stream Water to intrude into the upwelling region, in this case downstream of Cape Fear.

The north Florida shelf is a region of spreading isobaths. As a given volume of flow passes around Cape Canaveral and begins to follow the isobaths, the spreading flow is compensated by upwelling to replace the mass loss by horizontal spreading of the streamlines. In summer, this loss is made up by inducing the Gulf Stream Water to intrude across the bottom to shallower water. In regions where the isobaths do not spread (Georgia - South Carolina shelf), there is no inducement for an intrusion of this type to occur. The Georgia - South Carolina shelf has minimum differences in surface and bottom temperature in July and August (Fig. 2).

Wind-Induced Upwelling

Alongshore coastal winds favorable to upwelling prevail in the South Atlantic Bight during the months of June, July and August (Saunders, 1977; Weber and Blanton, 1980). Upwelling-favorable winds were thought to cause the cold coastal temperatures observed in northern Florida (Green, 1944; Taylor and Stewart, 1959). Upwelling-favorable winds are equally persistant off Georgia and South Carolina and yet we find no evidence that intrusions occur there in summer to the same degree found off the north Florida shelf.

Wave-Induced Upwelling

The upwelling of Gulf Stream Water is induced by waves in the Gulf Stream front. Satellite imagery shows that these waves are a consistent feature along the shelf break (Vukovich, Crissman, Bushnell and King, 1978; Legeckis, 1979) and appear to grow to much larger size north of the Charleston bump (Fig. 1) in the region of the Carolina Capes. They occur with a frequency of approximately 35 events/year, i.e., once/10 days, along the North Carolina shelf. Evidence suggests that these frontal disturbances intensify as they propagate north of Cape Canaveral, and presumably any upwelling they would produce would likewise intensify. One might hypothesize that upwelling of Gulf Stream Water would intensify with latitude and so would intrusions, particularly with the aid of the upwelling-favorable winds in summer. Our data (Fig. 2) do not support this hypothesis.

Speculations

We have shown data consistent with the hypothesis that the divergence due to spreading isobaths and related to vorticity changes in flow following curved isobaths induces upwelling that in turn causes denser Gulf Stream Water to flow shoreward along the bottom. This might be viewed as a process that enhances the upwelling produced at the shelf break by waves in the Gulf Stream front, and we pose the question of whether the upwelling induced by the capes might have a feedback effect that could intensify cyclonic circulation of the flow due to these events. Consider a wave propagating northward along the outer edge of the north Florida shelf. Colder Gulf Stream Water passes upward and shoreward through the wave (Fig. 10). The shoreward motion would be limited in the shelf area where no upwelling was induced by wind or topography, but the shoreward motion i.e., intrusion) is enhanced by the topographically-induced upwelling. Thus more water must pass upward through the wave to support the divergence in shelf flow.

Intensified upwelling caused by divergence in the overlying fluid has an analogy in meteorology. Surface low pressure areas frequently intensify as they propagate and pass beneath the exit region of an upper level (300-500 mb) trough in the jet stream (Haltiner and Martin, 1957). The low strengthens because the vertical motion already present is enhanced.

We do not presently have convincing evidence that meanders passing along the northern Florida shelf are intensified by spreading isobaths. This hypothesis is to be tested by future research in the South Atlantic Bight.

CONCLUSIONS

Historical data show that July and August bottom temperatures on the continental shelf off north Florida and in the Carolina Capes region in July and August are cooler than those found farther north. Vertical stratification is also stronger in the same areas which suggests that Gulf Stream Water intrudes along bottom into shallower water.

Shelf flow following curved isobaths can induce upwelling (Arthur, 1965) and regions of curved isobaths are found north of Cape Canaveral and in the Carolina Capes region. Upwelling in these regions is replaced by Gulf Stream Water uplifted by wave-like perturbations to levels above the shelf break. Replacement by Gulf Stream Water requires it to intrude across the bottom into the regions of curved isobaths. Intrusions off Georgia and South Carolina appear much weaker and are not indicated in the historical data. No curved isobaths exist here over a sufficiently large region to induce upwelling.

Predominant winds in July and August are favorable for upwelling throughout the South Atlantic Bight. If wind-induced upwelling were the sole agent responsible for the decreased bottom temperatures, we would expect to find evidence of these off Georgia and South Carolina. It is possible that Gulf Stream Water could intrude into these regions during spring when solar radiation begins to warm the cooler shelf water and produces a stratified water column. A density-driven flow such as the gravitational flow discussed in estuaries aided by northeastward wind stress could induce Gulf Stream Water to intrude closer to shore. The flow is obviously maintained for only one or two months after which winds and tidal mixing destroy the stratification. Off north Florida and North Carolina, Gulf Stream intrusions induced by shelf flow divergence maintain the stratification during the summer months with wind playing a less dominant role.

ACKNOWLEDGEMENTS

We are grateful to Dr. Gerold Janowitz for stimulating discussions in the early phases of this study. We thank Dr. David Menzel for his helpful comments on the original manuscript.

The following support from the U. S. Department of Energy is gratefully acknowledged: Contract No. EY-77-S-09-0125 and Contract No. EY-77-S-09-0889, to Skidaway Institute of Oceanography; Contract No. EY-76-S-09-0902 to North Carolina State University, and Contract No. EY-76-S-05-5163 to University of Miami. We acknowledge the support of Duke University through NSF Grant G-17669, which provided the R/V EASTWARD for the acquisition of data utilized in Figure 9 and Bureau of Land Management Contract No. 209-05 which supported the acquisition of some of the hydrographic data.

LIST OF FIGURES

Fig. 8. More bottom temperature charts illustrating that the front in bottom temperature is located in shallower depths south of Jacksonville, Florida. (A) 15-23 April 1978; (B) 4-7 July 1977.

Fig. 9. Bottom temperature chart across the shelf off Cape Lookout, North Carolina. Flow in summer is predominantly eastward and bottom temperatures are colder on the downstream side.

Fig. 10. Schematic representation of a summer intrusion of oceanic water onto the continental shelf. The wave along the cyclonic edge of the boundary current propagates poleward. Oceanic water is pulled upward through the wave trough and spreads shoreward along the shelf bottom into regions where flow on the shelf diverges. A bottom temperature front marks the extent of the intrusion.

LIST OF TABLES

REFERENCES

Arthur R. S. (1965) On the calculation of vertical motion in eastern boundary currents from determinations of horizontal motion. Journal of Geophysical Research, 70(12), 2799-2803.

Atkinson L. P. (1977) Modes of Gulf Stream intrusion into South Atlantic Bight Shelf Waters. Geophysical Research Letters, 4(12), 583-586.

Atkinson L. P., and L. J. Pietrafesa (1980) A flushing model of Onslow Bay, North Carolina based on intrusion volumes. Journal of Physical Oceanography, (in press).

Blanton, J. O. (1971) Exchange of Gulf Stream water with North Carolina Shelf Water in Onslow Bay during stratified conditions. Deep-Sea Research, 18, 167-178.

Blanton J. O. and L. J. Pietrafesa (1978) Flushing of the continental shelf south of Cape Hatteras by the Gulf Stream. Geophysical Research Letters, 5(6), 495-498.

Green C. K. (1944) Summer upwelling -- northeast coast of Florida. Science, 100 (2607), 546-547.

Haltiner G. J. and F. L. Martin (1957) Dynamical and physical meteorology. McGraw-Hill, New York. 470 pp.

Lee T. N. (1975) Florida current spin-off eddies. Deep-Sea Research, 22, 753-765

Lee T. N. and D. A. Mayer (1977) Low-frequency current variability and spin-off eddies of southeast Florida. Journal of Marine Research, 35(1), 193-220.

Lee T. N., L. P. Atkinson and R. Legeckis (1979) Detailed observations of a Florida current spin-off eddy on the Georgia continental shelf. (Submitted to Deep-Sea Research).

Legeckis R. (1975) Application of synchronous meterological satellite data to the study of time-dependent sea surface temperature changes along the boundary of the Gulf Stream. Geophysical Research Letters, 2(10), 435-438.

Legeckis R. (1979) Satellite observations of the influence of bottom topography on the seaward deflection of the Gulf Stream off Charleston, South Carolina. Journal of Physical Oceanography, 9(3), 483-497.

Leming, T.D. (1979) Observations of temperature, current and wind variations off the central eastern coast of Florida. NOAA Technical Memorandum NMFS-SEFC-6 (U.S. Dept. of Commerce). 172 pp.

Niiler P. P. and W. S. Richardson (1973) Seasonal variability of the Florida Current. J. Mar. Res., 31(3), 144-167.

Reid J., G. I. Roden and J. G. Wyllie (1958) Studies of California Current System. California Cooperative Fisheries Investigation Progress Report, July 1956-January 1958. Marine Research Commission, California, Department of Fish and Game, Sacramento, California.

Saunders P. M. (1977) Wind stress on the ocean over the eastern continental shelf of North America. Journal of Physical Oceanography, 7(4), 555-556.

Taylor C. B. and H. B. Stewart, Jr. (1959) Summer upwelling along the east coast of Florida. Journal of Geophysical Research 64(1), 33-40.

Uda M. (1959) Oceanographic Seminars. Fisheries Research Board of Canada. Manuscript Report Series No. 51, 110 pp.

von Arx W. S., D. Bumpas and W. S. Richardson (1955) On the fine structure of the Gulf Stream front. Deep-Sea Research, 3 46-65.

Vukovich F. M., B. M. Crissman, M. Bushnell and W. J. King (1978) Sea surface temperature variability analysis of potential OTEC sites utilizing satellite data. Final report to the U.S. Department of Energy (Contract No. EG-77-C-05-5444). 155 pp.

Weber A. H. and J. O. Blanton (1980) Monthly mean wind fields for the South Atlantic Bight. Journal of Physical Oceanography (in Press).

Webster F. (1961) A description of Gulf Stream meanders off Onslow Bay. Deep-Sea Research, 8, 130-143.

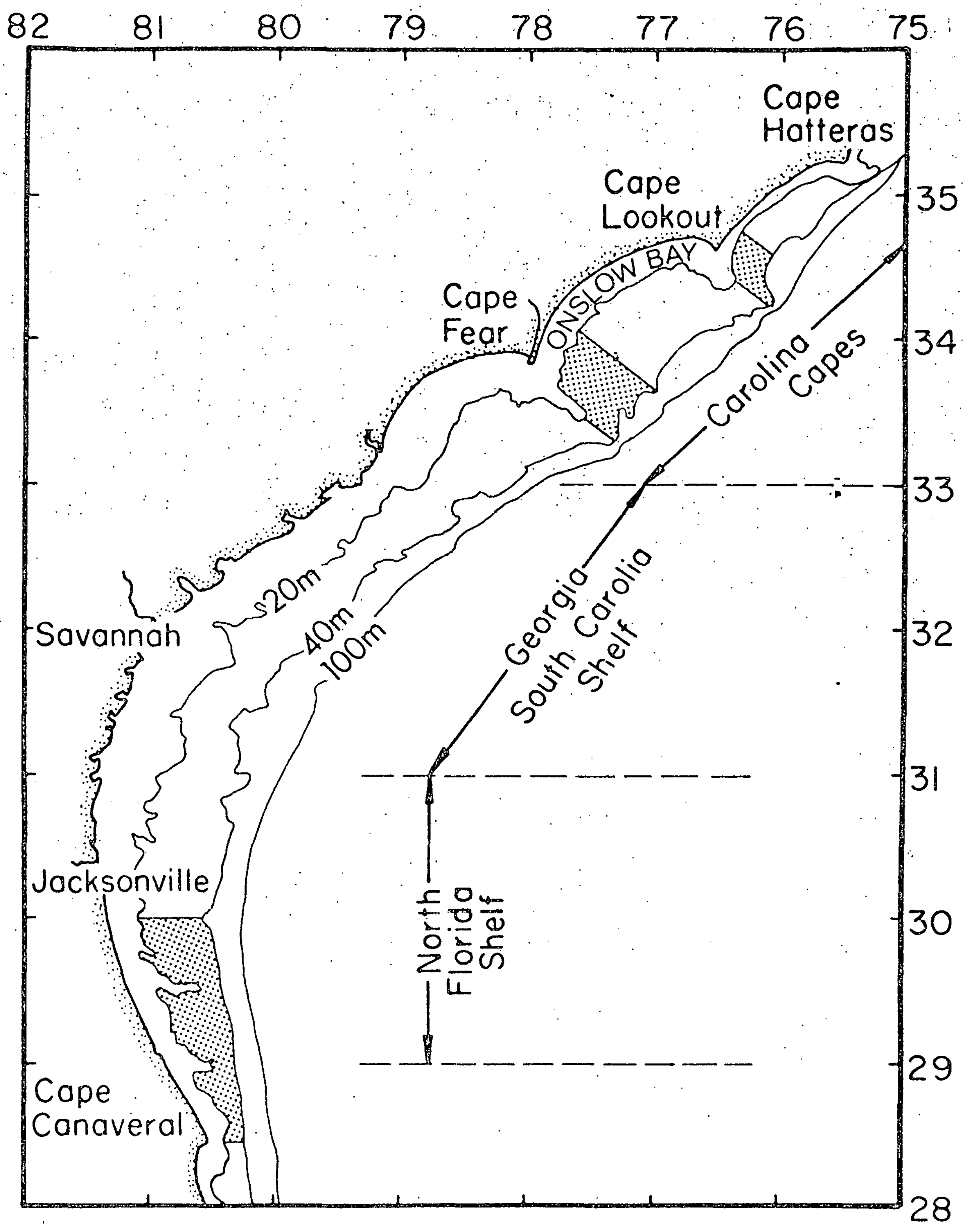

Fig 1. Blanton & all

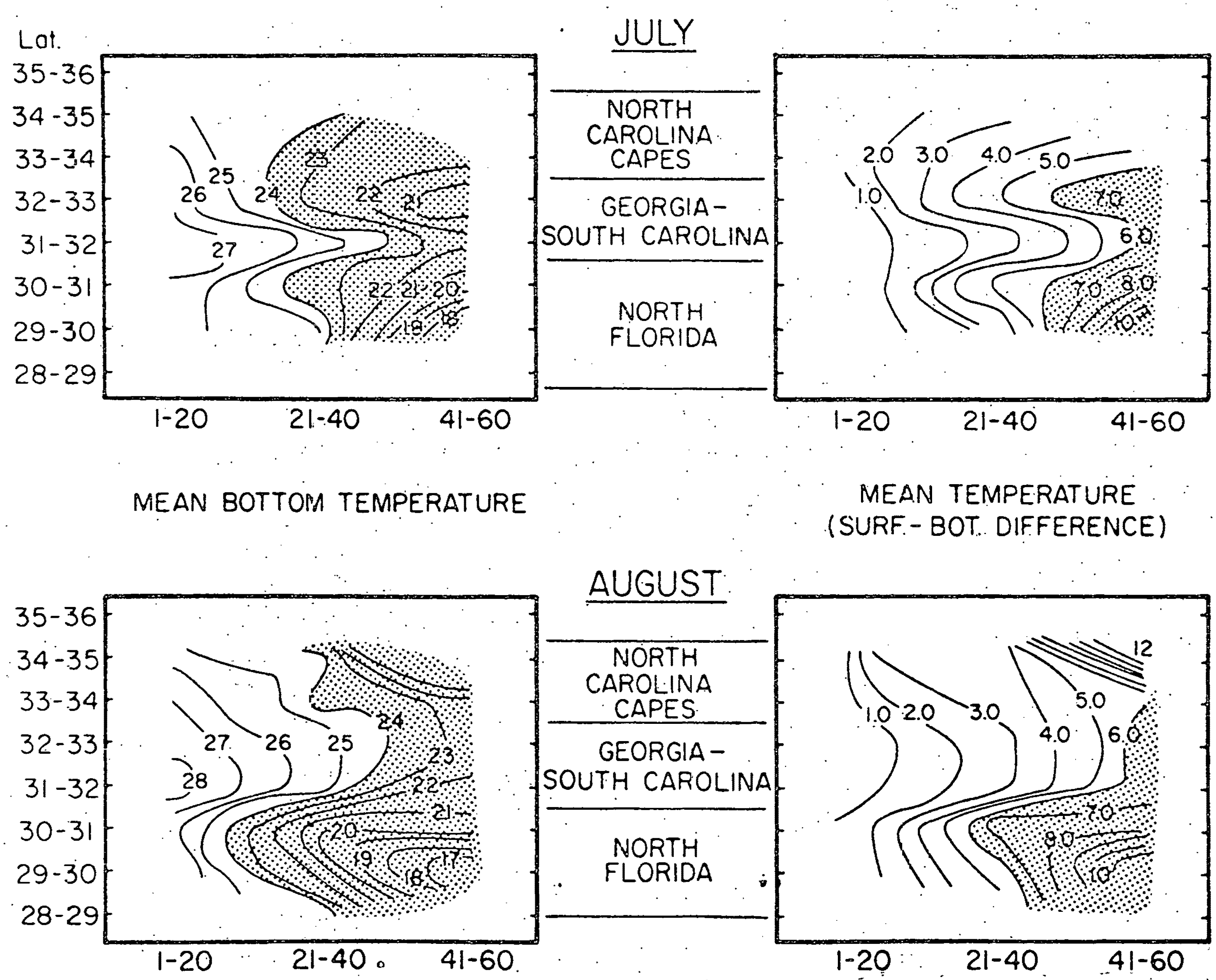

Fig. 2. Blanton et al.

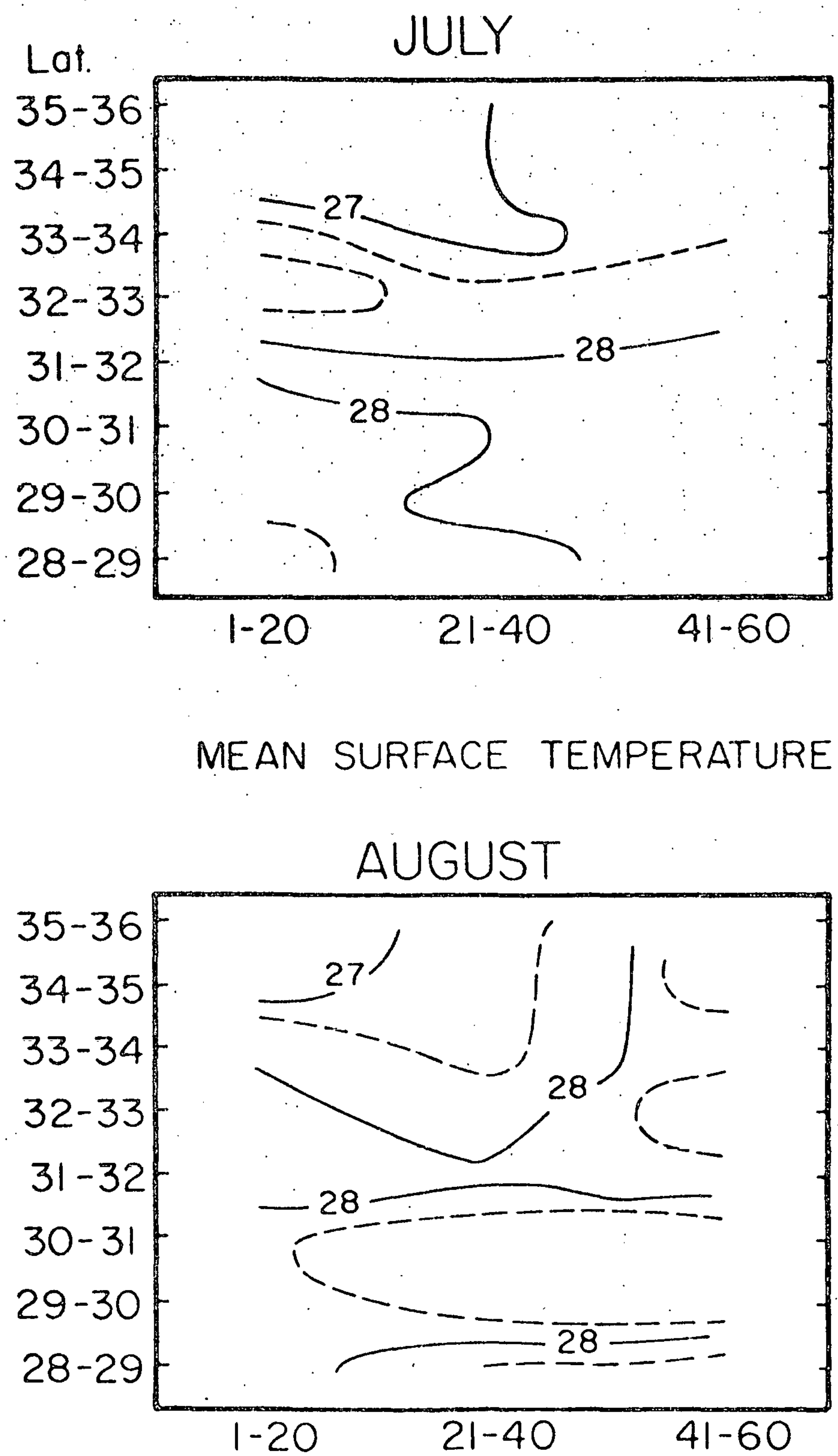

Fig. 3 Blanton et al.

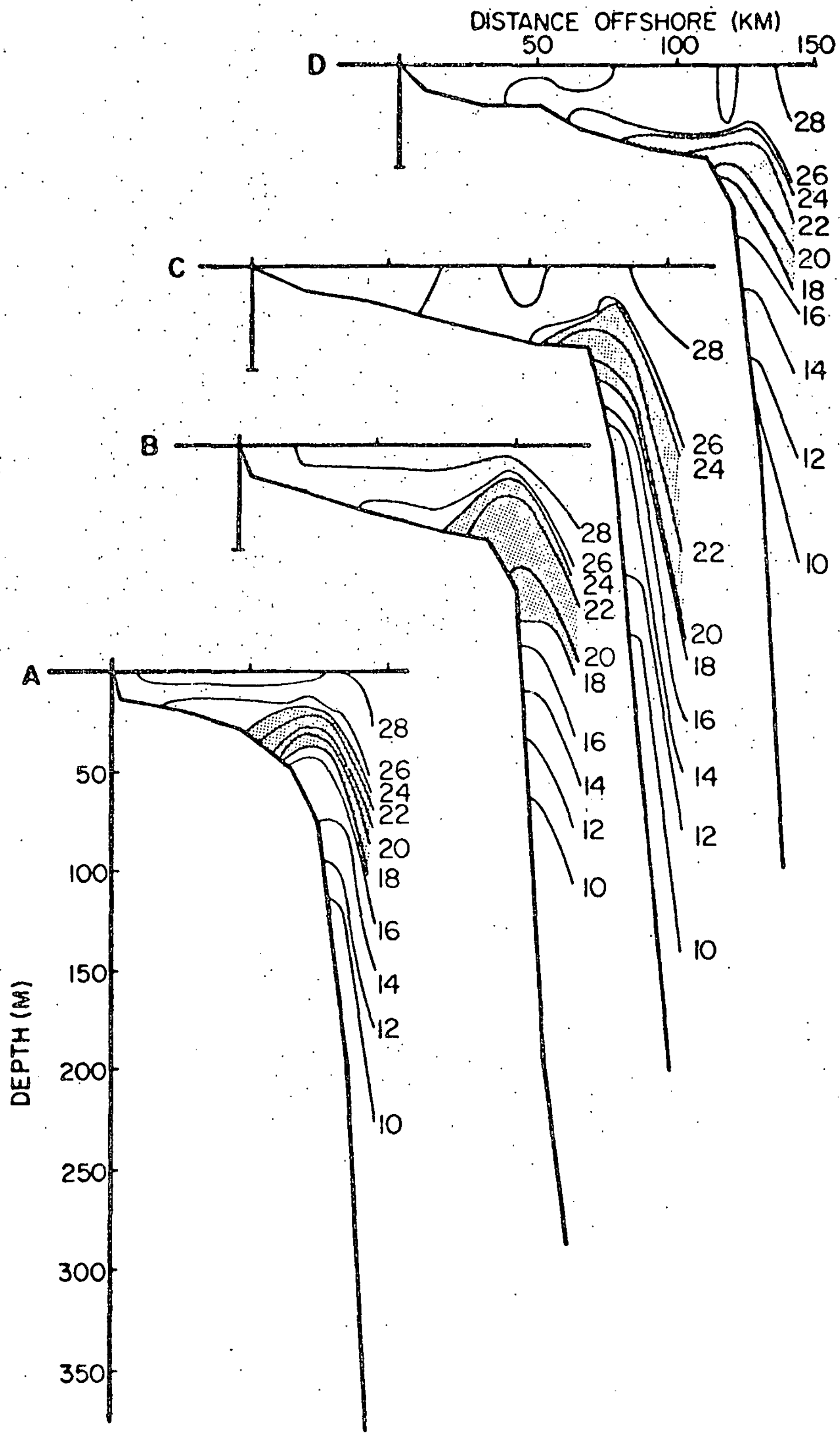

Fig 4. Blanton et al.

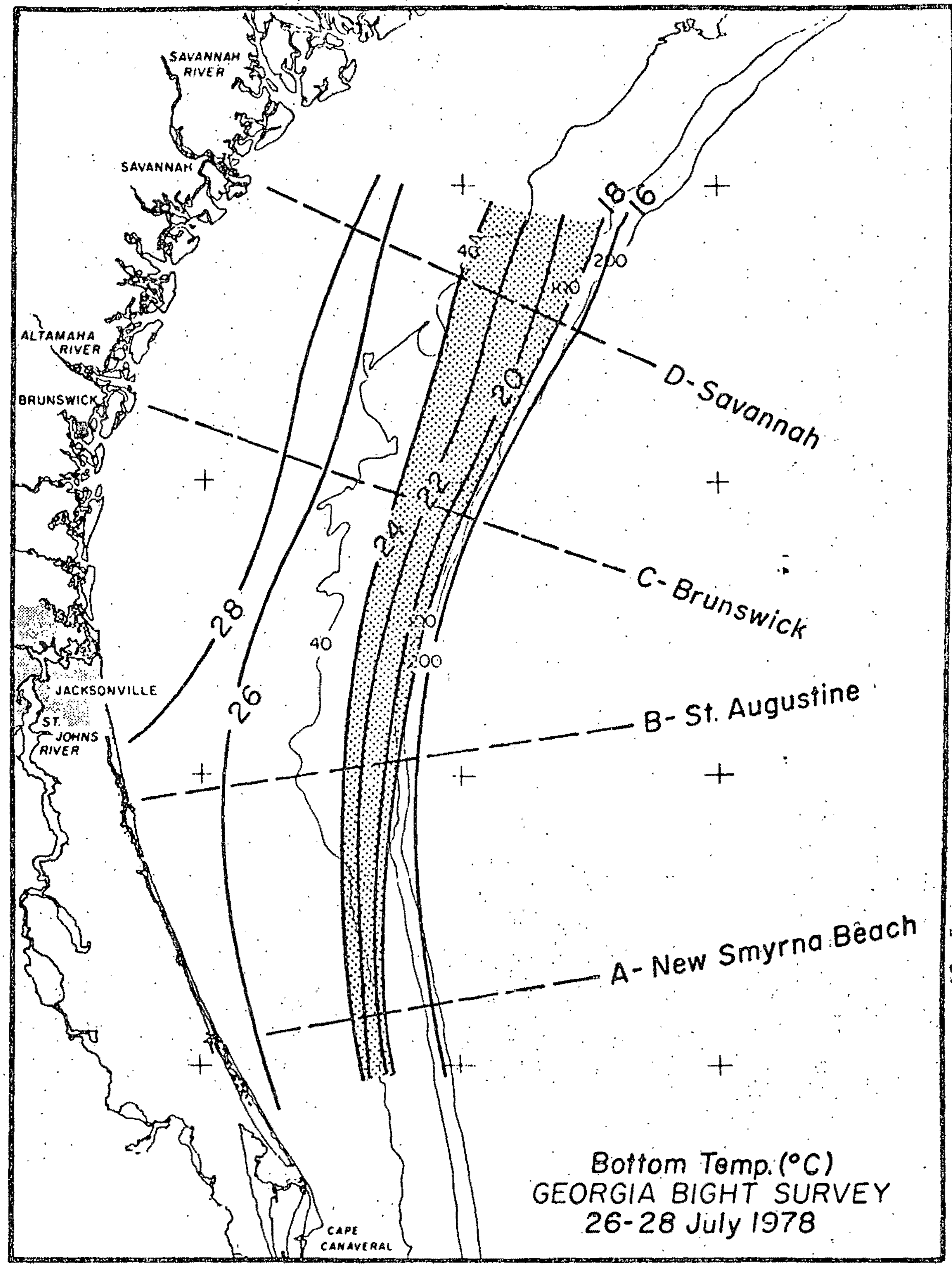

FIG. 5 Blanton et al.

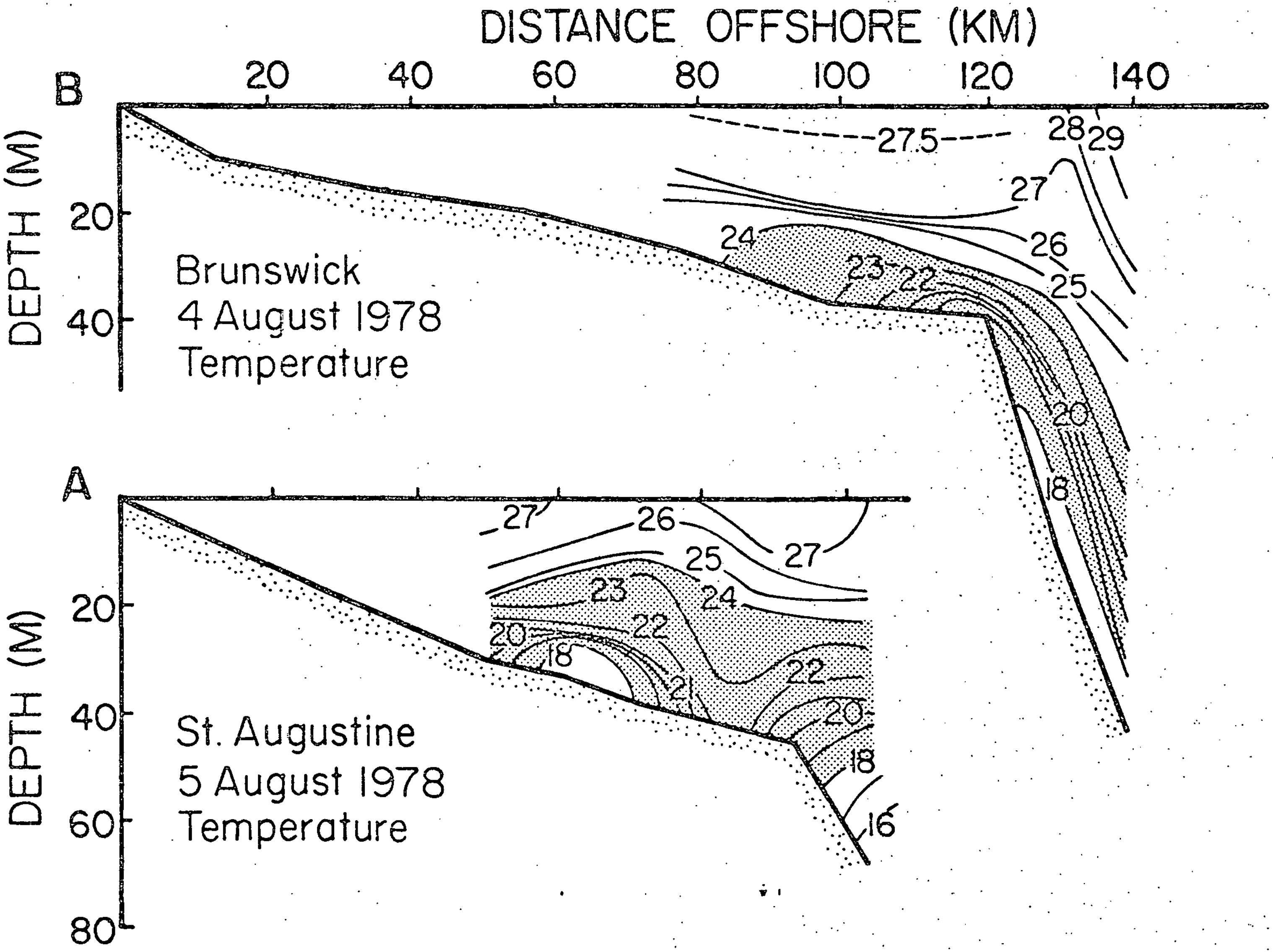

Fig. 4

Fig. 6 Blanton et al.

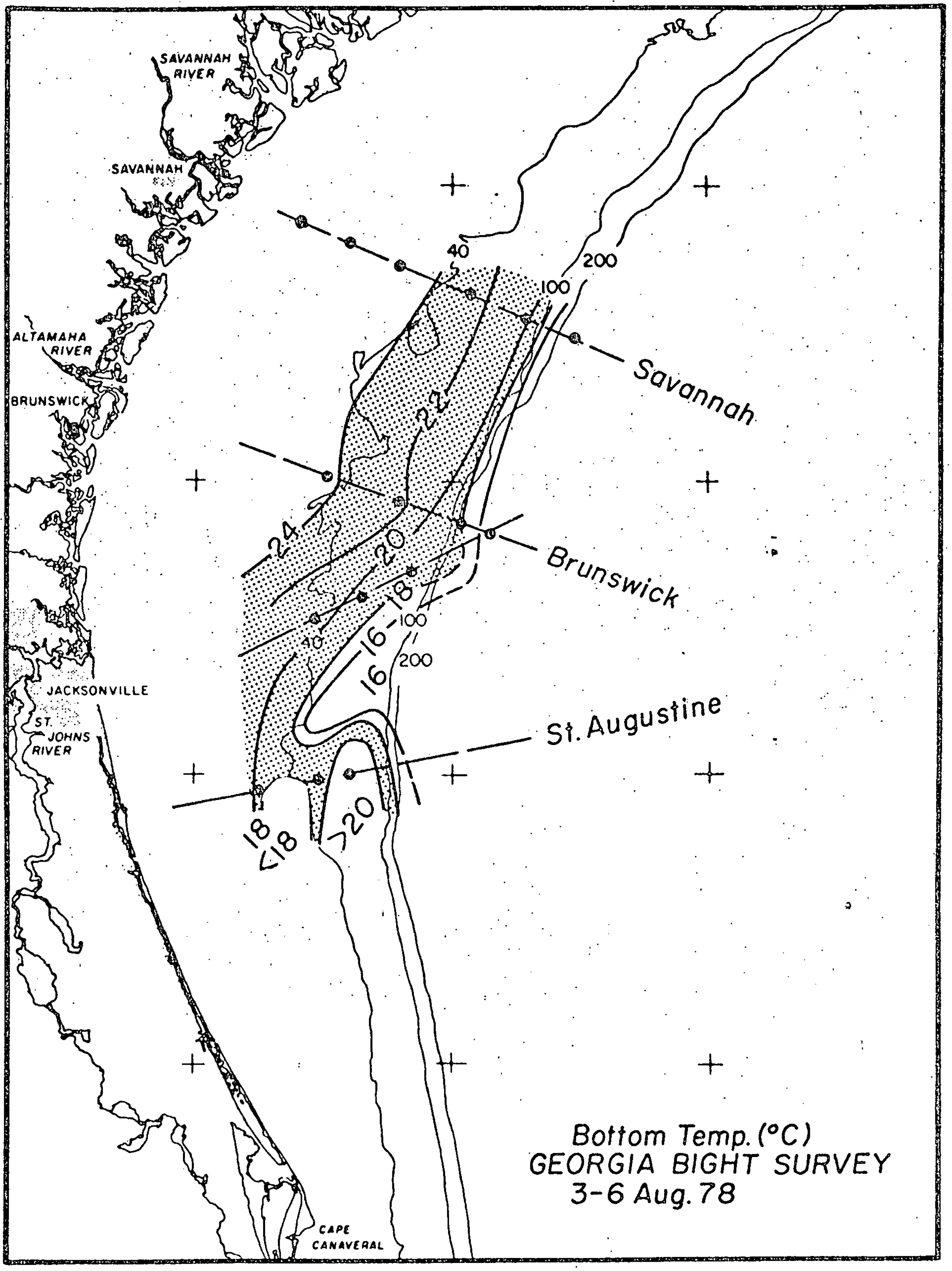

Fig. 7 Blanton et. al.

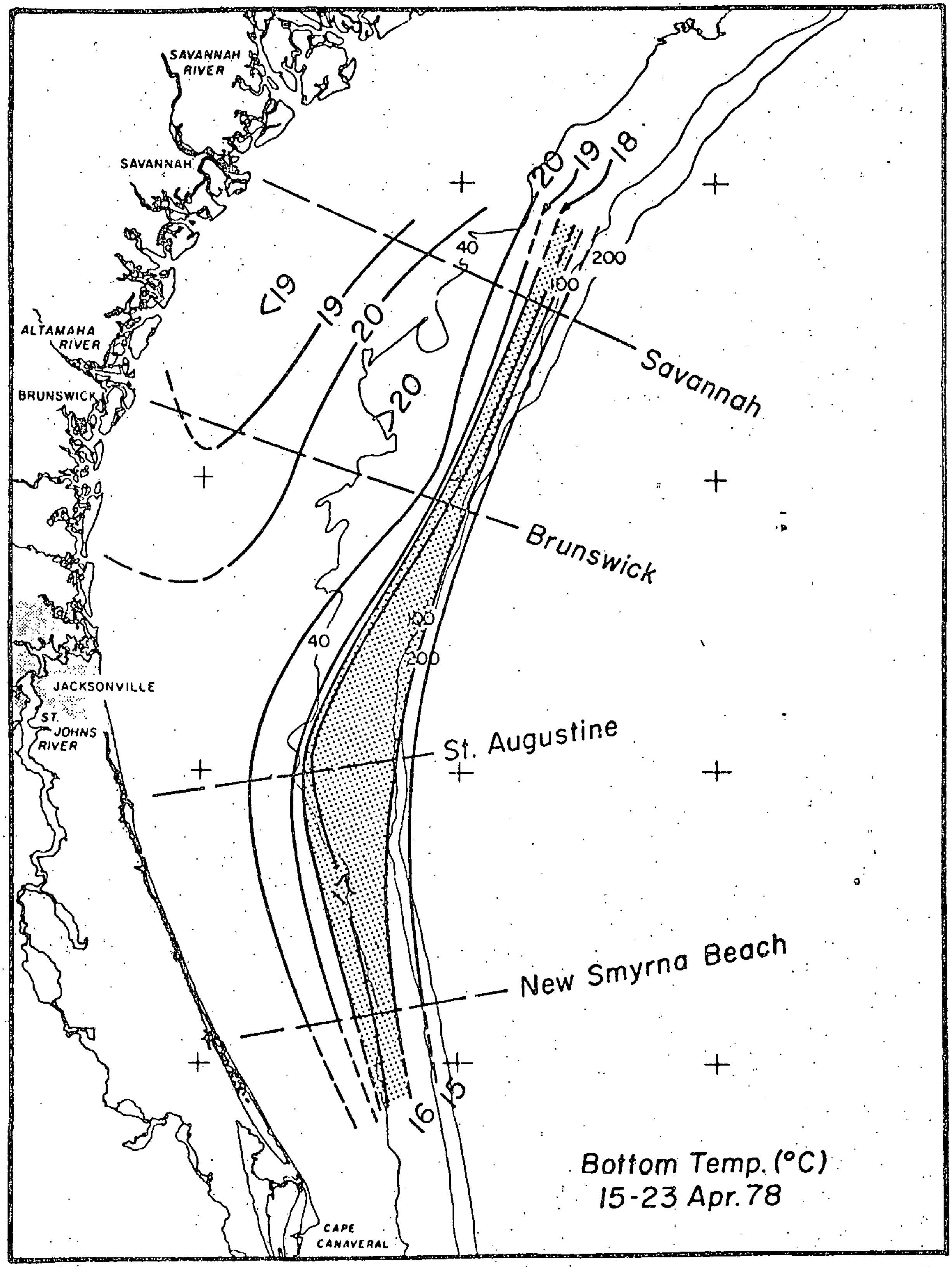

Fig. 8A. Blanton et al.

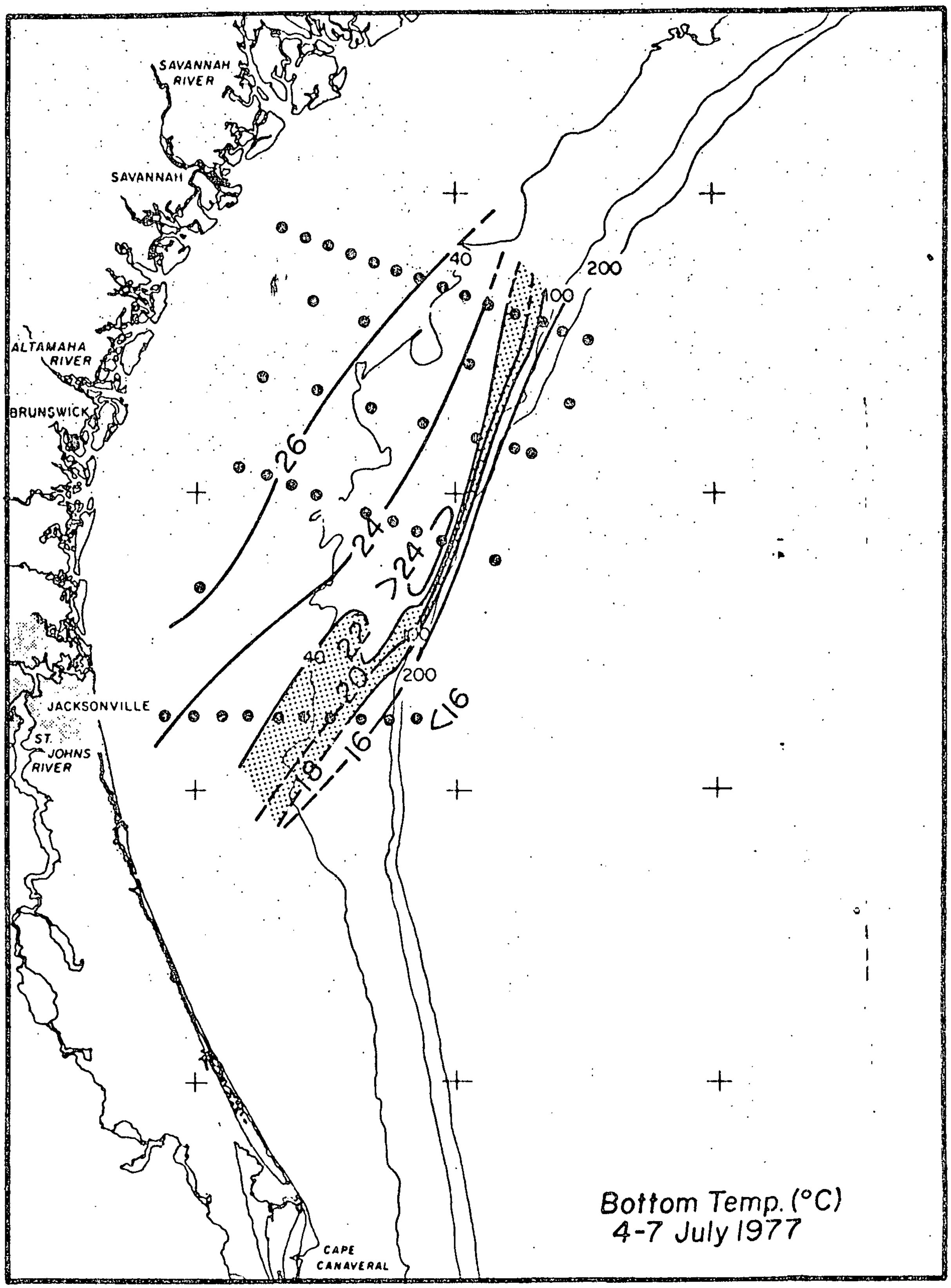

Fig. 8B. Blanton et al.

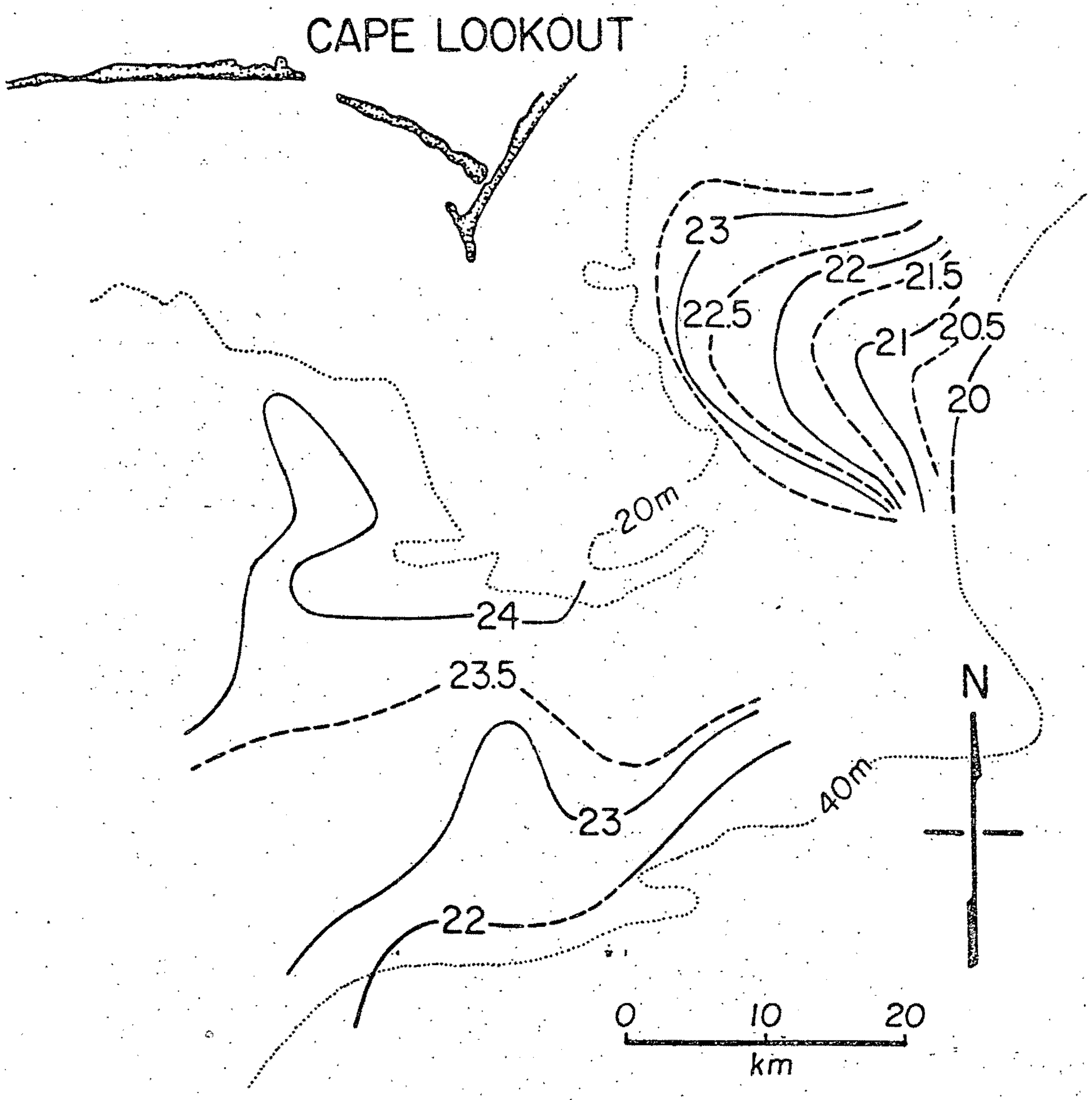

Fig. 9. Blanton et al.

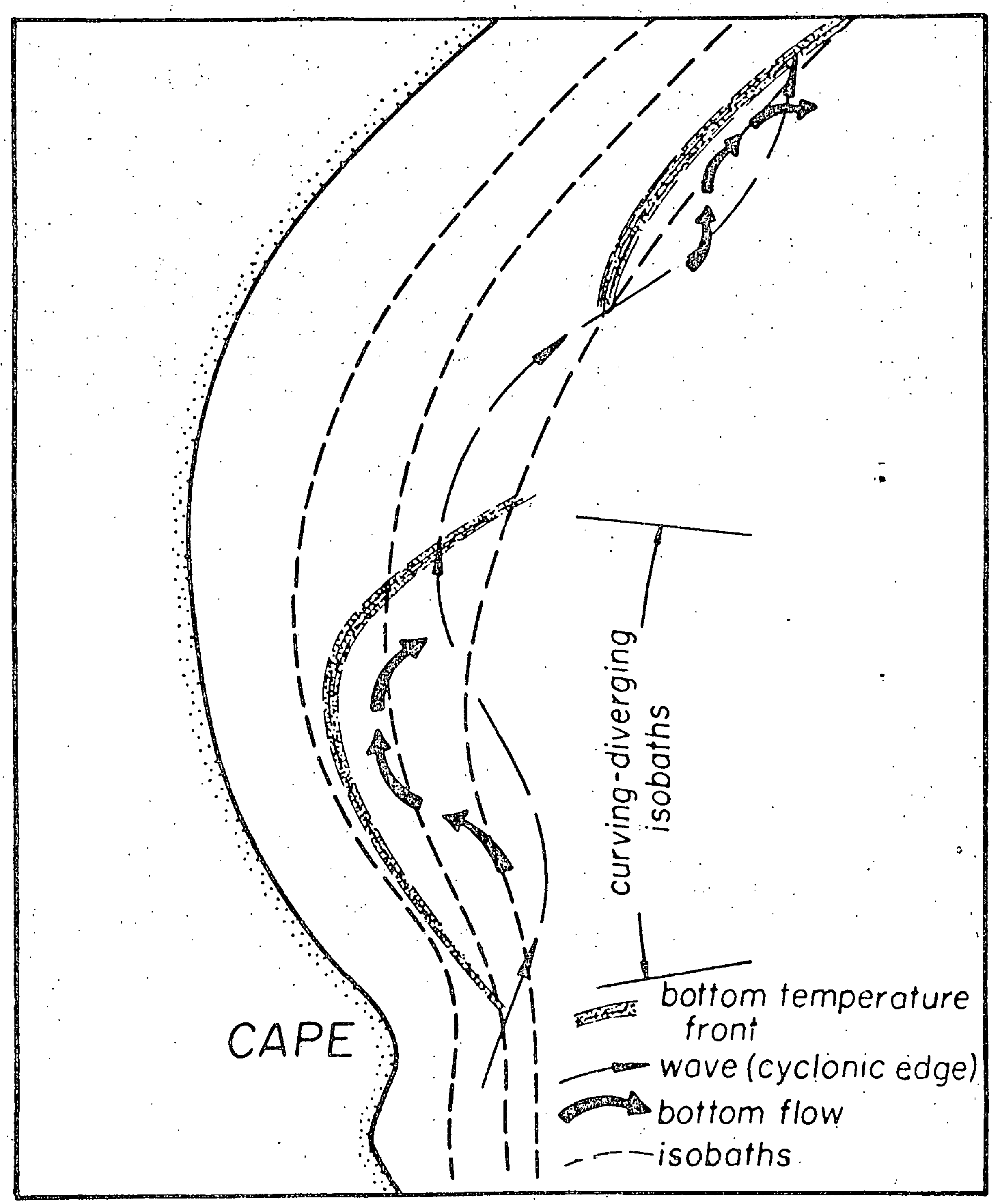

Fig. 10. Blanton et al.

7 August 1980

DETAILED OBSERVATIONS OF A GULF STREAM FRONTAL EDDY ON THE GEORGIA CONTINENTAL SHELF, APRIL 1977

Thomas N. Lee*, Larry P. Atkinson† and Richard Legeckis∇

Dedicated to Walter O. Düing; he has gone, but his spirit lives.

Abstract. Satellite, hydrographic and moored current meter data are used to show the effect of Gulf Stream frontal disturbances on low frequency current and temperature variability, water exchange and nutrient flux in the outer region of the Georgia shelf. Perturbations of the Gulf Stream cyclonic front are commonly observed as folded wave patterns in routine satellite-derived analyses of the Gulf Stream western boundary between Cape Hatteras and Miami. Those disturbances consist of southward-flowing warm filaments or of streamers near surface Gulf Stream water, 15-20 m deep, which can extend 35 to 40 km over the outer shelf around a cold upwelled core. Downstream dimensions of the warm filaments reach 100 to 200 km in the region from Jupiter, Florida, to Charleston, South Carolina, 10 to 50 km south of Jupiter, and 200 to 300 km between Charleston and Cape Hatteras. These features are defined as cyclonic, cold-core frontal eddies due to their flow and water mass properties. They appear to form from

* University of Miami, Rosenstiel School of Marine & Atmospheric Science, 4600 Rickenbacker Causeway, Miami, Florida 33149

† Skidaway Institute of Oceanography, P.O. Box 13687, Savannah, Georgia 31406

∇ National Environmental Satellite Services S33, National Oceanic and Atmospheric Administration, Washington, DC 20233

amplified waves in the Gulf Stream cyclonic front on an annual average of one every two weeks, but with considerable monthly variability. They can exist up to three weeks and travel to the north with the same phase speed as the waves, approximately 40 cm/sec.

The cyclonic circulation in frontal eddies provides a means for rapid shelf/Gulf Stream water exchange. They appear to control the residence time of the outer shelf waters, which is defined as the mean separation time between eddy events, or approximately two weeks. Upwelling in the cold core was observed to extend into the euphotic zone (45 m depth) and shoreward (35 to 40 km) beneath the southward flowing warm filament in a bottom intrusion layer 20 m thick. The annual nitrogen input to the shelf waters by this process is estimated as 55,000 tons/year, which is about a factor of two greater than all other estimated nitrogen sources combined, and can support an annual carbon production by phytoplankton of 32 to 64 gCm^{-2} yr^{-1} with no nitrogen recycling.

INTRODUCTION

Satellite-derived sea surface temperature (SST) data products routinely distributed by the National Oceanic and Atmospheric Administration (NOAA-NESS, 1974) and the U. S. Naval Oceanographic Office (NAVOCEANO, 1975) consistently reveal folded-wave patterns in the western boundary of the Gulf Stream from Cape Canaveral to Cape Hatteras. These features have been investigated in the Florida Straits and termed "spin-off eddies" due to their cyclonic rotation, cold core and exchange of heat and salt with adjacent shelf waters (LEE, 1975; LEE and MAYER, 1977). That terminology is discontinued in favor of a more general definition of the features as "frontal eddies".

Edge-eddies of this type appear in the surface waters as warm, southward-oriented, tongue-like extrusions of the Gulf Stream coupled to cold, upwelled cores. They were first measured as a succession of overlapping thermal segments termed "shingles" in the pioneering mapping of the Gulf Stream cyclonic front off the southeast U. S. by VON ARX, BUMPUS and RICHARDSON (1955). In the Florida Straits vortex diameters were found to be on the order of 10-30 km with downstream axes two to three times larger than the cross-stream (LEE, 1975; LEE and MAYER, 1977). They were observed to travel northward along the shelfbreak at speeds less than the mean speed of the Gulf Stream. They occurred on the average of one per week in the Florida Straits and resulted in large amplitude, subtidal, cyclonic flow reversals over the shelf that distorted the temperature and salinity fields to a depth of approximately 200 m (LEE, 1975; LEE and MAYER, 1977). The classification of these features as eddies stems from current meter observations of the cyclonic flow reversals produced by the passage of the warm filaments that appear to be geostrophically coupled to the cold uplifted cores. However, these features may never become completely detached vortices characteristic of the more common eddy types, such as warm and cold core rings. The shingle shapes of frontal eddies are more similar to "roll vortices", which are produced by wave-like rolling up of a shear zone (ROUSE, 1963); or "wake vortices" which are formed in the wake of islands as Karman vortex streets (WILLE, 1960). LEE (1975) was able to reproduce the observed cyclonic flow reversals and accurately predict eddy spatial dimensions and circulation using a kinematic, diagnostic model, which combined the effects of a moving vortex with a uniform background current. Sailing captains were probably the first to be aware of the transient southward flow generated on the shoreward side of the Gulf Stream by these events. STOMMEL (1965) reports that in 1590 a sailing vessel bound from Florida to Virginia had to stand far out to sea to avoid "eddy currents setting to the south and southwest" (KOHL, 1868).

Satellite thermal imagery indicates that frontal eddies evolve from growing wave-like meanders of the Gulf Stream cyclonic front (DE RYCKE and RAO, 1973; LEGECKIS, 1975; STUMPF and RAO, 1975). Thus an instability process may be involved, due either to the vertical shear (baroclinic instability) or horizontal shear (barotropic instability) across the front (ORLANSKI, 1969; ORLANSKI and COX, 1973; NIILER and MYSAK, 1971). It has been suggested that atmospheric forcing can trigger a disturbance in the front that travels northward with the Stream as an unstable wave, eventually evolving into a cyclonic edge-eddy (LEE and MAYER, 1977; DÜING, MOOERS and LEE, 1977; LEE and BROOKS, 1979). Eddies can form within a week of meander generation and then persist for another one to two weeks (LEE and MAYER, 1977; LEGECKIS, 1979). They appear to be forming all along the Gulf Stream boundary at any time of year, and may at times serve to dissipate kinetic energy from the mean flow (LEE, 1975). They also serve as an effective mechanism for exchange of shelf and Gulf Stream waters.

Frontal eddies appear to grow to larger dimensions north of Jupiter, Florida, where the shelf begins to widen. The size increase occurs primarily in the downstream direction, resulting in elongated tongues of warm Gulf Stream water 100 to 200 km in length. A second elongation is observed north of the "Charleston bump", a topographic anomaly of the slope extending seaward into the Stream, where downstream dimensions can reach up to 300 km (LEGECKIS, 1979). The Gulf Stream is observed to have a quasi-persistent eastward displacement downstream of the "bump", which is believed to be the cause of the enhanced meanders and eddies between the "bump" and Cape Hatteras (PIETRAFESA, ATKINSON and BLANTON, 1978; BROOKS and BANE, 1978; BANE and BROOKS, 1979; LEGECKIS, 1979). LEGECKIS (1979) classified the wave-like features of the Gulf Stream surface front between Charleston and Cape Hatteras into five types. The type V pattern had large amplitude east-west displacements accompanied by the warm filament structure, suggestive of eddy development. BROOKS and BANE (1980) used current meter data and satellite imagery from the outer shelf area off Onslow Bay to show that the type V filament structure was associated with cyclonic subsurface current reversals similar to that found in the Florida Straits (LEE and MAYER, 1977) and off the Georgia Shelf (LEE and BROOKS, 1979). East of Cape Hatteras, Gulf Stream meanders are no longer restricted by a shallow shelf as along the southeast U. S. coast and the well-known warm and cold core "rings" develop north and south of the Stream, respectively (SAUNDERS, 1971; THOMPSON and GOTTHARDT, 1971; GOTTHARDT, 1973; FUGLISTER, 1972, BARRETT, 1971; PARKER, 1971).

OBSERVATIONAL METHODS

Current meter, wind, hydrographic and satellite SST data were obtained for the Georgia shelf and bordering Gulf Stream regions during April 1977 as part of a Department of Energy supported interdisciplinary study of the physical, chemical and biological processes affecting the southeast U. S. continental shelf. Current and temperature measurements were taken every 20 minutes with Aanderaa current meters located 17 m below the surface and 3 m above the bottom in a 7-element box array of subsurface, taut-wire moorings (Fig. 1). The array was initially deployed for four months from

December 7, 1976, to April 11, 1977 ("Winter 76/77"), and then expanded to 9 moorings and redeployed for a 4 month period from June 30, 1977, to November 5, 1978 ("Summer 77"). Between box array deployments a 2-element array (moorings E and F) was installed for a 2.5 month period from April 11, 1977, to June 30, 1977 ("Spring 77"). Information regarding these mooring deployments is given in Table 1. Wind speed and direction time series were constructed from 6-hourly estimates made for the center of the box array. These estimates were produced (PARTAGAS, 1978) by determining the surface wind from the isobaric configuration shown in surface weather charts prepared by the National Hurricane Center, Miami, Florida, and utilizing wind observations from coastal stations, weather buoys and ships. Effects of friction on the wind speed and direction estimates were also taken into account. Hourly values of sea level height were obtained from the National Ocean Survey, NOAA, Rockville, Maryland. Low frequency (subtidal) time series of all data sets were generated by smoothing the original data with a 40-hour low-pass Lanczos filter kernal to remove variance associated with tidal and inertial fluctuations. Diurnal tides are attenuated by more than 10^5 by the filtering operation, which results in a 4-day truncation at both the start and end of the time series. The filtered data were subsampled every 6 hours and current and wind vectors rotated clockwise 30 degrees into a "normal" coordinate system in which the off-diagonal of the Reynolds stress is near zero (FOFONOFF, 1969). The rotated vectors were converted to cross-shelf (u+ at 120°T) and along-shelf (v+ at 30°T) components. The orientation of the along-shelf component agrees with the alignment of local isobaths to within 5% or 18 degrees at all current meters and should therefore be the primary axis for low frequency flow.

Hydrographic sections were made at the cross-shelf current meter locations and at additional sections to the south on each mooring exchange cruise. Transect identifications are presented in Table 2. Salinity and temperature were determined with a Plessey 9400 CTD interfaced to a Hewlett-Packard 9825 desk-top computer and Kennedy incremental recorder. Additional temperature profiles were obtained with an expendable bathythermograph system. Water samples were taken at selected depths with Niskin bottles mounted on a rosette sampler coupled to the CTD. Continuous measurements of surface temperature and salinity were made underway with a Bissett-Berman 6600 T thermosalinograph. Phosphate, silicate and oxygen were determined according to STRICKLAND and PARSONS (1965) and nitrate according to GARDNER, WYNNE and DUNSTAN (1976). The complete hydrographic data set and discussion of methods can be found in O'MALLEY, ATKINSON, SINGER, CHANDLER and LEE (1978).

Sea surface temperatures (SST) were measured by a Very High Resolution Radiometer (VHRR) on a polar orbiting satellite (NOAA-5) operated by NOAA. The scanning radiometer measures thermal infrared (IR) radiation emitted by the earth and atmosphere in the 10.5 to 12.5 μm band and visible radiation reflected in the 0.6 - 0.7 μm spectral band. The VHRR is capable of resolving SST changes of 0.5 C with a spatial resolution of 1 km at nadar. The satellite data are available over the Gulf Stream twice daily at 0200 and 1400 GMT. According to BRAUN (1971) clouds can completely obscure the SST features associated with the current while atmospheric water vapor degrades the SST gradients observed under cloud-free conditions. Observations of the Gulf Stream are also limited by the seasonal disappearance of recognizable SST gradients during the warmer months of the year (usually June through October for the Gulf Stream south of Cape Hatteras). Although atmospheric moisture limits the accuracy of satellite derived temperature measurements, the position of the western SST boundary can be established accurately in cloud free areas. This is accomplished by geometrically correcting the VHRR data as described by LEGECKIS and PRITCHARD (1976), and projecting the IR images on a bathymetry map (UCHUPI, 1968). The Gulf Stream boundary can be located within an uncertainty of 5 km provided landmarks are recognizable in the images. Between April 7 and 17, 1977, nearly 20 IR observations of the Gulf Stream were made during unusually cloud free conditions. This allowed the evolution of two frontal eddies to be described in a time series of satellite derived SST.

RESULTS

Synoptic Observations

A shipboard telefax system was used on the mooring exchange cruise of April 1977 to receive satellite SST images from the NOAA-NESS field station in Miami, Florida. With the use of this information and high speed shipboard mapping of the Gulf Stream cyclonic surface front, a shingle feature (eddy F) was located and mapped on two successive occasions between April 12 and 16 (Figs. 2 and 3). Each mapping took approximately 1.5 days including hydrographic sections made through the event. Hydrographic transects were also made before and after the mapping period (Table 2).

The disturbance was first mapped on April 13 and 14 (Fig. 2). It appeared as an elongated tongue of warm (22-23 C) Gulf Stream water extruding out of the front and over the shelf toward the south around a cold core (21 C). At this time it was about 160 km long and 40 km wide. When next observed about 1.5 days later (Fig. 3) it was almost 220 km long and 70 km wide and maximum temperature in the warm tongue had increased to 24 C. This rapid growth appeared to occur by extension of the northern portion of the structure along the front, perhaps due to the strong horizontal shear across the Gulf Stream boundary. The cool core of 21 C water had also doubled in size. The center of the cool core was advected to the north at a speed of about 30 cm/sec.

A satellite VHRR-IR image taken on April 16, 1977, at 0200 GMT (orbit 3223 NOAA-5) clearly displays this feature and its Gulf Stream roots (Fig. 4). The warmest water is represented by the darkest tones of gray. Both the western and eastern frontal boundaries of the Gulf Stream are clearly defined. The SST data were averaged in 2 km squares in the box outlined in Fig. 4 and are displayed as alpha-numeric characters at intervals of about one degree Celsius in Fig. 5. The contours are used to separate areas of similar temperature. Comparison of the temperatures in Fig. 5 with those obtained on the hydrographic survey on April 14-16 (Fig. 3) shows that the coldest water detected in the core of the feature measured 21 C (ship) and 20.1 ± 0.5 C (VHRR). The warmest Gulf Stream water adjacent to this cold core was 25 C (ship) and 23.6 ± 0.5 C (VHRR). This shows that the satellite measurements were about 1 to 2 C lower than the ship measurements. Estimates of the atmospheric water vapor correction to the IR temperatures are not available, but this comparison implies that the atmosphere was relatively dry. The cross-stream SST differences in the vicinity of eddy F are 4 C (ship) and 3 to 4 C (satellite). This indicates that the SST gradients are represented in Fig. 4 within an uncertainty of 1 C. A quantitative intercomparison of shipboard and satellite-derived SST in this event (BROWN and EVANS, 1979) found a mean square difference of 1.2 C between several thousand observation pairs, with the shipboard measurements being higher. The difference between the standard deviations computed from the two data sources was only 0.1 C. The general position, size and shape of the disturbance as plotted from shipboard SST data (Fig. 3) are also in close agreement with that shown by the satellite IR image. The length and width estimated from the dark filament shown in the satellite image (Fig. 4) are 230 and 70 km, respectively, which are within about 4% of the shipboard estimates and indicate that the observed spatial growth did not seriously affect the ship-derived estimates.

A composite of hydrographic sections made across eddy F from 1900 GMT on April 14 to 1400 on April 16 are shown in Figs. 6 and 7. The northern-most section off Savannah on April 16 was made from east to west across moorings E and F just north of the event (Fig. 3). The steeply sloping 24 and 25 C isotherms identify the western boundary (cold wall) of the Gulf Stream front (Figs. 3 and 4) in a layer about 20 m deep. The westward deepening isopycnals suggest southward flow within the warm tongue and throughout the water column over the outer shelf, which is in approximate The sections made across the disturbance south of the Savannah transect show the warm surface filament of 22 to 24 C water extruding from the Gulf Stream front (Figs. 3 and 4) to extend to a depth of about 20 m. The westward deepening isopycnals suggest southward flow within the warm tongue and throughout the water column over the outer shelf, which is in approximate geostrophic balance with the uplifted cold core. Northward flow is indicated east of the cold core. Ship drifts measured during the hydrographic stations support the indicated flow directions. Southward flow of about 50 cm/sec was estimated from ship drifts at stations within the warm filament and northward flows greater than 100 cm/sec were observed for stations east of the cold core. Strong upwelling of deeper Gulf Stream waters occurred within the cold core and extended shoreward beneath the warm surface tongue. The Gulf Stream source of the upwelled waters is indicated by the low temperatures, salinities and oxygen values and high nutrient concentrations. Near the bottom (63 m) at the shelfbreak (68 m) in the St. Augustine South section, temperature was 12.5 C, salinity 35.6 $^o/oo$, σ_t 26.97, dissolved oxygen 3.12 mℓ ℓ^{-1} and nitrate 20.5 μ mole ℓ^{-1}. Similar values could not be found even at a depth of 185 m in the Savannah section made north of the event. Historical data from sections taken in the same region but without evidence of eddy structure indicate that water with these characteristics comes from a depth of approximately 200 to 300 m. This suggests that the near-bottom waters found along the shelfbreak in eddy F could have been upwelled a vertical distance of 140 to 240 m. Thus subsurface Gulf Stream intrusions of this type provide a source of nutrients to the outer shelf euphotic zone. The Ormond transect appears to have been near the southern extremity of the disturbance, as indicated by the horizontal temperature and density distributions (Figs. 3, 8 and 9). The lack of doming in the temperature and density sections suggests that the flow has returned to a northerly direction. Also there does not appear to be any significant upwelling in the vertical section data (Figs. 6 and 7) judging from the high salinity and oxygen values and low nutrient concentrations.

Cyclonic circulation in eddy F is indicated by the horizontal distribution of temperature at the surface, 16 and 30 m (Figs. 3 and 8) and the subsurface topography of the 26 σ_t surface (Fig. 9). Southward flow appears to occur in the warm filament and northward flow in the Gulf Stream east of the cold core. There also appears to be a convergence zone at the southern extremity of the feature and along the Gulf Stream boundary. This zone can be formed by the convergence of southerly flow in the warm filament with the northward flow of the Gulf Stream south of the disturbance which forces a flow toward the east that merges with Gulf Stream and strengthens the front. A similar feature has been observed in the Florida Straits (LEE, 1975; LEE and MAYER, 1977).

Temporal Observations

Nearly 20 IR observations of the western SST boundary of the Gulf Stream were made between Florida and Cape Hatteras from April 7 to 17, 1977. The northward propagation of two frontal eddies was observed through the region of the current meter array during this period (Figs. 10 and 11). The first event, eddy E, traveled through the area between April 8 and 15 at a rate of approximately 47 cm/sec (Fig. 10). It passed the current meter locations on the 10th and 11th, which unfortunately is when the box array was being removed and moorings E and F redeployed. However, current meter data were obtained during a small portion of the disturbance on April 12. The second event, eddy F, was observed to move northward through moorings E and F around April 16 and 17 (Fig. 11) at a speed of about 42 cm/sec.

Time series of low frequency (subtidal) current, wind and temperature for the "Spring 77" observation period are shown in Figs. 12 and 13. Eddy F is clearly identified in the first week of data from all current meters as a cyclonic flow reversal coupled to a decrease in temperature (Figs. 12 and 13, event #1). Data from these instruments were expanded in time over the period from April 12 to 23 in order to highlight the event. Hourly vectors from 3-hour low-pass filtered time series were used (Fig. 14) because the 4-day truncation of the beginning of the subtidal records overlapped with the start of eddy F and had completely cut off eddy E.

The cyclonic current reversal from southerly to northerly flow on April 12 indicates the passage of the southern portion of eddy E. Satellite IR images showed the warm filament to be passing the current meters at this time. Southerly flow in the warm filament was also indicated in hydrographic sections (not shown) taken at St. Simons on April 10 and at Savannah on April 11 (Table 2) by doming isotherms and isopycnals east of the filament. These section data further showed a significant increase in nutrient concentrations in the near bottom waters of the outer shelf within this event.

Eddy F first influenced currents at the mooring locations near the start of April 15, as seen by the low frequency cyclonic rotation superimposed on the semi-diurnal tidal variations (Fig. 14). The reversal occurred at mooring F about one day prior to mooring E. Current meter FT worked for only about 1.5 days at the start of the event. The passage of eddy F produced a coherent, in phase cyclonic current rotation in the upper and lower current meters at both the 45 and 75 m locations (Figs. 12, 13 and 14). Large temperature decreases were observed to occur almost simultaneously with the flow reversals (Fig. 13). Local winds were weak and toward the north during the period of southward flow and appear to be unrelated to the flow reversal. Strongest southward currents were recorded at current meter ET, where speeds reached 60 cm/sec (Fig. 14). The weakest southward currents of about 15 cm/sec were measured at EB. The mean vertical shear over the 55 m instrument separation was about 3.6×10^{-3} sec^{-1} during the period of southward flow. The temperature drop was largest near the bottom at the shelfbreak (EB), where temperature declined about 5 C during onshore flow which reached a speed 9 cm/sec. The temperature decrease and onshore flow near the bottom at the 45 m isobath (FB) were also about 5 C and 9 cm/sec respectively. In the upper layer at the shelfbreak (ET), temperature dropped by about 2.5 C during onshore flow which reached speeds of 7 cm/sec. The occurrence of 18 C water at the 45 m isobath appeared to lag that at the shelfbreak by about 2.5 days. This suggests an onshore advection velocity of approximately 8 cm/sec in the lower layer between the 17 km mooring separation, which agrees well with the observed flow. Temperature and salinity sections taken through the filament (Figs. 6 and 7) also indicate that these large temperature decreases were produced by advection of newly upwelled Gulf Stream water past the moorings in a bottom layer approximately 20 m thick.

The end of eddy F occurred toward the beginning of April 21 when current vectors revolved back toward the north, thus completing a cyclonic rotation. Near-bottom temperature at the shelfbreak increased to nearly the pre-eddy values, during offshore flow of about 10 cm/sec, signaling the end of the event. The total time for the disturbance to pass the mooring (eddy duration) was approximately 7 days, from April 15 to 21. The most probable path of eddy F past the moorings is approximated by the dotted line from mooring E in Fig. 8a. This path was estimated by comparing the contoured temperature field at the depth of current meter ET to measured temperature at ET during the passage of the event (Fig. 13, event 1). The arrows are estimated current directions necessary to produce the observed cyclonic flow reversal. The length of the filament, determined from an average of shipboard and satellite SST estimates (Figs. 3 and 4) was about 225 km. The northward phase speed computed from the eddy length and duration is 37 cm/sec, which is close to the 42 cm/sec speed previously determined from time series of satellite IR images (Fig. 11). Either this agreement from the two completely separate data sources is extremely fortuitous or the eddy length must have remained relatively constant during the passage of the event by the moorings, suggesting that eddy growth had stabilized at this time.

Weekly averaged SST maps of the Gulf Stream produced by the U. S. Naval Oceanographic Office (NAVOCEANO, 1975) reveal an unusually large warm filament on the Georgia shelf during the weeks of May 12-18, 1977, and May 19-25, 1977 (Figs. 15a and b). The spatial dimensions estimated from these maps were 185 x 80 km during the first week and 240 x 110 km in the second week, which indicate that the width of the disturbance was almost the same size as the width of the Gulf Stream at this location and time. The current meter records show the effect of this feature from about May 20 through May 26, giving a duration of approximately 7 days (Figs. 12 and 13, event 6). Assuming the filament length of 240 km remains relatively unchanged over the duration gives a rough estimate of its northward phase speed of 40 cm/sec. The disturbance appeared to occur at the 75 m and 45 m isobaths almost simultaneously and produced a cyclonic current reversal in the upper layer at the shelfbreak of + 100 cm/sec to -60 cm/sec in about one day. A temperature drop of 7 C occurred in the bottom layer at the shelfbreak during the period of onshore flow, which reached speeds of -20 cm/sec in the lower layer and -30 cm/sec in the upper layer.

Low Frequency Variability

Subtidal current, wind and coastal sea level time series from the "Winter 76/77" and "Summer 77" periods are shown in Figs. 16 and 17. At the shelfbreak (75 m isobath) current amplitudes in the upper layer ranged from ± 40 to ± 80 cm/sec about a mean northward flow of 65 cm/sec in the winter (Fig. 16) and 55 cm/sec in the summer (Fig. 17). These energetic fluctuations produced broad-banded spectral peaks (not shown) at periods of 2.5, 3.5, 5 and 10 days that were coherent between the cross-shelf (u) and along-shelf (v) components, with the cross-shelf leading by 90° in phase, suggestive of propagating wave motion. Downstream current meter pairs of the winter experiment revealed northward propagation that was coherent over the greatest along-shelf array separation of 40 km at periods of 3.5 and 10 days in the upper layer and 10 days in the lower layer. During the summer coherent northward propagation of velocity and temperature fluctuations was found over the 90 km along-shelf spacing at periods of 5 to 12 days in the upper layer. Southward propagation was observed during the winter in the lower layer at periods of 9 to 12 days and during the summer in both upper and lower layers at periods of 2 to 3 days. Temperature fluctuations with amplitudes ranging from ± 2 to ± 4 C occurred throughout the year and were significantly coupled to the velocity variations (Fig. 13). Largest temperature changes occurred in the lower layer. Current and temperature fluctuations were coherent over the 55 m vertical instrument separation at periods of 3.5, 5 and 10 days during the winter and at periods of 2 to 2.5 days only during the summer. Significant coherence was also found during the winter between along-shelf current fluctuations and the local cross-shelf wind at the 4 and 10 day periods in the upper layer and at periods near 2.5 days near the bottom. Along-shelf winds and currents were only coherent for 10 day period fluctuations near the bottom. Bottom temperature was highly coherent with the cross-shelf wind at the 3 and 5 day periods and significantly coherent with the along-shelf wind at 5 and 10 day periods. No significant coherence was found between currents at the shelfbreak and coastal sea level.

Low frequency heat and momentum fluxes at the shelfbreak were found to be selectively grouped in the frequency bands of the more energetic motions. Largest values were usually associated with fluctuations in the 5 and 10 day period bands, with the Gulf Stream giving up heat and momentum to the shelf waters in the upper layer and the lower layer normally indicating an offshore heat flux. The offshore heat flux is believed to be produced by the coupling of lower layer onshore flow events to cold anomalies (Fig. 13), which results in a positive $\overline{u'T'}$. The seasonal average momentum flux was found to be onshore in the upper layer during both winter and summer at about -70 and -40 cm^2 sec^{-2} respectively. The seasonal average heat flux in the upper layer was onshore at about -4 C cm sec^{-1} in the winter and -2 in the summer. In the lower layer the heat flux was offshore at about +0.5 in the winter and +2 in the summer. The negative momentum flux indicates that the shelfbreak strip off Georgia is a region of energy dissipation associated with the transfer of energy from the mean Gulf Stream current to the fluctuations. A significant portion of the energy transfer appears to be occurring with fluctuations having periods in the 5 to 10 day period band. On the continental slope off Onslow Bay BROOKS and BANE (1980) recently found that the fluctuations were supplying energy to the mean flow as was found previously by WEBSTER (1961). In the near bottom water BROOKS and BANE (1980) also found an offshore heat flux of similar magnitude as found here for the Georgia shelfbreak.

At mid-shelf locations (30 m isobath) low frequency along-shelf current fluctuations were highly coherent over the 90 km array separation distance and nearly in phase for all periods >2 days during the winter with very similar results for the summer season (Figs. 16 and 17). Current variations were also coherent with coastal sea level and local wind with phase lags of 12 to 20 hours (Figs. 16 and 17). Thus at mid-shelf, subtidal currents are largely generated by the same mechanism, the local winds, by producing surface and bottom Ekman transports which cause the coastal sea level to set-up and set-down and thereby drive a barotropic along-shelf flow over the mid-shelf and inner-shelf (BEARDSLEY and BUTMAN, 1974; SCOTT and CSANADY, 1976; LEE and BROOKS, 1979). The amplitude of these current variations ranged from ± 10 to ± 40 cm/sec about a 4 month mean flow in the upper layer of 5 cm/sec toward the north in the winter and 1 cm/sec toward the north over the summer 4-month period. LEE and BROOKS (1979) found no evidence of southward-propagating continental shelf waves in the Georgia coastal sea level data as was found south of Cape Canaveral by BROOKS and MOOERS (1977). PIETRAFESA and JANOWITZ (1980) also recently reported on the lack of evidence for southward-propagating shelf waves in Onslow Bay, North Carolina. The width (120 km) and shallowness (≈90% of shelf width <50 m) of the Georgia shelf was believed to effectively isolate the inner region from propagating disturbances at the shelfbreak.

Coherence between along-shelf currents measured at mid-shelf and the shelfbreak during the winter was low except for the 9 to 12 day period range. This is also the only period band for which propagating wave motion was indicated for the mid-shelf location (u and v in coherent quadrature). The effect of Gulf Stream events appears to be more pronounced in the summer at mid-shelf than during the winter (Fig. 17). Coherence between along-shelf currents from the mid- and outer-shelf was found to be generally higher at this time. This suggests that inclined isopycnal surfaces in the summer allow Gulf Stream events to penetrate further onto the shelf than in the winter when shelf density is higher and horizontally stratified.

DISCUSSION

Eddy Signature

Frontal eddies appear to be a common feature in the Spring 77 time series (Figs. 12 and 13, events 1-10) and they can probably account for a significant portion of the low frequency variability in the outer shelf region. Ten cyclonic current reversals occurred at the shelfbreak during the 74-day recording period, or approximately one per week on the average. Each cyclonic reversal is accompanied by a large decrease in near-bottom temperature, which is the typical eddy signature in shelfbreak current and temperature records in the region from Miami to Savannah, where the Gulf Stream boundary follows the shelfbreak. A schematic characterization of a typical frontal eddy on the Georgia shelf is shown in Fig. 18. Satellite

IR images, hydrographic and current meter data indicate that southward flow occurs within the warm filament extruding out of the Gulf Stream front toward the south (Figs. 4, 6, 12, 14 and 15). Southward flow extends to the bottom in the outer shelf region and is in approximate geostrophic balance with the uplifted density structure of the cold core (Fig. 6). The vertical shear estimated from the thermal wind equation; $\frac{\partial v}{\partial z} = \frac{g}{\rho f} \frac{\partial \rho}{\partial x}$, using density ($\rho$) data from stations across the warm filament in the St. Augustine south transect (Fig. 6), is within 2% of the average shear measured at the shelfbreak during the period of southward flow. The decrease in near-bottom temperature appears to be produced by the northward advection of upwelled waters in the cold core, which extends onto the shelf beneath the warm filament (Figs. 6 and 18). Upper layer temperature signatures are not as consistent and depend on the location of the sensor relative to the depth of the warm filament and location of the cold core. The larger current data base from the Georgia shelf indicates that for the 11-month period from December 1976 through October 1977 approximately one eddy occurred every two weeks on the average (Figs. 12, 16 and 17, eddy event lines). The occurrence of these disturbances appears to be a random process, for at times several reversals may occur in succession and at other times they can be separated by several weeks. Similar eddy signatures in current meter data have recently been shown to be related to the large Gulf Stream filament structures that form off Onslow Bay (BROOKS and BANE, 1980). However, measurements from the shelfbreak region off Cape Romain (PIETRAFESA and JANOWITZ, 1979), where the Gulf Stream boundary is deflected seaward by the Charleston bump, indicate that the eddy signature in current and temperature records is more complicated than on the Georgia, Florida and North Carolina shelfs. The signature is observed to vary according to the location of the current meter relative to eddy center and propagation direction. In the lee of the Charleston bump eddy filament sizes can become larger and apparently propagated onshore across the "bump" as well as northward. Thus measurements from the shelf-break at Cape Romain sometimes show a clockwise current rotation coupled to a temperature increase apparently resulting from the onshore motion of a southward flowing filament whose cold core lies south of the mooring (PIETRAFESA and JANOWITZ, 1979).

Gulf Stream Meanders

Current and temperature time series from the Georgia outer shelf have been compared to hydrographic data from repeated sections made across the current meter locations and into the Gulf Stream in December 1976 (ATKINSON and LEE, 1980). The results of this analysis indicate that the large amplitude subtidal current and temperature fluctuations that occur along the shelfbreak with periods of 2 days to 2 weeks and without cyclonic current reversals (Figs. 12 and 13, events 11-15) are produced by northward-propagating, wave-like disturbances of the Gulf Stream cyclonic front, i.e., Gulf Stream meanders. Offshore meanders result in a decrease in northward current speeds throughout the water column and upwelling of cool, deeper Gulf Stream waters with increased nutrient concentrations in the lower layer. Onshore meanders produce downwelling and increased northward current speeds. These onshore-offshore meanders produce coherent in-phase fluctuations of velocity and temperature at periods of 2.5 to 3 and 5 to 10 days throughout the year. On many occasions offshore meanders produced velocity and temperature decreases at the shelfbreak, which appear to follow northward wind events (Figs. 12 and 13, events 12, 13 and 15), indicating that the offshore meanders and associated upwelling may at times be generated by offshore and onshore Ekman transports in the surface and bottom layers, respectively.

Eddy Formation

Time series of satellite-derived thermal images have clearly shown that edge-eddies form from growing northward propagating wave-like meanders of the Gulf Stream cyclonic front (LEGECKIS, 1975; STUMPF and RAO, 1975). The folded-wave pattern, characteristic of eddy development, has been observed to occur within two days of meander formation (STUMPF and RAO, 1975). Wave folding appears to occur from the shoreward extension of a meander producing a southward flowing warm filament of Gulf Stream water over the outer shelf (Figs. 3, 4, 15 and 18). Current meter and hydrographic observations indicate that southward currents in the warm filament associated with eddy F were in approximate geostrophic balance with the uplifted cold core.

The above results suggest the following conceptual model for the life cycle of spin-off eddies: perturbation of the Gulf Stream cyclonic front produced by either offshore surface Ekman transport associated with northward wind events or interaction of the flow with bottom features can generate an offshore meander that travels to the north as an unstable shelf wave in the upper part of the Current where the mean current speed is greater than the southward phase speed of the wave. The wave grows rapidly in time, possibly feeding upon the potential energy of the mean current (baroclinic instability) and it may eventually evolve into an elongated edge-eddy, which can act to dissipate the newly acquired kinetic energy into the shelf waters. Time sequences of satellite IR images (similar to Fig. 4) between April 7 to 17 reveal that the folded-wave patterns, which typify edge-eddy development, begin to evolve from the onshore crests of the waves as the crests shoal over the outer shelf. Once the folding process is initiated, the shallow (20-30 m) southward flowing filament of warm Gulf Stream water becomes rapidly elongated by the downstream extension of the northern Gulf Stream connection to the filament (Figs. 2 and 3). The feature literally shears apart from the Gulf Stream and becomes stranded in the outer shelf, awaiting its final dissipation over the shelf. The total cycle from growth to decay may take only 2 to 3 weeks: 2 days to one week of wave development, about one week of eddy growth and one week of dissipation. This process appears to be occurring about once every 2 weeks on the average between Miami and Cape Hatteras, with further amplification of the disturbances north of the Charleston bump.

Eddy F was observed to undergo a significant elongation in the along-shelf direction over the 2 day interval between measurements (Figs. 2 and 3). The growth appeared to occur primarily by the extension of the northern Gulf Stream source portion of the filament, possibly due to the strong horizontal shear across the Gulf Stream boundary. Thus an instability process appears to be involved in the evolution of both meanders and eddies. The exact nature of the instability is uncertain. Both barotropic and baroclinic unstable waves can develop in the Gulf Stream cyclonic front due to the intense horizontal and vertical shears there. NIILER and MYSAK (1971) theorized that the fastest growing barotropic waves would propagate to the north with wavelengths of about 150 km and periods of about 10 days. ORLANSKI (1969) obtained similar results for amplified baroclinic waves, i.e., wavelengths of 220 km with periods around 10 days. DÜING, MOOERS and LEE (1977) found that the most energetic current fluctuations in the Florida Straits had periods of about 9 to 12 days. The downstream component was coherent at these periods across the entire Florida Straits, from the shelf waters off Miami to those off Bimini, Bahamas, and was also coherent with the local cross-stream wind component. Current fluctuations in this period band propagated to the north with phase speeds of 26 to 33 cm/sec and wavelengths of 200 to 450 km.

Coherence in the downstream direction sharply decreased for distances greater than 55 km. It was suggested (DÜING et al., 1977) that these results could have been produced by wind forced, unstable, baroclinic shelf waves. ROONEY, JANOWITZ and PIETRAFESA (1978) also suggest that filaments may result from an unstable meander initiated by a wind event. BROOKS and BANE (1980) indicate that the Charleston bump may trigger a local instability, causing an internal energy redistribution downstream of the bump through both baroclinic and barotropic energy conversions.

Eddy Interaction with Shelf Waters

The water mass properties of eddy F and of the shelf waters are good indicators of the type and degree of shelf-Gulf Stream interactions during eddy passage. Significant amounts of shelf water within the vortex would imply interaction by entrainment and mixing, whereas a paucity of shelf water would imply interaction by displacement. The water type "slope water" is seldom observed south of Cape Hatteras and then only as far south as Onslow Bay (STEFÁNSSON, ATKINSON and BUMPUS, 1972). A composite T-S plot of data from all stations of the April cruise (Fig. 19) shows that shelf water tends to stratify primarily due to salinity at this time of year and Gulf Stream waters have a tendency towards thermal stratification. The waters of the Gulf Stream are fortunately quite constant in their T-S relationship and easily discernable from shelf water. T-S plots of stations taken across eddy F (Fig. 20b) clearly show the characteristic Gulf Stream T-S profiles at all stations with no trace of shelf water (salinity <36.0 $^{o}/oo$). Stations taken across the outer shelf north of the event (Fig. 20a) show that Gulf Stream water extends to at least the 46 m isobath. The subsurface salinity maximum of subtropical underwater with a salinity of about 36.5 $^{o}/_{oo}$ is clearly visible near the 90 m depth. The composite T-S plot reveals that shelf water never extended further offshore than the 46 m isobath. The absence of shelf water over the outer shelf (46 to 75 m isobaths) and within the vortex indicates that edge-eddies are efficient mechanisms for rapid and persistent shelf-Gulf Stream water exchange. The repeated renewal of waters by this means tends to displace the Gulf Stream salinity front shoreward, thus creating an effective Gulf Stream front at approximately the 45 m isobath, whereas the instantaneous front (maximum horizontal temperature and current shear) normally meanders about the 100 m isobath. The reason shelf water was not found in eddy F is that it was interacting with residual Gulf Stream waters from previous vortices. The outer shelf waters are continually renewed by this means so that a residence time can be defined as the average separation time between spin-off eddies, or approximately 2 weeks.

Nitrate Flux

Upwelling in the cold core of edge-eddies transports deeper Gulf Stream waters with high nutrient concentrations into the euphotic zone (<50 m) along the outer shelf. Nitrate concentrations of 10 μ moles ℓ^{-1} were found at the 30 m depth in the uplifted core of eddy F (Fig. 7). Nutrient-enriched waters were also observed to intrude onto the shelf in a bottom layer 20 to 30 m thick extending a distance of 35 km from the shelfbreak beneath the southward flowing warm Gulf Stream filament. Nitrate concentrations in the outer shelf are generally less than 1.0 μ moles ℓ^{-1} when eddies are not present. The vertically averaged net nitrate flux $\langle \overline{u' NO_3'} \rangle$ at the shelfbreak was calculated using current and temperature data from mooring E for the 7 day duration of eddy F, April 15-21. Temperature time series from meter EB were used to construct an inferred nitrate time series, since in this area temperature and nitrate are linearly related for newly upwelled waters with temperatures $\leq$ 20 C (STEFANSSON and ATKINSON, 1971; O'MALLEY et al., 1978); according to the empirical relationship:

$$[NO_3] = 53.0 - 2.6 \cdot T$$

The nitrate concentration at meter ET is assumed to be zero since temperatures are greater than 20 C, and the meter is located in the euphotic zone where planktonic uptake occurs. Nitrate section data (Fig. 7) also show near zero concentrations at this location. The net nitrate flux at EB for the period of eddy passage was computed from:

$$\overline{u'NO_3'} = \overline{(u - \tilde{u})\ (NO_3 - \tilde{NO_3})}$$

where the overbar represents a time average of the 7 day period of eddy F; u and NO_3 are daily averages to suppress tidal variations; $\tilde{u}$ and $\tilde{NO_3}$ are one month averages over the period from April 16 to May 16, which was used to average the influence of several eddies. The vertically averaged net nitrate flux was found from:

$$\left\langle \overline{u'NO_3'} \right\rangle = \frac{\overline{u'NO_3'}\ (72\ m) + \overline{u'NO_3'}\ (17\ m)}{2}$$

$$\left\langle \overline{u'NO_3'} \right\rangle = -18.6\ \mu\ \text{moles}\ m^{-2}\ sec^{-1}$$

The negative sign indicates a net flux of nitrate to the shelf waters. The amount of nitrate flux through a 1 m^2 column (55 m x 1.82 cm) at the shelf-break is -18.6 μ moles sec^{-1}. This is nearly equivalent to the 4 month winter average of -25 μ moles sec^{-1} onshore nitrate flux found for a 1 m^2 column at the seaward edge of the very productive Scotian shelf (SMITH, 1978). The vertical eddy averaged nitrate flux was converted to a nitrogen flux Q_N giving a value of Q_N = -0.26 mg N m^{-2} sec^{-1}. This was used to find the total

260μg/sec

nitrogen transported to the shelf by the eddy, N_T:

$$N_T = Q_N \cdot H \cdot L \cdot T$$

where H is the height of the shelfbreak water column (55 m), L is the eddy length (225 km) and T is the eddy duration (7 days). Using these values $N_T = 1.94 \times 10^9$ gN/eddy or 2128 tons N/eddy. Assuming that on the average about one eddy occurs every two weeks, then an estimated yearly input of nitrogen to the outer shelf by eddies is 5.5×10^4 tons N/year. The net flux of nitrate at the shelfbreak from low frequency current and temperature fluctuations during the winter period from December 76 to April 77 was estimated at -8.5 μ moles m^{-2} sec^{-1} using the same methods as above with 40 HLP time series. If we assume this rate is constant over the year then the annual nitrogen input through a length of shelfbreak equivalent to the eddy length (225 km) is 5.1×10^4 tons N/year. The close agreement of these two independent estimates over different time periods and averaging lengths suggests that the rate of nitrogen transport is reasonably constant for time periods longer than one month and that spin-off eddies are a major contributor to the transport.

Impact of Eddy Nitrate Flux on Phytoplankton Production

The computed net onshore flux of nitrate will have an impact on phytoplankton production that can be estimated knowing the area influenced by the disturbance. Hydrographic sections (Figs. 6 and 7) and surface temperature maps (Figs. 2 and 3) indicate that the eddy, which was observed to be 225 km in along-shelf dimension, influences a region approximately 35 km in the onshore direction, an area of 7.88×10^9 m^2. Assuming one eddy occurs on the average every two weeks, or 26 events per year, the annual direct areal nitrogen input is -6.4 g N m^{-2} yr^{-1}. Carbon:nitrogen ratios in phytoplankton range from 5:1 to 10:1, implying that the supplied nitrate could support an annual carbon production of 32 to 64 g C m^{-2} yr^{-1} with no nitrogen recycling.

The estimated carbon production is based on the computed net flux from a spring eddy only, but the rate appears to be representative of the annual input. HAINES and DUNSTAN (1975) found an annual outer shelf production of 132 g C m^{-2} yr^{-1} and April production of only 18 g C m^{-2} yr^{-1} on an annual basis. Since their samples were taken from a predetermined grid which did not emphasize the shelfbreak area or attempt to identify or sample within eddy-upwelled waters, their values are not representative of outer shelf carbon production. HAINES (1974) attempted a nitrogen budget for the South Atlantic Bight that is schematically shown in Fig. 21. Our estimate of Gulf Stream induced eddy nitrate flux has been included on this figure for comparison. The eddy estimate of 55,000 tons N per year is a factor of 2 greater than the combined nitrogen sources as determined by HAINES and is a factor of 7 greater than HAINES Gulf Stream estimate, which was based on diffusion of subsurface Gulf Stream waters. However at the time of the HAINES measurement the capability to conduct satellite directed field sampling had not been developed. Clearly, the newly calculated net nitrate flux due to eddy passage is a major source of new nitrogen for the South Atlantic Bight and may control carbon production in the outer shelf.

SUMMARY AND CONCLUSIONS

We have combined a unique set of satellite IR images, hydrographic sections and current and temperature time series to conclusively show that the folded-wave patterns commonly observed in routine satellite-derived analyses of the Gulf Stream western boundary from Cape Hatteras to Miami are produced by geostrophic, southward flowing warm filaments of near-surface

Gulf Stream water coupled to cold upwelled cores. We define these features as cyclonic frontal eddies partly for historical reasons, partly from their formation process (they appear to develop from growing wave-like meanders of the Gulf Stream front), and partly from their eddy-like cyclonic circulation produced by the warm southward flowing Gulf Stream waters on the west side and northward Gulf Stream flow on the east side of the cold uplifted core, which is in approximate geostrophic balance with the cyclonic circulation. They may never become completely detached from the Stream except during the final stages of decay when stranding over the shelf and eventual dissipation is in evidence.

Eddy dimensions appear to have 3 characteristic length scales, which are influenced by topography and can be classified by 3 geographic areas along the southeast U. S. shelf. South of Jupiter, Florida, the disturbances are restricted by the narrow shelf and channelized boundaries of the Florida Straits. Eddy diameters here range from about 10 to 30 km, with the downstream axis being 2 to 3 times larger than the cross-stream. Between Jupiter and the Charleston bump the shelf widens and edge-eddies take on the characteristic elongated folded-wave patterns. The filaments can extend 35 to 40 km over the shelf with downstream lengths ranging from 100 to 200 km. A second elongation is observed following a seaward deflection of the Stream by the Charleston bump and downstream lengths may reach up to 300 km.

The eddy formation process is not completely understood. It is evident from time series of satellite IR-images that they form from growing wave-like meanders of the Gulf Stream cyclonic front. It is also apparent that at times wind events can initiate a frontal meander, which propagates to the north and may evolve into an edge-eddy; but whether this occurs through a barotropic or baroclinic instability process is unknown. The uncertainty rises because the Gulf Stream front appears to satisfy the instability criteria for either process and both predict similar wave properties, which agree with the observed properties (wave lengths 100 to 200 km and wave period $\simeq$ 10 days). However, edge-eddies have been found to dissipate kinetic energy of the mean flow, which points to a barotropic instability (LEE, 1975). They form on the average of one every 2 weeks and travel to the north along the shelfbreak at about 40 cm/sec, which is about the same as the northward phase speed of the meanders. Their total life cycle, from meander to dissipation over the shelf, usually takes place in less than 3 weeks: approximately 2 days to one week of meander growth, one week of eddy growth and one week of decay. They appear to form along the boundary of any major current system and are often observed along the outer edges of the larger warm and cold core Gulf Stream rings, which suggests that they may play a role in the exchange of water across ring fronts.

Frontal eddies are observed to be a major component of the low frequency current and temperature variability over the outer 35 to 40 km of the Georgia shelf during all seasons. Eddy signature in current and temperature time series from the shelfbreak along Florida and Georgia consists of a cyclonic flow reversal throughout the water column coupled to a large temperature decline that is more intense near the bottom. There is some indication that there is more eddy activity in the spring, but it will take longer time series to be conclusive. Edge-eddies provide a means of rapid water renewal for the outer shelf. The frequency of vortex passage tends to create an effective Gulf Stream front (as measured by salinity, 36.0 $^{o}/oo$ or greater) 35 to 40 km shoreward of the actual front (maximum horizontal temperature and current gradient), which is normally located seaward of the shelfbreak. The residence time of the outer shelf waters can be defined as the average time interval between eddy events, or approximately 2 weeks.

Upwelling in the cold core of frontal eddies was observed to transport deeper nutrient-enriched Gulf Stream waters onto the shelf in a bottom intrusion layer 20 m thick beneath the warm southward flowing filament. The intrusion can extend 35 to 40 km across the outer shelf in the winter and spring and possibly even further in the summer when the shelf waters are vertically stratified. These nutrient-enriched waters reach into the euphotic zone, which is approximately 45 m in this area, and thus provide a food source for phytoplankton. Estimates of nitrate flux indicate that eddies transport approximately 55,000 tons of nitrogen annually to the outer shelf, which is almost a factor of 7 greater than previous Gulf Stream estimates and is about a factor of 2 greater than all other estimated shelf nitrogen sources combined. We estimate that this nitrogen input could support an annual carbon production of 32 to 64 $gCm^{-2}\ yr^{-1}$ with no nitrogen recycling. The estimated rate of nitrate input is only a factor of 2 less than that estimated for the seaward edge of the very productive Scotian shelf. The question then is: why is the Georgia shelf usually considered to have low biological productivity? Since we feel our nitrate flux estimates are reasonably accurate, we can think of two possible answers: (1) It is highly productive, at least in the outer shelf, but past sampling strategies have not been adequate to resolve such an event-dominated region. This could have easily occurred because only recently, with the advent of routine satellite coverage, have the eddy upwelling events been observed in any detail; (2) The eddy-induced upwelling events do not last long enough to establish a well-structured food chain. In the 2 to 3 week duration of upwelling events there is ample time for primary producers to respond and for some of the faster growing zooplankton, however, the time may not be sufficient for higher trophic level organisms.

If the answer to the above question is number 1, then there should exist undiscovered fisheries along the southeast U.S. outer shelf. If number 2 is the answer, then since the nutrient food source is almost continuous this region would seem ideal for establishing artificial reefs within the euphotic zone along the shelfbreak strip.

Acknowledgements--We thank Captain Hartshorne of the R/V Columbus Iselin and Captain Bennet of the S/S Advance II and their crews for aid in the field operations. Special thanks are extended to Rich Findley and Neddra Chalker, who prepared the current meter instrumentation, and Jim Singer, Bill Chandler and Pat O'Malley, who made the hydrographic observations. Pat O'Malley is also thanked for preparing data in technical report form. Sherman Chiu is thanked for computer processing of the current meter data and José Partagas for surface wind analysis. We greatly appreciate the assistance our colleagues gave, especially Dr. J. Yoder, who helped in evaluating the possible impact of the observed physical processes on the biota; Drs. C. Rooth and C.N.K. Mooers for many germane discussions, and Dr. P. McClain and D. Olson for their critiques. We particularly wish to acknowledge the help of Dr. Steve Baig of NOAA/NESS, Miami, for without his analysis of satellite images we may never have found the eddies. We also thank Jere Green for typing and Dan McIntosh and Gary Rosiello for drafting.

This research was supported by the Department of Energy under contracts EY-76-S-05-5163 and EY-76-S-09-0889 to T. N. Lee and L. P. Atkinson, respectively.

REFERENCES

ATKINSON L. P. and T. N. LEE (1979) Shelf break upwelling induced by Gulf Stream meanders. (In preparation)

BANE J. M. Jr. and D. A. BROOKS (1979) Gulf Stream meanders along the continental margin from the Florida Straits to Cape Hatteras. Geophysical Research Letters, 6(4), 280-282.

BARRETT J. R. (1971) Available potential energy of Gulf Stream rings. Deep-Sea Research, 18, 1221-1231.

BEARDSLEY R. C. and B. BUTMAN (1974) Circulation on the New England continental shelf: response to strong winter storms. Geophysical Research Letters, 1, 181-184.

BRAUN C. (1971) Limits on the accuracy of infrared measurements of sea surface temperature from satellite. NOAA Tech. Memo. NESS 30, NOAA, Washington, DC, 1-28.

BROOKS D. A. and C. N. K. MOOERS (1977) Wind forced continental shelf waves in the Florida Current. Journal of Geophysical Research, 82, 2569-2576.

BROOKS D. A. and J. M. BANE JR. (1978) Gulf Stream deflection by a bottom feature off Charleston, South Carolina. Science, 201, 1225-1226.

BROOKS, D. and J. M. BANE JR. (1980) Gulf Stream meanders: observations of their formation, structure, propagation, and energetics from Charleston to Cape Hatteras. (Submitted to Journal of Physical Oceanography)

BROWN O. B. and R. H. EVANS (1979) Processing of NOAA VHRR Infrared data for geophysical applications. Presented at Second Working Conference on Oceanographic Data Systems, WHOI, September 26-28, 1978.

DE RYCKE R. J. and P. K. RAO (1973) Eddies along a Gulf Stream boundary viewed from a very high resolution radiometer. Journal of Physical Oceanography, 3, 490-492.

DÜING W., C. N. K. MOOERS and T. N. LEE (1977) Low frequency variability in the Florida Current and relations to atmospheric forcing from 1972 to 1974. Journal of Marine Research, 35(1), 129-161.

DUNSTAN W. M. and L. P. ATKINSON (1976) Sources of new nitrogen for the South Atlantic Bight. Proceedings of 3rd International Estuarine Research Conference, Galveston, Texas (Martin Wiley, ed.) 1:69-78.

FOFONOFF N. P. (1969) Spectral characteristics of internal waves in the ocean. Deep Sea Research, supplemental to Vol. 16, 59-71.

FUGLISTER F. C. (1972) Cyclonic rings formed in the Gulf Stream 1965-1966, in Studies in Physical Oceanography, A. Gordon, ed., New York, Gordon and Breach, 137-168.

GARDNER, W. S., D. S. WYNNE and W. M. DUNSTAN (1976) Simplified procedure for the manual analysis of nitrate in seawater. Mar. Chem., 4, 393-396.

GOTTHARDT G. A. (1973) Observed formation of a Gulf Stream anticyclonic eddy. Journal of Physical Oceanography, 3, 237-238.

HAINES E. B. (1974) Processes affecting production in Georgia coastal waters. PhD dissertation. Duke University, Durham, North Carolina.

HAINES, E. B. and W. M. DUNSTAN (1975) The distribution and relation of particulate organic material and primary productivity in the Georgia Bight, 1973-1974. Estuarine and Coastal Mar. Sci., 3, 431-441.

KOHL J. G. (1868) Geschichte der Golfstroms und seiner Erforschung. Bremen: C. E. Müller.

LEE T. N. (1975) Florida current spin-off eddies. Deep Sea Research 22, 753-765.

LEE T. N. and D. MAYER (1977) Low frequency current variability and spin-off eddies on the shelf off southeast Florida. Journal of Marine Research, 35(1), 193-220.

LEE T. N. and D. A. BROOKS (1979) Initial observations of current, temperature and coastal sea level response to atmospheric and Gulf Stream forcing on the Georgia shelf. Geophysical Research Letters, 6(4), 321-324.

LEGECKIS R. (1975) Applications of synchronous meteorological satellite data to the study of time dependent sea surface temperature changes along the boundary of the Gulf Stream. Geophysical Research Letters, 2, 435-438.

LEGECKIS R. (1979) Satellite observations of the influence of bottom topography on the seaward deflection of the Gulf Stream off Charleston, South Carolina. Journal of Physical Oceanography, 9(3), 483-497.

LEGECKIS R. and J. PRITCHARD (1976) Algorithm for correction of VHRR imagery for geometric corrections due to earth curvature, earth rotation and spacecraft roll attitude errors. NOAA Tech. Memo. NESS 77, Washington, DC, 1-31.

NAVOCEANO (1975) Experimental ocean frontal analysis charts. U.S. Naval Oceanographic Office, Code 3710, 1975-1977.

NIILER P.P. and L. A. MYSAK (1971) Barotropic waves along an eastern continental shelf. Geophysical Fluid Dynamics, 2, 273-278.

NOAA-NESS (1974) Experimental Gulf Stream Analysis, NOAA-2 Satellite Thermal Infrared (VHRR), U.S. Department of Commerce, Environmental Products Group, F.O.B. #4, Room 3301, Washington, D.C. 20233.

O'MALLEY, P.G., L. P. ATKINSON, J. J. SINGER, W. S. CHANDLER and T. N. LEE (1978) Hydrographic observations in the Georgia Bight (April 1977). Georgia Marine Science Center Technical Report 78-5. 208 pp.

ORLANSKI I. (1969) The influence of bottom topography on the stability of jets in a baroclinic fluid. Journal of Atmospheric Science, 26, 1216-1232.

ORLANSKI I. and M. D. COX (1973) Baroclinic instability in ocean currents. Geophysical Fluid Dynamics, 4, 297-332.

PARKER C.E. (1971) Gulf Stream rings in the Sargasso Sea. Deep-Sea Research, 18, 981-993.

PARTAGAS J.F. (1978) Surface winds in the Georgia Embayment. University of Miami, RSMAS, Final Report to Science Applications, Inc., on subcontract 025-06. 34 pp.

PIETRAFESA L. J., L. P. ATKINSON and J. O. BLANTON (1978) Evidence for deflection of the Gulf Stream by the Charleston Rise. Gulf Stream, IV (9), 3-7.

PIETRAFESA L. J. and G. S. JANOWITZ (1979) A note on the identification of a Gulf Stream Spin-off Eddy from Eulerian Data. Geophysical Research Letters, 6 (7), 549-552.

PIETRAFESA L. J. and G. S. JANOWITZ (1980) Lack of evidence of southerly propagating shelf waves in Onslow Bay, N.D. Geophysical Research Letters, 7(2), 113-116.

ROONEY, D., G. JANOWITZ and L. PIETRAFESA (1978) A simple model of the reflection of the Gulf Stream by the Charleston Bump. Gulf Stream Monthly, 4(11), 3-7.

ROUSE, H. (1963) On the role of eddies in fluid motion. American Scientist, 285-314.

SAUNDERS, P. M. (1971) Anticyclonic eddies formed from shoreward meanders of the Gulf Stream. Deep Sea Research, 18, 1207-1219.

SCOTT, J. T. and G. T. CSANADY (1976) Nearshore currents off Long Island. Journal of Geophysical Research, 81, 5401-5409.

SMITH, P. C. (1978) Low-frequency fluxes of momentum, heat, salt and nutrients at the edge of the Scotian shelf. Journal of Geophysical Research, 83(C8), 4079-4096.

STEFÁNSSON, U., L. P. ATKINSON and D. F. BUMPUS (1971) Hydrographic properties and circulation of the North Carolina shelf and slope waters. Deep-Sea Research, 18, 383-420.

STEFANSSON, U., and L. ATKINSON (1971) Nutrient-density relationships in the western North Atlantic between Cape Lookout and Bermuda. Limnol. Oceanography, 16(1), 51-59.

STOMMEL, H. M. (1965) The Gulf Stream. University of California Press, 248 pp.

STRICKLAND, J. D. H. and T. R. PARSONS (1965) A manual of sea water analysis. Bulletin Fisheries Research Board of Canada. 125: 185 pp.

STUMPF, H. G. and P. K. RAO (1975) Evolution of Gulf Stream eddies as seen in satellite infrared imagery. Journal of Physical Oceanography, 5, 388-393.

THOMPSON, B. J. and G. A. GOTTHARDT (1971) Life cycle of a North Atlantic eddy. Trans. American Geophysical Union, 52, 241 (abstract only).

UCHUPI, E. (1968) Atlantic continental shelf and slope of the United States physiography. Geolog. Survey Professional Paper 529-C, U. S. Government Printing Office, Washington, D.C. 1-30.

VON ARX, W. S., D. F. BUMPUS and W. S. RICHARDSON (1955) On the fine structure of the Gulf Stream front. Deep-Sea Research, 3, 46-65.

WEBSTER, R. (1961) The effect of meanders on the kinetic energy balance of the Gulf Stream. Tellus, 13, 392-401.

WILLE, R. (1960) Karman vortex streets. Advances in Applied Mechanics, 4, 185-196.

FIGURE CAPTIONS

Fig. 1. Location of current meter moorings A-G (⊙), coastal sea level (▲) and wind (⊛) stations.

Fig. 2. Surface temperatures from T/S mapping April 12 (0925 hr.) to 14 (1030 hr.), 1977. Circles with dots show mooring locations. Ship track is shown by straight lines and stations by small dots. Stations at section ends are shown in brackets. Arrows indicate current direction.

Fig. 3. Surface temperatures from T/S mapping April 14 (1030 hr.) to 16 (0921). Circles with dots show mooring locations. Ship track is shown by straight lines and stations by small dots. Stations at section ends are shown in brackets. Arrows indicate current direction.

Fig. 4. Satellite VHRR IR image of a Gulf Stream frontal eddy from orbit 3223 NOAA-5 on April 16, 1977, at 0200 GMT.

Fig. 5. SST contours from alpha-numeric presentation of orbit 3223 NOAA-5 VHRR IR images averaged every 2 km.

Fig. 6 Composite of hydrographic sections through eddy F, April 14-16. Stations are identified on bottom profiles.

Fig. 7. Composite of nutrient sections through eddy F, April 14-16. Stations are identified on bottom profiles.

Fig. 8a. Horizontal temperature (C) distribution at 16 m through eddy F, April 14-16. Circles with small dots are mooring locations. Dots are for station location. Section end stations are in brackets.

Fig. 8b. Horizontal temperature (C) distribution at 30 m through eddy F, April 14-16. Circles with small dots are mooring locations. Dots are for station locations. Section end stations are in brackets.

Fig. 9. Depth of the 26 σ_t surface through eddy F, April 14-16. Dots are for station location.

Fig. 10. Sequential positions of eddy E on April 8 to 15, taken from infrared VHRR images from NOAA-5 night (0200 GMT) orbits. Circles show the current meter locations.

Fig. 11. Sequential positions of eddy F on April 15-17, taken from infrared VHRR images from NOAA-5 day (1400 GMT) orbits. Circles show the locations of current meters E and F.

Fig. 12. Time series of 6-hourly, rotated current and wind vectors from 40-HLP filtered records for April 15 to June 29, 1977. Magnitude and rotation of wind and current vectors are shown by the scale arrows on the left. Instrument depth and water depth are shown on the right. Vertical lines are for eddy and meander event identification.

Fig. 13. Time series of rotated velocity components u (-O-O-O-), v (-+-+-+-), cm/sec, and temperature T (-X-X-X-), C, from 40-HLP filtered records for April 15 to June 29, 1977. Vertical lines are for eddy and meander event identification.

Fig. 14. Time series of 1-hourly, rotated current and wind vectors from 3-HLP filtered records for April 12-24, 1977. Magnitude and rotation of wind and current vectors are shown by the scale arrows on the left.

Fig. 15. Gulf Stream boundaries off the southeast U. S. as shown by U. S. Naval Oceanographic Office in Experimental Ocean Frontal Analysis charts for weeks of a) May 12-18, 1977 and b) May 19-25; arrows indicate current direction.

Fig. 16. Time series of 6-hourly, rotated current and wind vectors, and corrected sea level from Charleston (Chs.) and Daytona (Day.), 40-HLP filtered records for December 14, 1976, to April 6. Sea level corrected for atmospheric pressure by 1 mb pressure = 1.01 cm sea level. Magnitude and rotation of vectors shown by scale arrows on left. Instrument depth and water depth are shown on right. Vertical lines are for eddy event identification.

Fig. 17. Time series of 6-hourly, rotated current and wind vectors, and corrected sea level from Charleston (Chs.) and Daytona (Day.), 40-HLP filtered records for July 6, 1977 to October 31. Sea level corrected for atmospheric pressure by 1 mb pressure = 1.01 cm sea level. Magnitude and rotation of vectors shown by scale arrows on left. Instrument depth and water depth are shown on right. Vertical lines are for eddy event identification.

Fig. 18. Schematic characterization of a Gulf Stream frontal eddy on the Georgia shelf.

Fig. 19. Composite T-S plot of all hydrographic station data taken during April 8-16, 1977. Station nos. are given beside some of the identifiable shelf stations.

Fig. 20a. T-S distributions from stations of Savannah (4) section, April 16.

20b. T-S distributions from stations of St. Augustine North section, April 15.

Fig. 21. Schematic of annual nitrogen inputs to the Georgia shelf as computed by HAINES (1974). Values are in tons of nitrogen per year. Arrows indicate flux direction. Our estimate of annual eddy induced flux is shown in parenthesis.

Table 1. Relevant instrument information for Georgia shelf current meter deployments.

mooring no.	coordinates	instr. no.	water depth (m)	instr. depth (m)
A	31° 00.5'N	AT	30	17
A	80° 27.9'W	AB	30	27
B	30° 50.8'N	BT	75	17
B	80° 02.0'W	BB	75	72
C	31° 11.3'N	CT	75	17
C	79° 53.1'W	CB	75	72
D	31° 25.0'N	DT	75	17
D	79° 45.4'W	DB	75	72
E	31° 35.8'N	ET	75	17
E	79° 40.2'W	EB	75	72
F	31° 39.6'N	FT	45	17
F	79° 50.9'W	FB	45	42
G	31° 44.8'N	GT	30	17
G	80° 08.5'W	GB	30	27

current record lengths

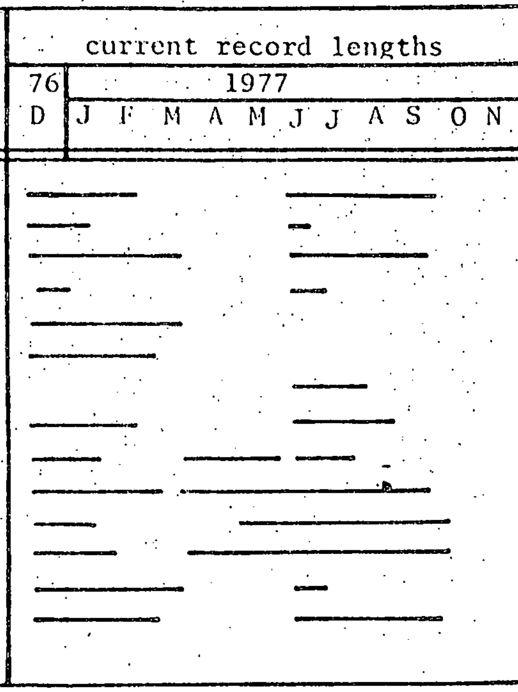

Table 2. Sequence of hydrographic sections, April 8-20, 1977.

start (hour/day) EST	end (hour/day) EST	section	section type	stations	ship
14.8/ 8	4.4/ 9	Savannah 1	STD/XBT	1- 14	S/S Advance II
1.4/10	9.4/10	St. Simons 1	STD/XBT	21- 32	"
3.1/11	10.6/11	Savannah 2	STD/XBT	33- 43	"
15.4/12	23.8/12	Savannah 3	STD/XBT	53- 65	"
17.7/13	2.1/14	Jacksonville-South	STD/XBT	100-113	"
19.1/14	0.1/15	St. Augustine-South	STD/XBT	174-182	"
4.1/15	8.1/15	Ormond	STD/XBT	192-199	"
12.1/15	16.6/15	St. Augustine-North	STD/XBT	213-220	"
16.6/15	23.0/15	Jacksonville-North	XBT	229-236	"
2.7/16	5.7/16	St. Simons 2	XBT	249-258	"
8.7/16	14.4/16	Savannah 4	STD/XBT	259-267	"
15.3/19	4.0/20	Savannah 5	XBT	A-P	R/V Blue Fin

Table 3. Data used in nitrate flux calculations, values are daily averages.

date (April 1977)	u (17m) cm/sec	u (72m) cm/sec	$\langle u \rangle$ cm/sec	T (72m) °C	NO_3 (72m) μ moles ℓ^{-1}	$\langle NO_3 \rangle$ μ moles ℓ^{-1}	$\langle u \rangle'$ cm/sec	$\langle NO_3 \rangle'$ μ moles ℓ^{-1}
15	3.5	-2.3	0.60	18.2	5.7	2.85	0.04	-2.75
16	-5.3	-8.2	-6.75	17.1	8.7	4.35	-7.31	-1.25
17	-4.0	-3.5	-3.75	14.5	15.3	7.65	-4.31	2.05
18	-4.7	-1.6	-3.15	14.0	16.7	8.35	-3.70	2.75
19	3.6	2.4	3.00	14.7	14.9	7.49	2.44	1.89
20	14.0	8.5	11.25	16.5	10.2	5.10	10.69	-0.50
21	7.0	-1.5	2.75	17.8	6.8	3.40	2.19	-2.20

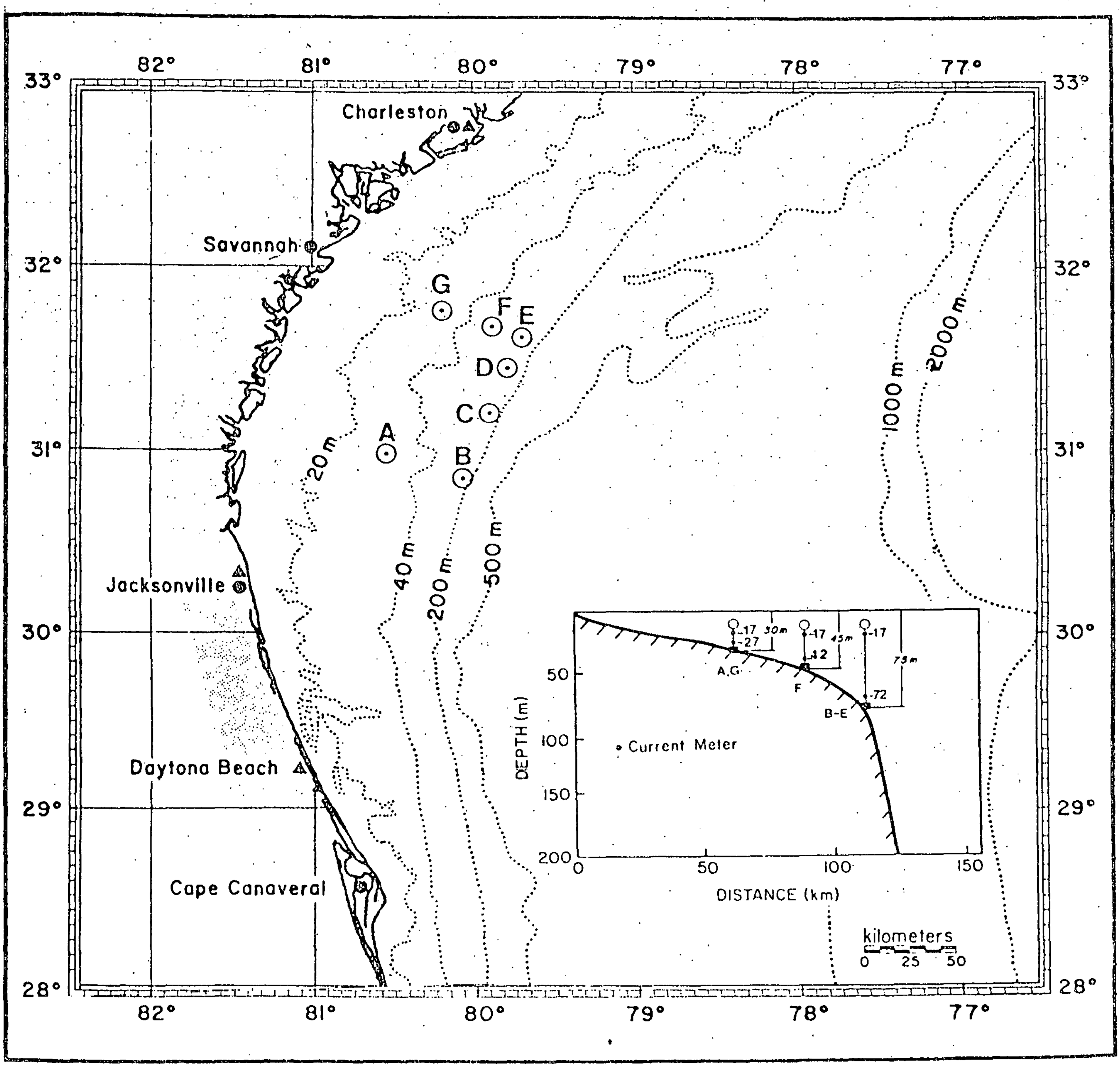

Fig. 1. Location of current meter moorings A-G (⊙); coastal sea level (▲); and wind stations (⊗).

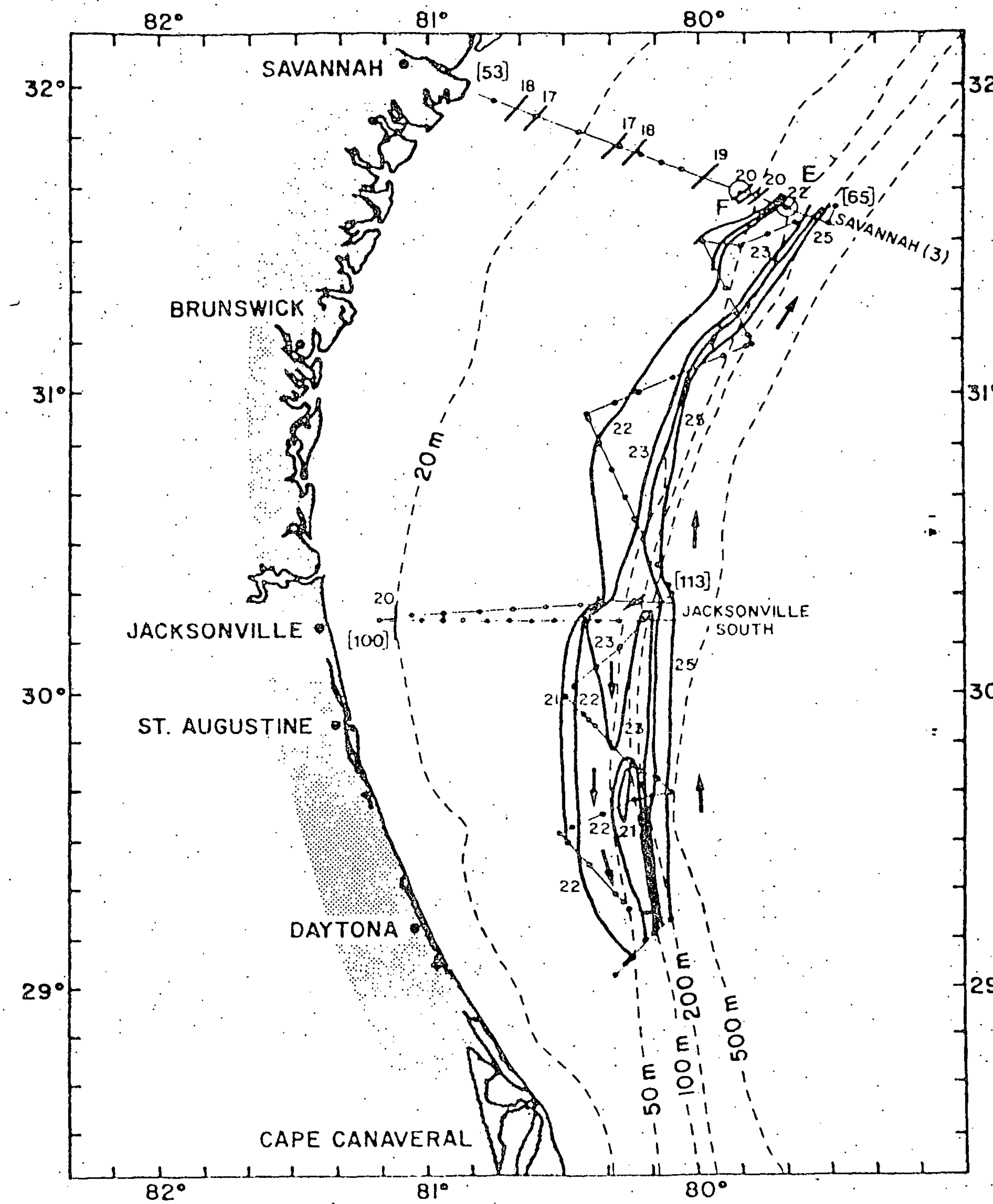

Fig. 2. Surface temperatures from T/S mapping April 12 (0925 hr.) to 14 (1030 hr.), 1977. Circles with dots show mooring locations. Ship track is shown by straight lines and stations by small dots. Stations at section ends are shown in brackets. Arrows indicate current direction.

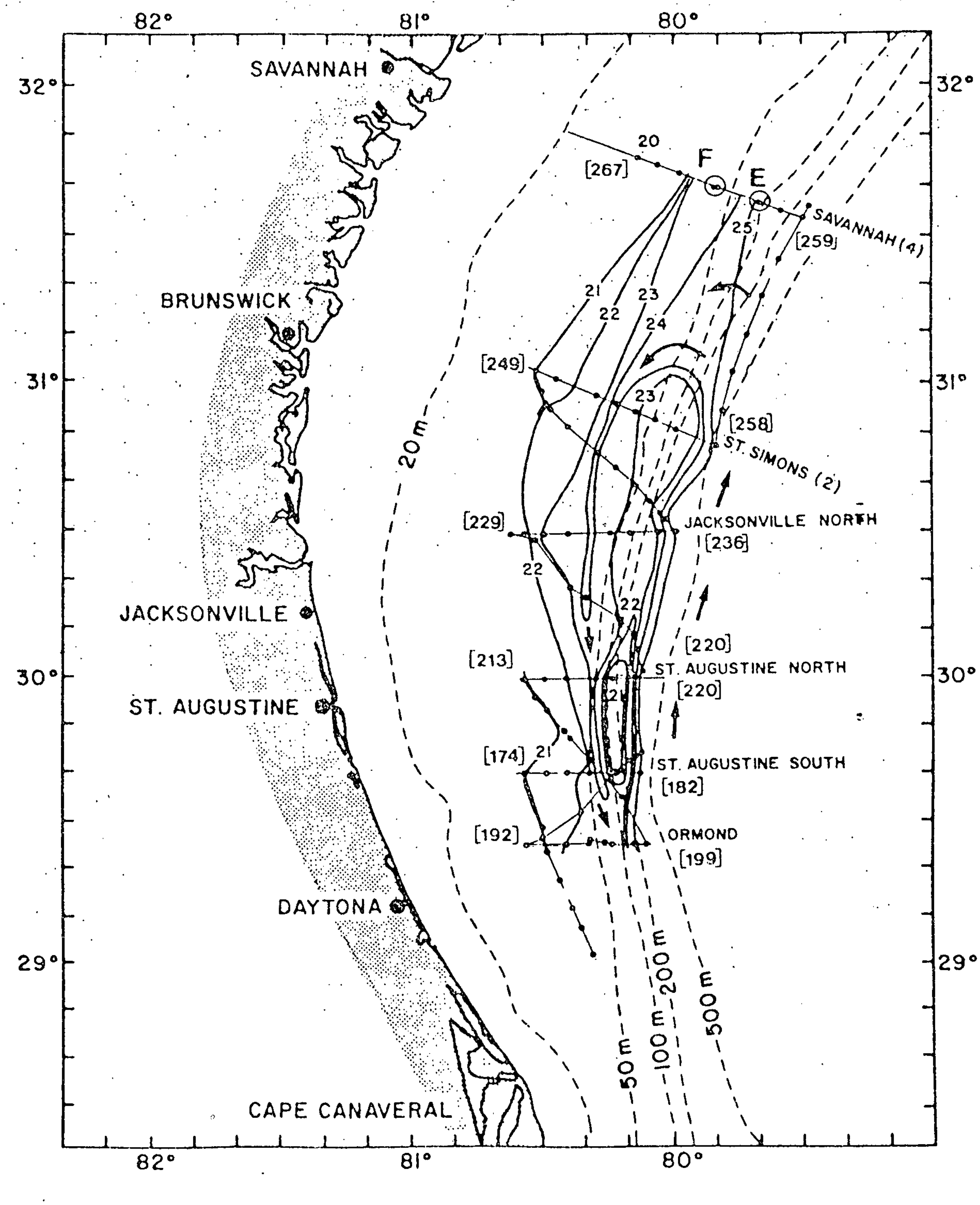

Fig. 3. Surface temperatures from T/S mapping April 14 (1030 hr.) to 16 (0921). Circles with dots show mooring locations. Ship track is shown by straight lines and stations by small dots. Stations at section ends are shown in brackets. Arrows indicate current direction.

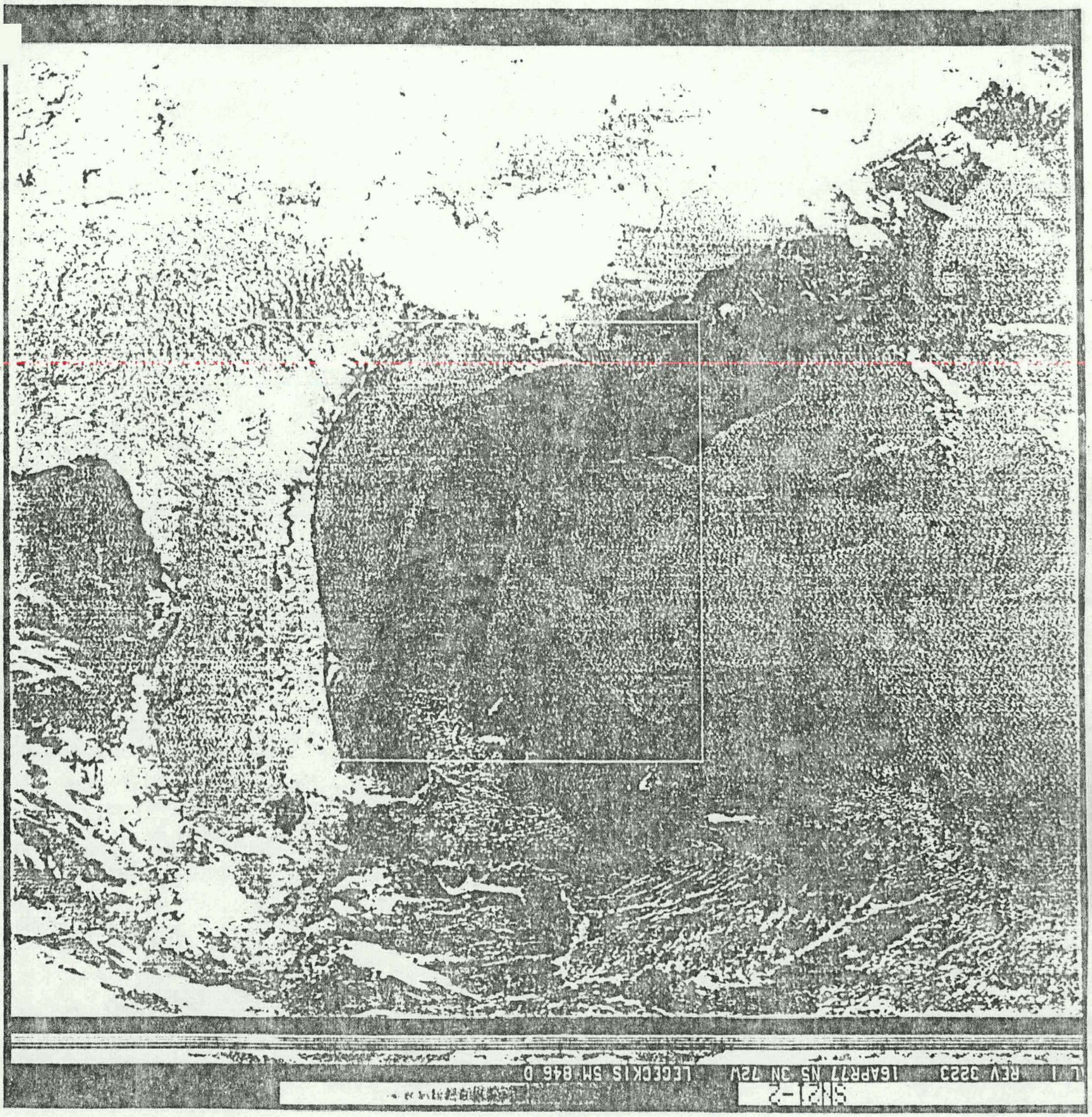

Fig. 4. Satellite VHRR IR image of a Gulf Stream frontal eddy from orbit 3223 NOAA-5 on April 16, 1977, at 0200 GMT.

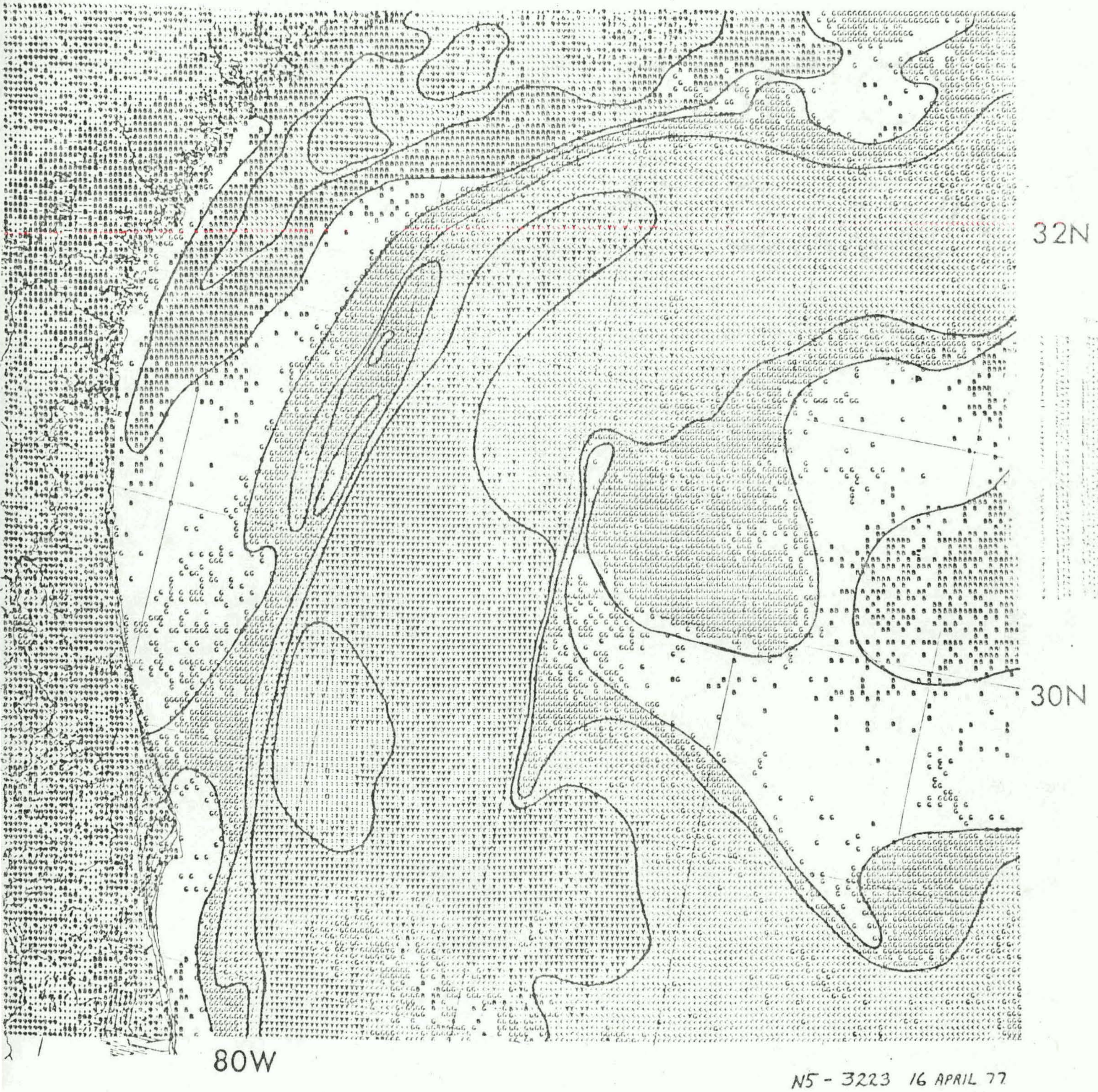

Fig. 5. SST contours from alpha-numeric presentation of orbit 3223 NOAA-5 VHRR IR images averaged every 2 km.

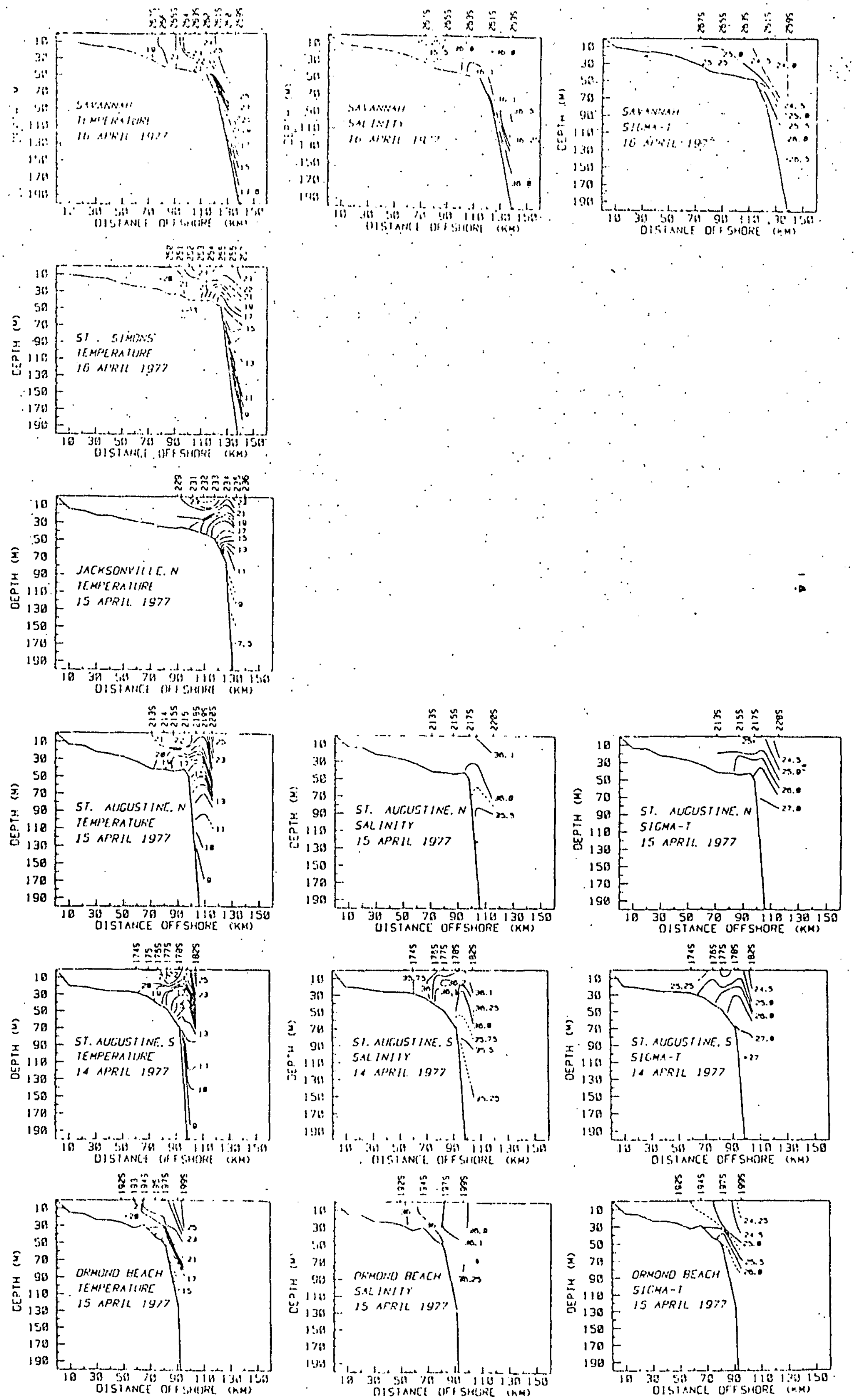

Fig. 6. Composite of hydrographic sections through eddy F, April 14-16. Stations are identified on bottom profiles.

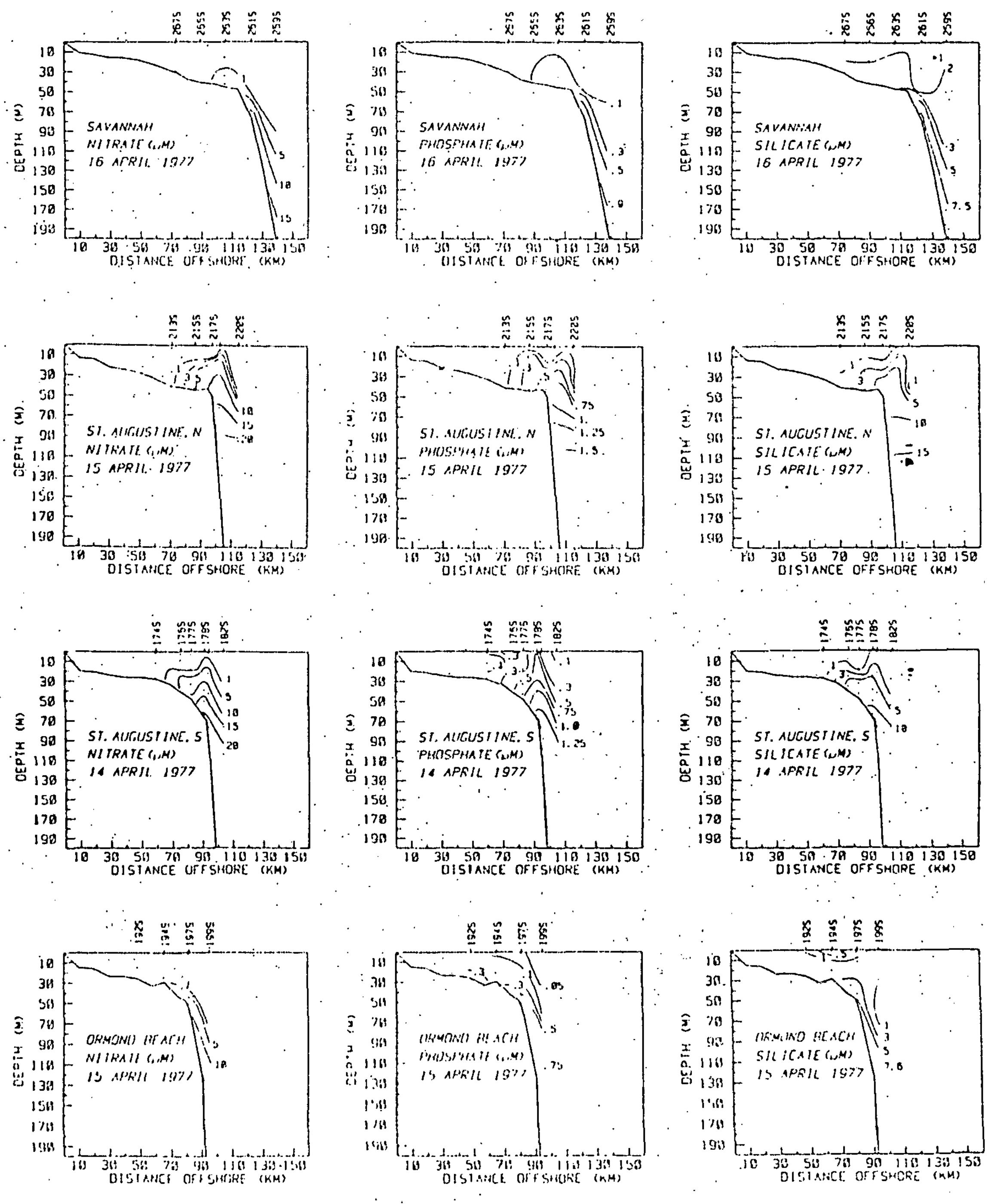

Fig. 7. Composite of nutrient sections through eddy F, April 14-16. Stations are identified on bottom profiles.

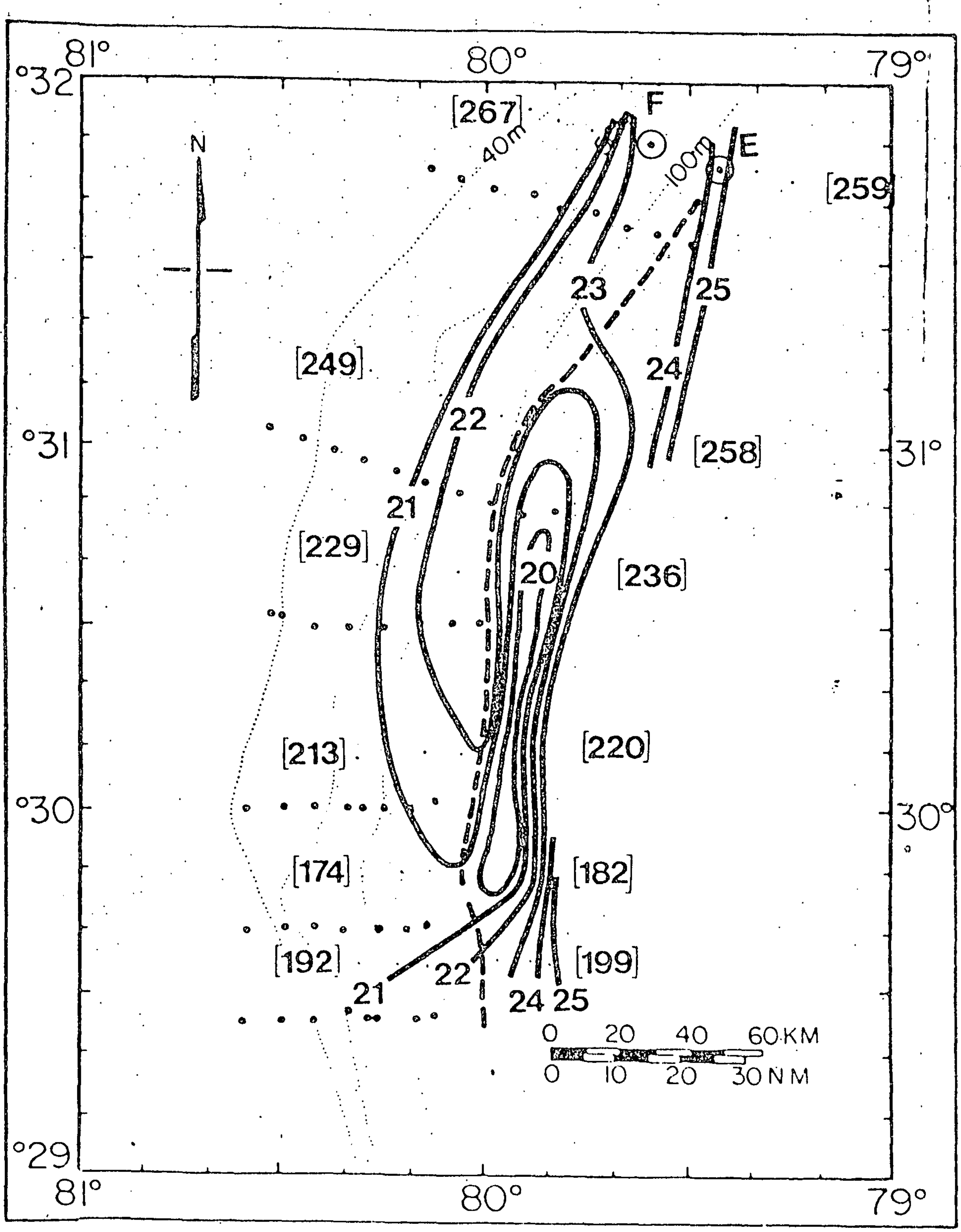

Fig. 8a. Horizontal temperature (C) distribution at 16 m through eddy F, April 14-16. Circles with small dots are mooring locations. Dots are for station location. Section end stations are in brackets.

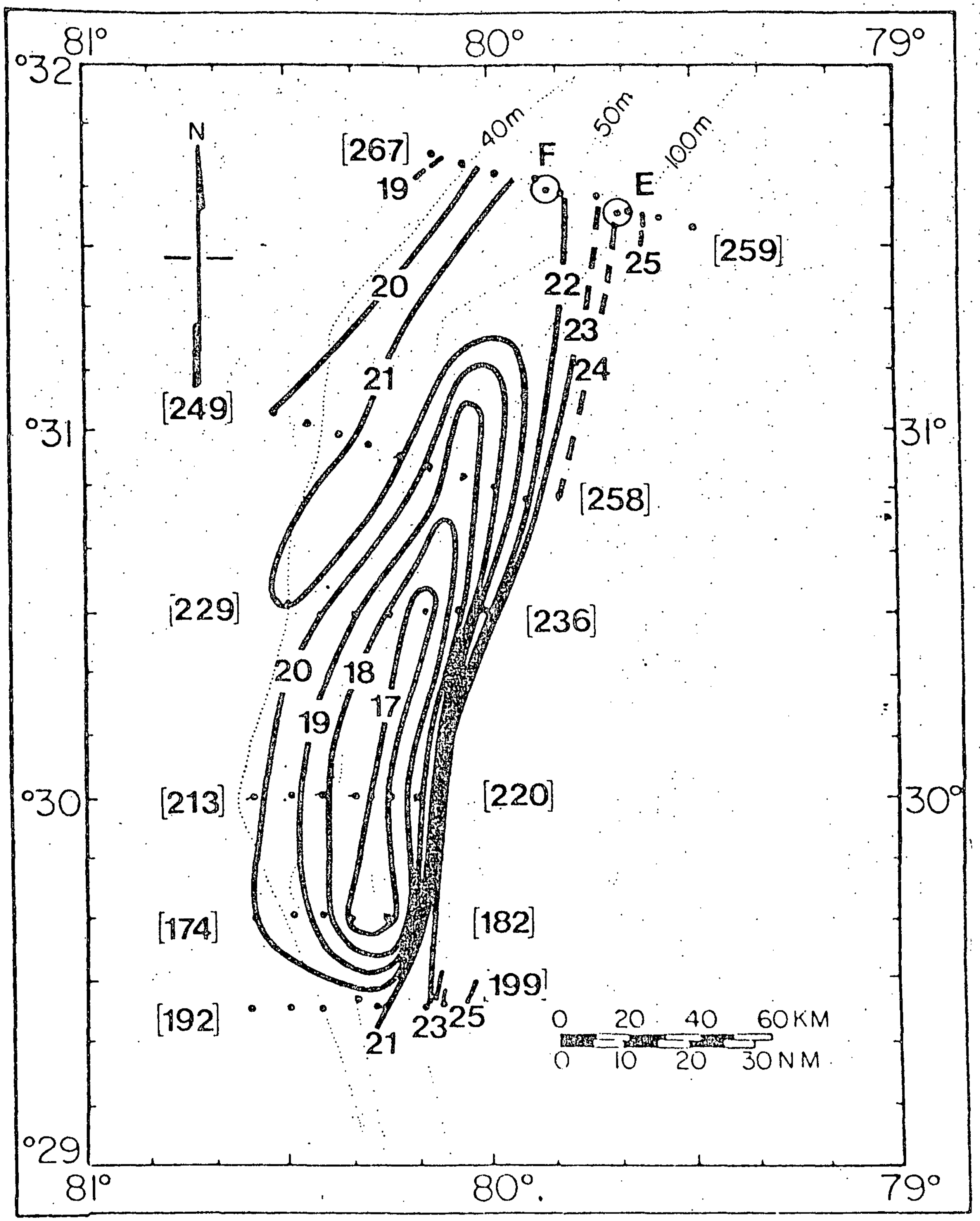

Fig. 8b. Horizontal temperature (C) distribution at 30 m through eddy F, April 14-16. Circles with small dots are mooring locations. Dots are for station locations. Section end stations are in brackets.

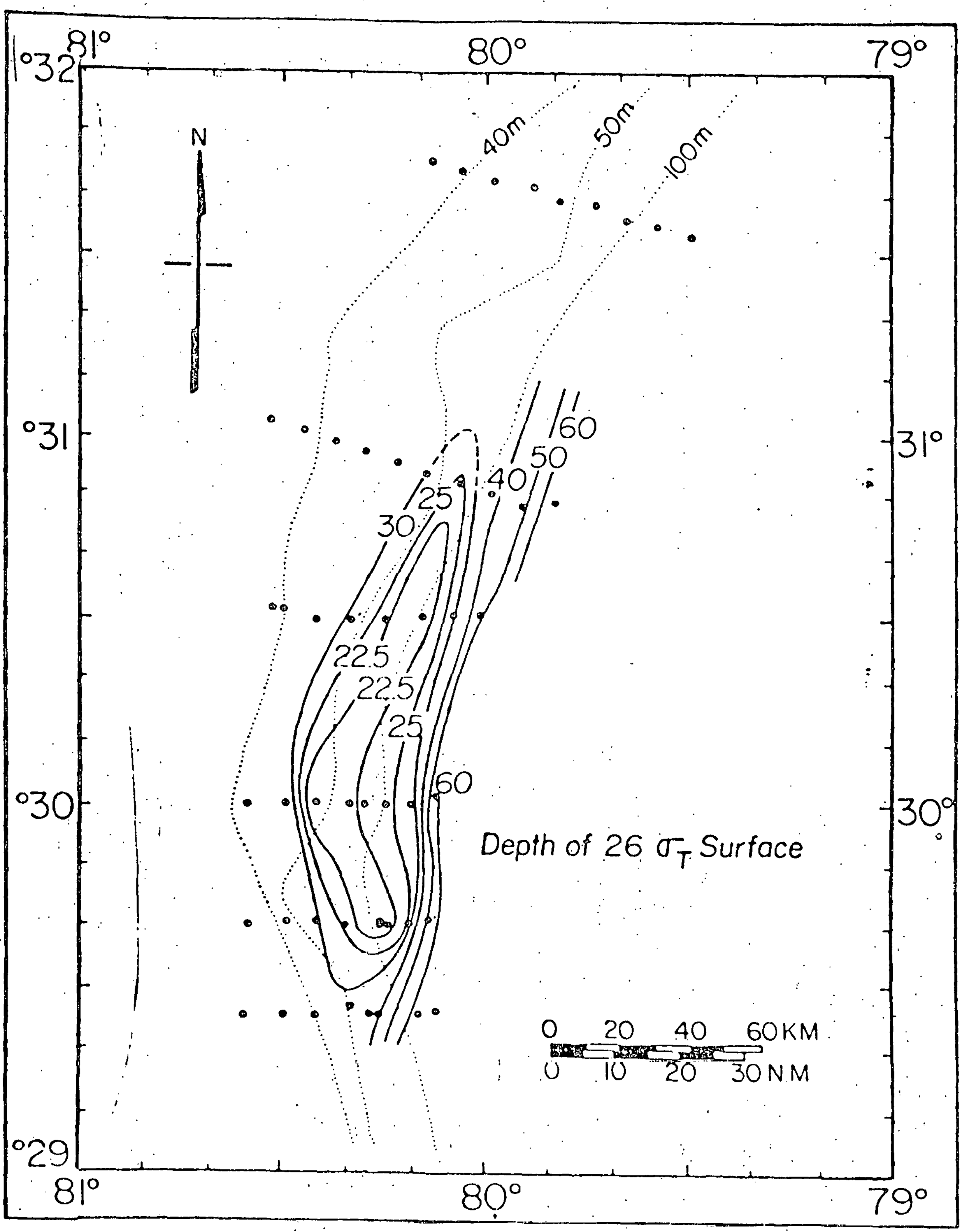

Fig. 9. Depth of the 26 σ_t surface through eddy F, April 14-16. Dots are for station location.

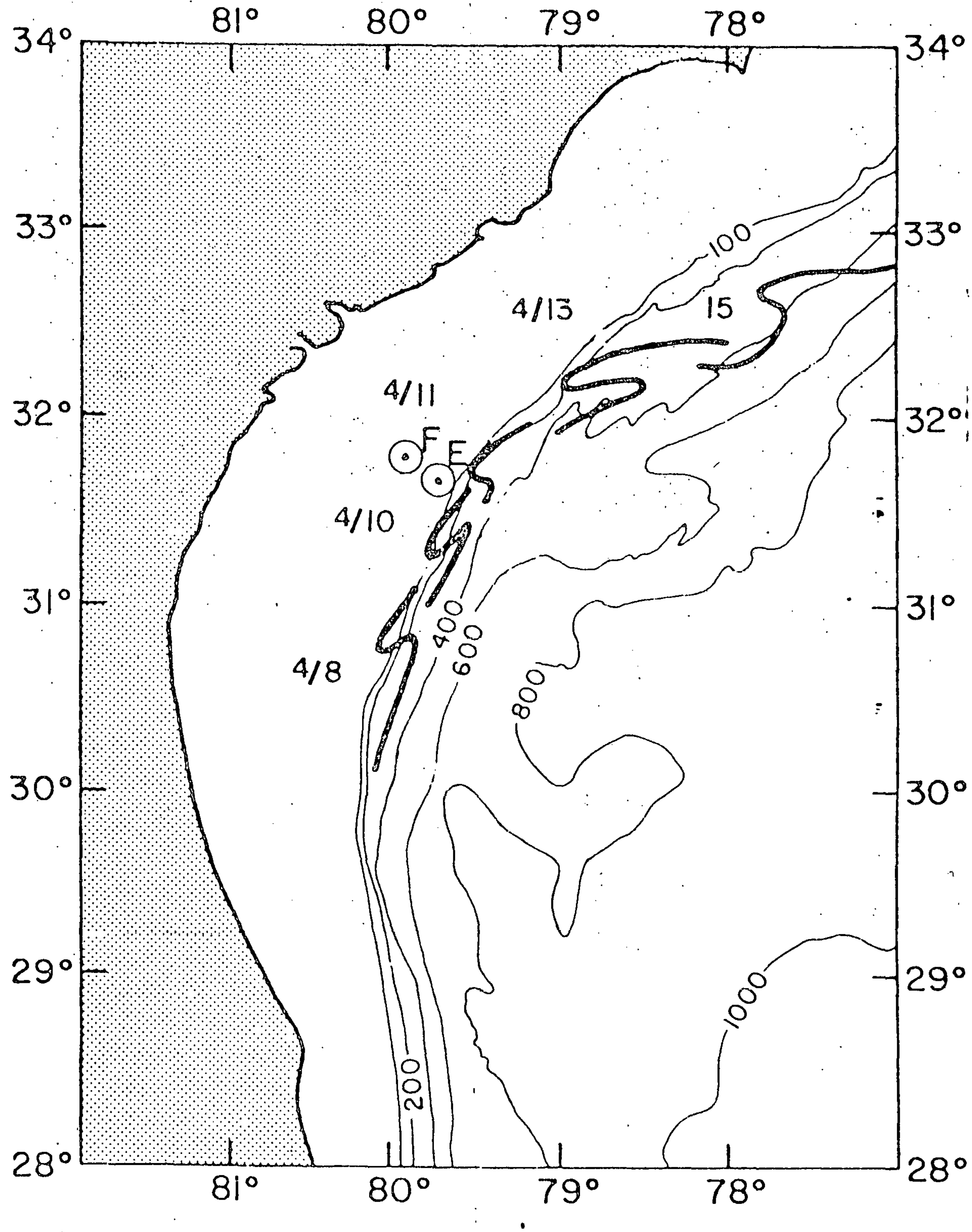

Fig. 10. Sequential positions of eddy E on April 8 to 15, taken from infrared VHRR images from NOAA-5 night (0200 GMT) orbits. Circles show the current meter locations.

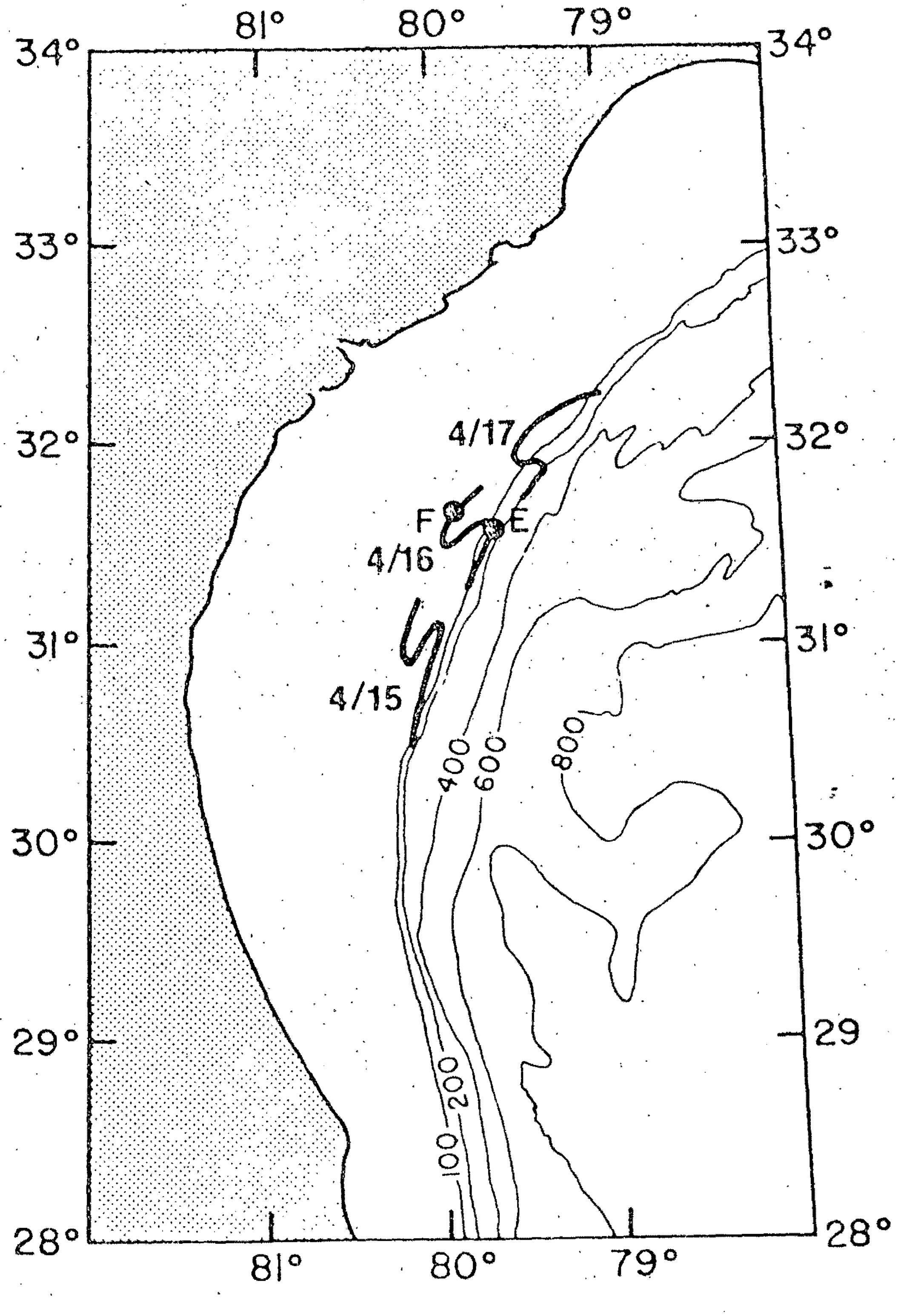

Fig. 11. Sequential positions of eddy F on April 15-17, taken from infrared VHRR images from NOAA-5 day (1400 GMT) orbits. Circles show the locations of current meters E and F.

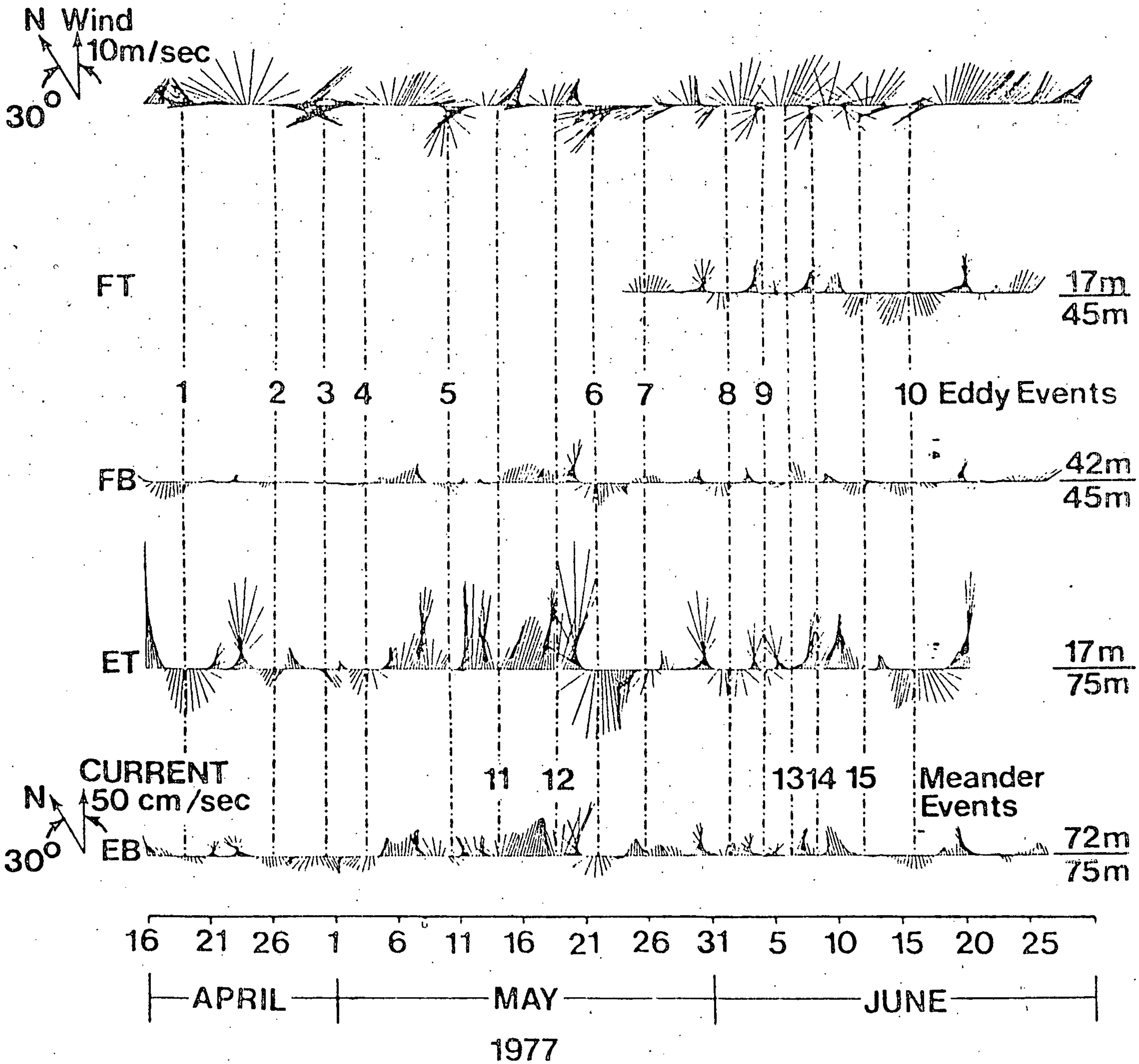

Fig. 12. Time series of 6-hourly, rotated current and wind vectors from 40-HLP filtered records for April 15 to June 29, 1977. Magnitude and rotation of wind and current vectors are shown by the scale arrows on the left. Instrument depth and water depth are shown on the right. Vertical lines are for eddy and meander event identification.

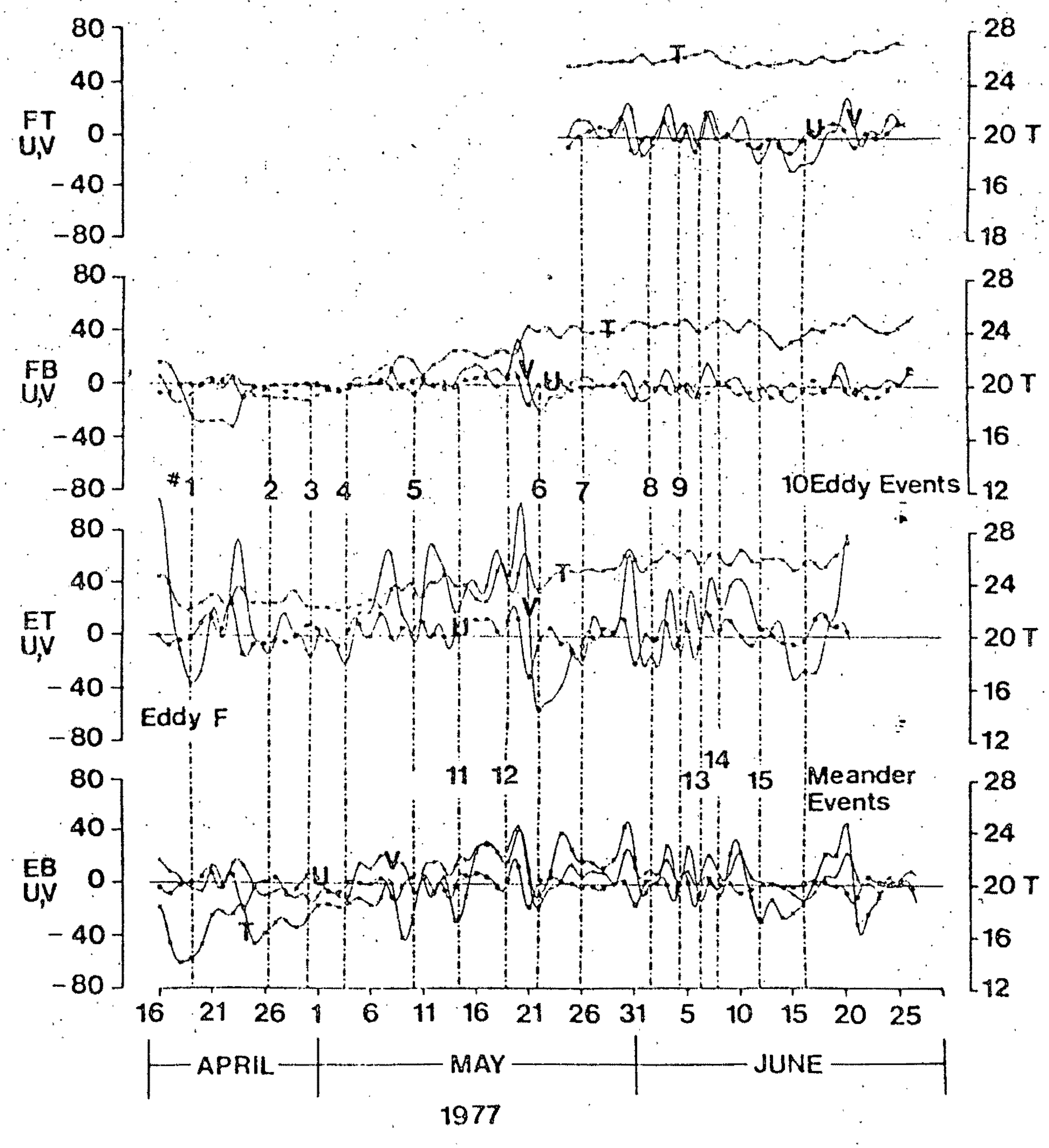

Fig. 13. Time series of rotated velocity components u (-O-O-O-), v (-+-+-+-), cm/sec, and temperature T (-X-X-X-), C, from 40-HLP filtered records for April 15 to June 29, 1977. Vertical lines are for eddy and meander event identification.

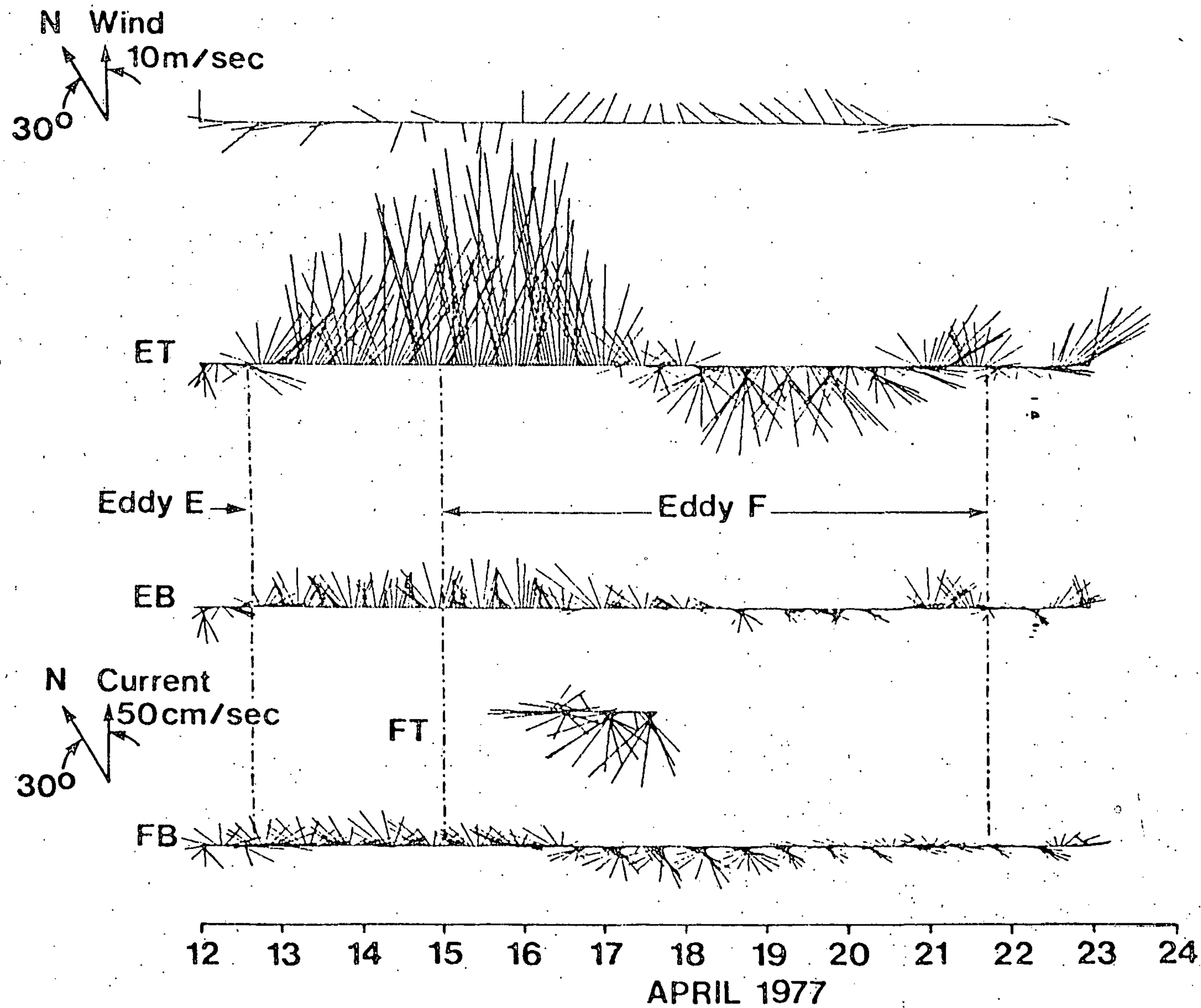

Fig. 14. Time series of 1-hourly, rotated current and wind vectors from 3-HLP filtered records for April 12-24, 1977. Magnitude and rotation of wind and current vectors are shown by the scale arrows on the left.

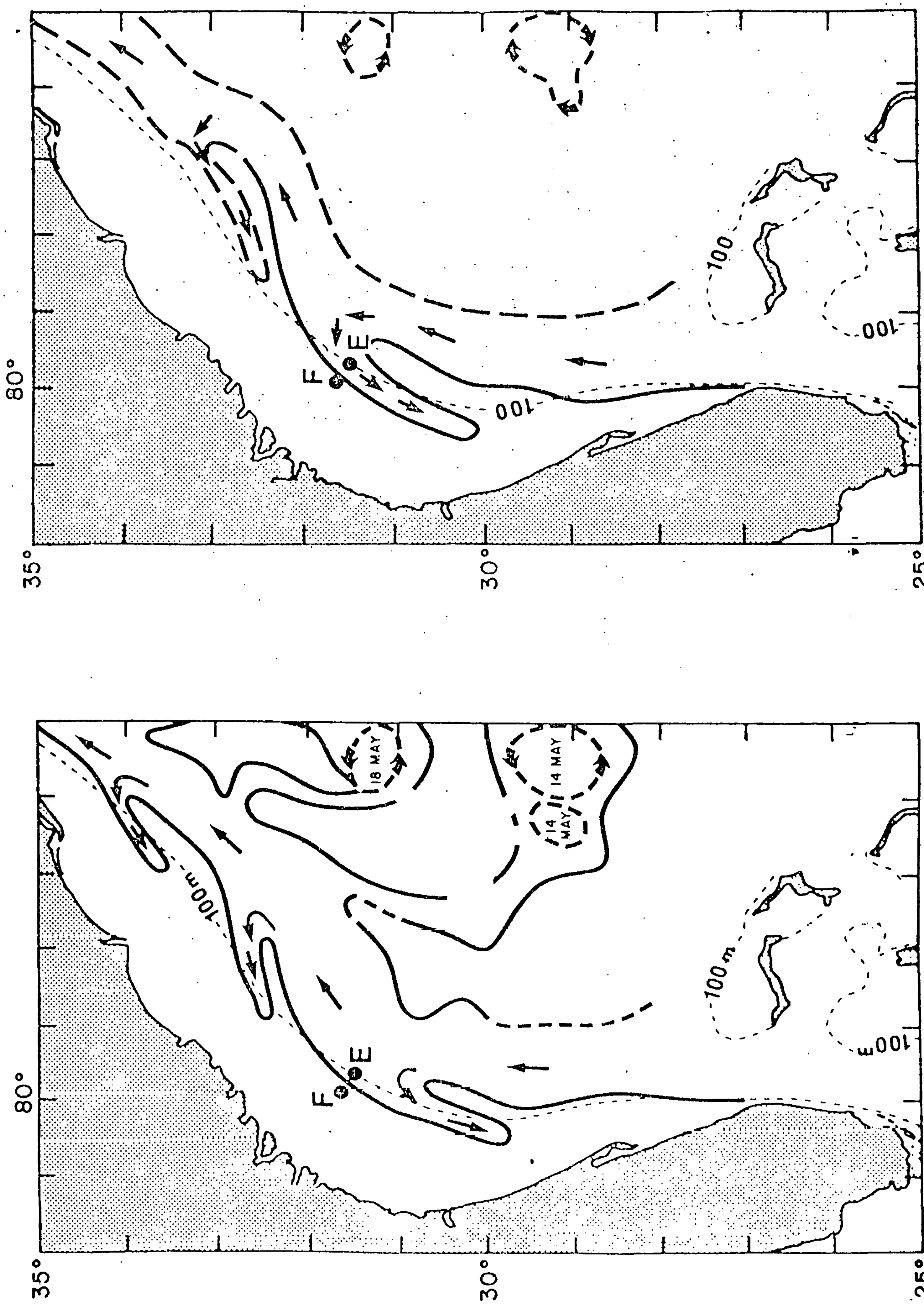

Fig. 15. Gulf Stream boundaries off the southeast U.S. as shown by U.S. Naval Oceanographic Office in Experimental Ocean Frontal Analysis charts for weeks of a) May 12-18, 1977, and b) May 19-25; arrows indicate current direction.

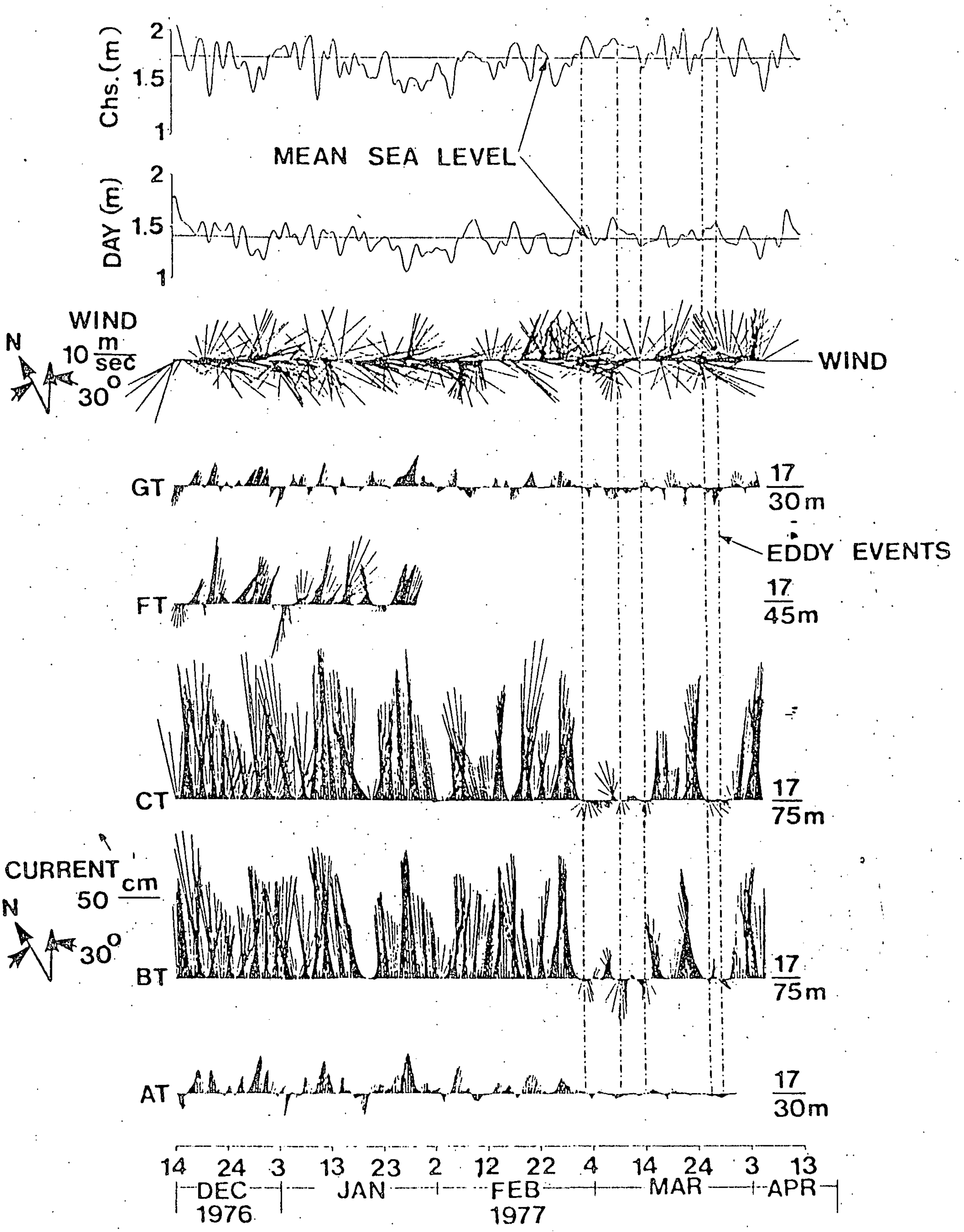

Fig. 16. Time series of 6-hourly, rotated current and wind vectors, and corrected sea level from Charleston (Chs.) and Daytona (Day.), 40-HLP filtered records for December 14, 1976, to April 6. Sea level corrected for atmospheric pressure by 1 mb pressure = 1.01 cm sea level. Magnitude and rotation of vectors shown by scale arrows on left. Instrument depth and water depth are shown on right. Vertical lines are for eddy event identification.

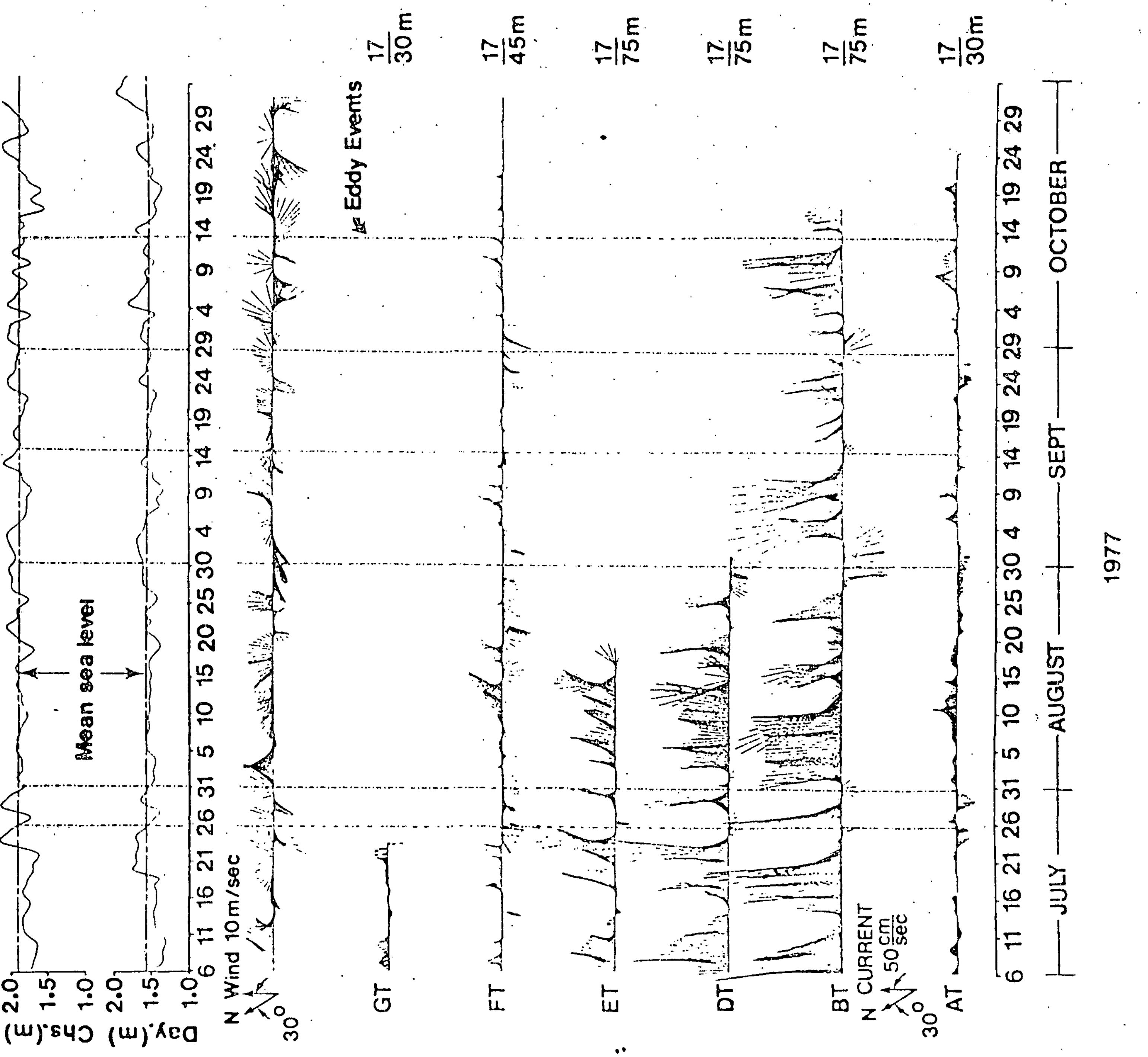

Fig. 17. Time series of 6-hourly, rotated current and wind vectors, and corrected sea level from Charleston (Chs.) and Daytona (Day.), 40-HLP filtered records for July 6, 1977 to October 31. Sea level corrected for atmospheric pressure by 1 mb pressure = 1.01 cm sea level. Magnitude and rotation of vectors shown by scale arrows on left. Instrument depth and water depth are shown on right. Vertical lines are for eddy event identification.

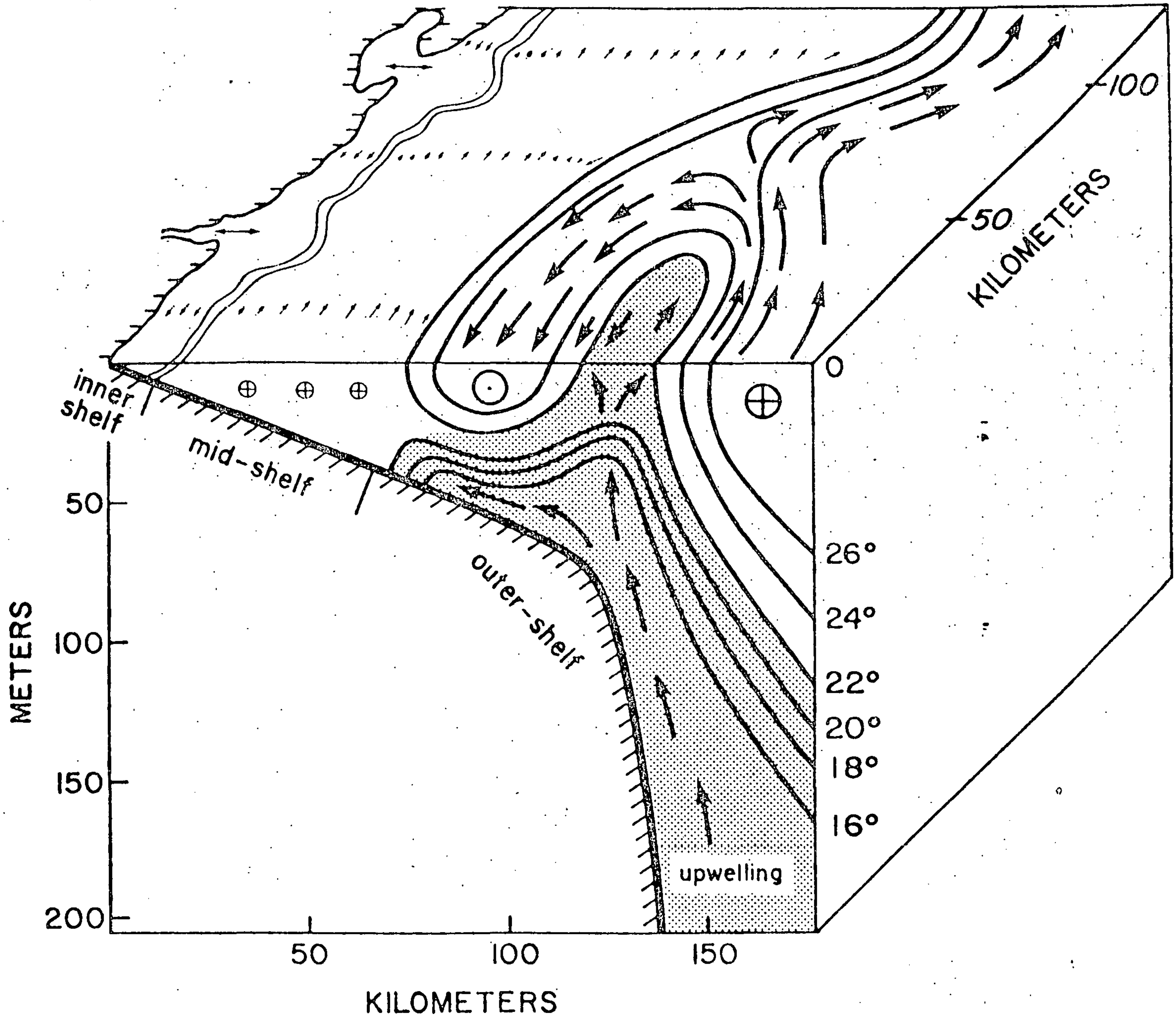

Fig. 18. Schematic characterization of a Gulf Stream frontal eddy on the Georgia shelf.

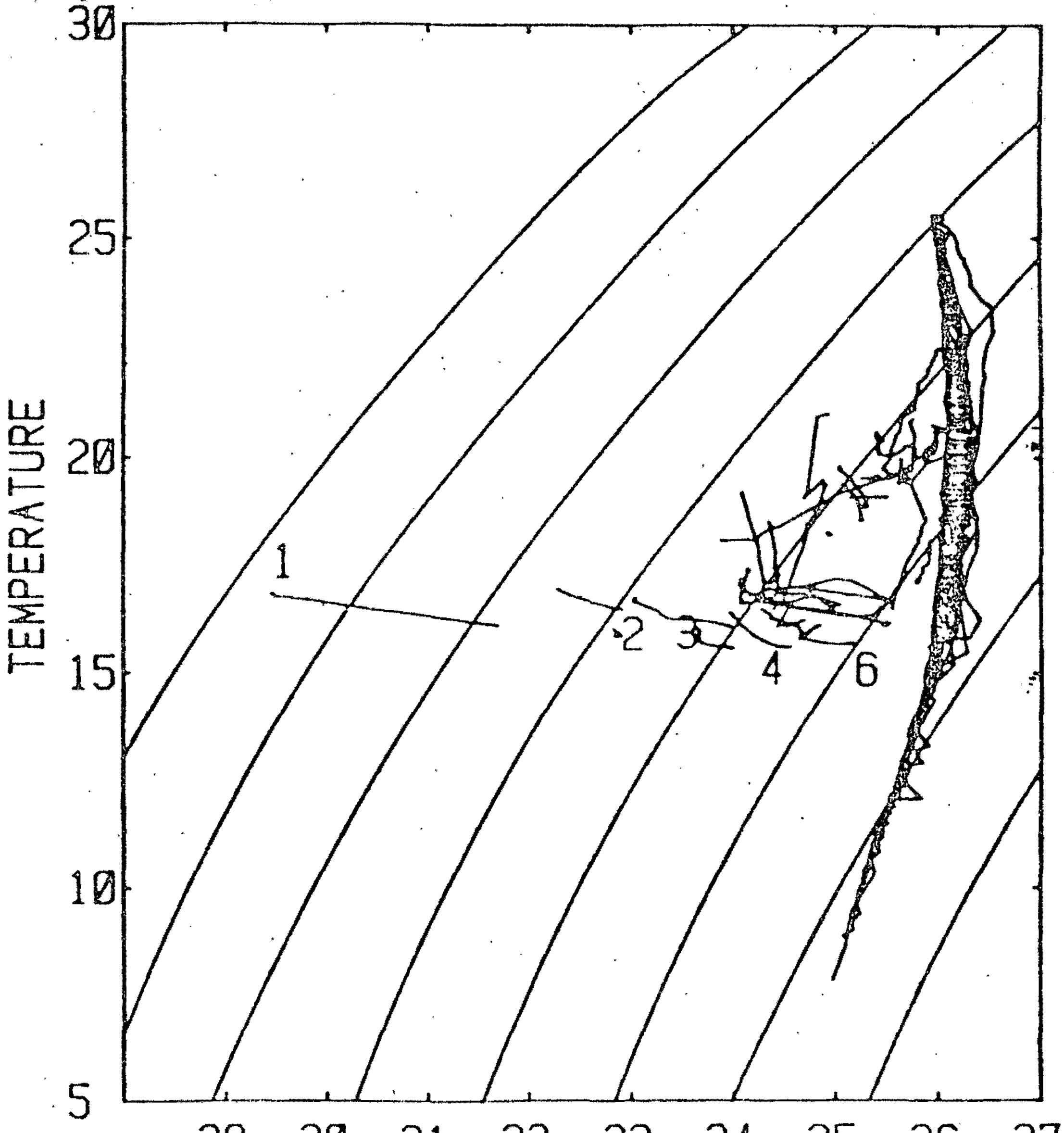

Fig. 19. Composite T-S plot of all hydrographic station data taken during April 8-16, 1977. Station numbers are given beside some of the identifiable shelf stations.

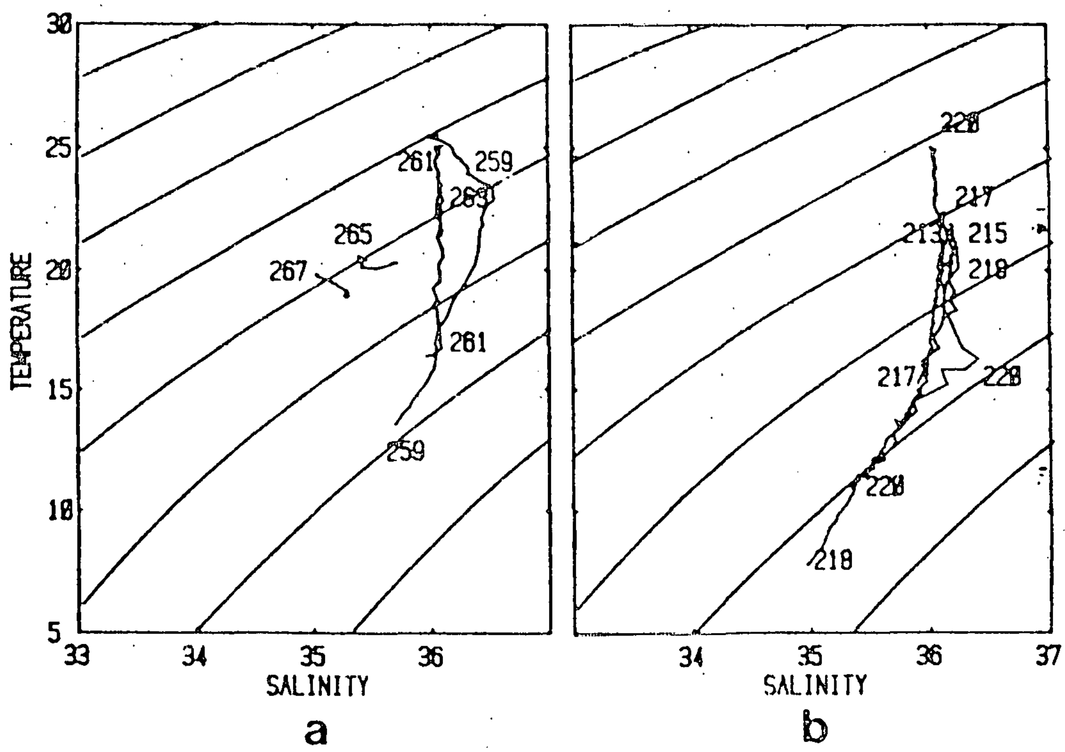

Fig. 20a. T-S distributions from stations of Savannah (4) section, April 16.

Fig. 20b. T-S distributions from stations of St. Augustine North section, April 15.

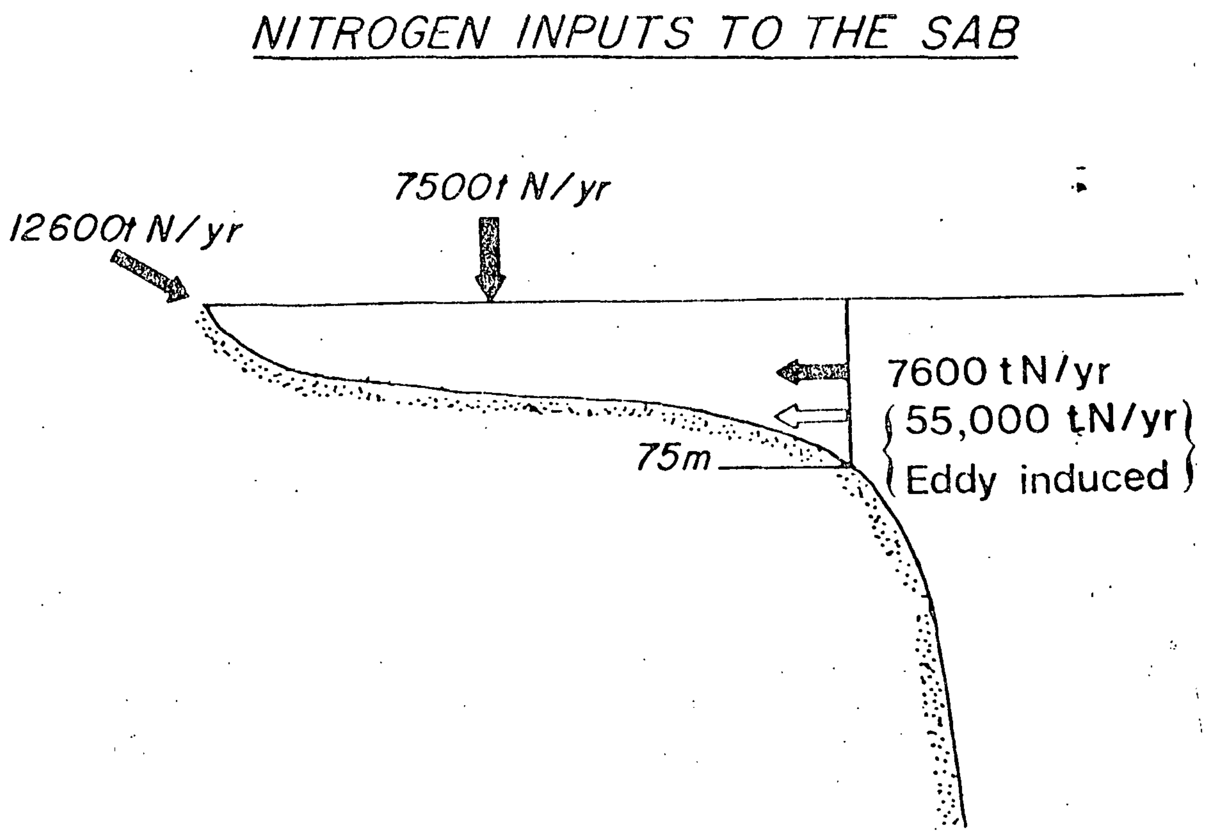

Fig. 21. Schematic of annual nitrogen inputs to the Georgia shelf as computed by HAINES (1974). Values are in tons of nitrogen per year. Arrows indicate flux direction. Our estimate of annual eddy induced flux is shown in parenthesis.

NATURAL FLUORESCENCE AS A TRACER FOR DISTINGUISHING BETWEEN PIEDMONT AND COASTAL PLAIN RIVER WATER IN THE NEARSHORE WATERS OF GEORGIA AND NORTH CAROLINA

Joan D. Willey

Marine Science Program and Department of Chemistry

P. O. Box 3725

University of North Carolina at Wilmington

Wilmington, North Carolina 28406

and

Larry P. Atkinson

Skidaway Institute of Oceanography

P. O. Box 13687

Savannah, Georgia 31406

Keywords: tracers; fluorescence; silica concentrations; salinity variations; humic substances; coastal waters; Georgia; North Carolina

Natural fluorescence, dissolved silica and salinity were investigated as possible tracers to distinguish between piedmont river and coastal plain river waters discharged into the ocean off North Carolina and Georgia. In the Georgia study area, dissolved silica was not suitable for use as a tracer because silica concentrations were variable and did not mix conservatively with seawater. In the North Carolina study area, dissolved silica concentrations exhibited too much short term variability for tracer use. In both areas, natural fluorescence was a suitable tracer. Additional investigations relevant to tracer application were made of the method for determining natural fluorescence; these include dependence on temperature of analysis; pH dependence, sample storage effect, sensitivity, correlation with total organic carbon, and possible interferences from chlorophyll-a, lignin sulfonates, petroleum, and iron.

Introduction

The purpose of this study was to investigate whether dissolved silica and natural fluorescence can be used to distinguish between coastal plain and piedmont river waters where they flow into the nearshore areas of Georgia and North Carolina. Rivers which originate in the piedmont area of the southeastern United States (the eastern margin of the Appalachian Mountains) flow down steeper gradients and so flow faster and tend to have higher suspended sediment loads and may therefore have higher concentrations of dissolved silica than coastal plain rivers. Coastal plain rivers originate in swamps and marshes on the flat coastal plain, are slower flowing rivers and tend to have higher organic matter content than piedmont rivers. Because of this, coastal plain rivers should have higher natural fluorescence than piedmont rivers.

Development of parameters which can be used as chemical tracers should allow better definition of circulation patterns in the nearshore area. This is of particular importance in industrialized areas like Savannah, Georgia, and Wilmington, North Carolina. Dissolved silica and natural fluorescence are of interest because they have the possibility of distinguishing between water from closely spaced individual rivers. This may allow better resolution on a small scale of water sources where other tracers are inadequate. For example, stable isotopes (oxygen-18 and deuterium) can be used to distinguish between water from the South Atlantic Bight, the Mid-Atlantic Bight and the Gulf of Maine, but because these tracers depend on climate (temperature), precise resolution is not possible (Torgerson, 1979). Natural fluorescence and dissolved silica may help to distinguish waters from different sources which experience the same climate.

A chemical tracer is defined as any chemical parameter that can be used to follow the movements and mixing of water from different sources. Dissolved silica has been used as a tracer in other areas (for example, Gardner, 1977; and Hunt, 1978), however, its use is limited because of biological utilization of dissolved silica (Fanning and Pilson, 1973a; Van Bennekom, et. al., 1974; and Hunt, 1978). Natural fluorescence, which in fresh water is thought to result from the presence of humic compounds (Kalle, 1963), has been used as a tracer by Kalle (1949) in the Gulfs of Bothnia and Finland, by Duursma (1961) in the Dutch Wadden Sea, and by Otto (1967) and Zimmerman and Rommets (1974) in the North Sea. In each case, natural fluorescence and salinity were negatively correlated, indicating conservative mixing.

Several criteria must be satisfied if a parameter is used as a chemical tracer (Zimmerman and Rommets, 1974). The concentration of the tracer must differ by at least a factor of two between the end members; the concentration of the tracer must remain constant in the end members over the time period of interest; and the tracer must mix conservatively with seawater. These criteria were evaluated in the present study for both dissolved silica and natural fluorescence in two areas, northeastern Georgia and southeastern North Carolina (Figure 1). The rivers studied in Georgia are the Savannah River, which is a piedmont river, and the Ogeechee plus Canooche River which are coastal plain rivers. The Canooche River drains into the Ogeechee River; both the Ogeechee and Savannah rivers discharge directly into the ocean near Savannah, Georgia. In North Carolina, the Cape Fear River, which is a piedmont river, and the Northeast Cape Fear River and the Black plus South Rivers which are coastal plain rivers were investigated. The South River drains into the Black River; the other three rivers flow into the Cape Fear River Estuary near Wilmington, North Carolina.

Sampling methods

Sampling in the Georgia study area was conducted on May 16 and 17, 1979. All samples were collected from a boat in or near the estuarine regions up to 4 km offshore. The intention was to obtain samples over a wide salinity range. This was achieved by measuring the salinity on board using a refractometer, and obtaining more precise salinities in the laboratory. Samples were also collected for analysis of dissolved silica and natural fluorescence.

The North Carolina study area was sampled during March, May and November of 1979, and during March and May of 1980. River water samples from up to 80 km west of the ocean were collected from bridges or docks, and seawater samples were collected from a boat 20 km east of Wrightsville Beach, North Carolina. All samples were analyzed for salinity, dissolved silica and natural fluorescence. The intention of this sampling was to define the tracer concentrations in the rivers, and to evaluate temporal variability.

Analytical methods

Dissolved silica was measured using the method of Strickland and Parsons (1972) as modified by Fanning and Pilson (1973b). Samples were frozen soon after collection and were stored frozen until analyzed.

Natural fluorescence was measured using the method of Kalle (1963). A standard solution of 0.1 mg/ℓ quinine bisulfate in 0.01N H_2SO_4 (0.236 μM quinine) was set to read 73 mFl relative to the 0.01N H_2SO_4 blank solution. Since samples were measured relative to this standard setting, fluorescence readings are not in absolute units (Duursma and Rommets, 1961). The excitation wavelength of 365 nm, and emission wavelength of 460 nm (Kalle, 1963), corresponded with the maxima for these river water samples. A Turner 430 spectrofluorometer was used to measure fluorescence; this is a monochromator and not a filter instrument so sensitivity is reduced but specificity is improved. On this instrument calibration required a scale expansion of X 10. To prevent internal quenching (self absorption by solutions which contain high concentrations of fluorescing material) samples which read greater than 100 mFl were diluted prior to analysis (Kalle, 1963, Duursma and Rommets, 1961). Another reason for diluting is that fluorescence is linear with respect to concentration only when a small fraction of the incident light is absorbed (St. John, 1973). The standard deviation of the quinine solution (73 mFl) based on 16 determinations was 1.8, corresponding to a relative error of 2.4%. Two North Carolina samples (33.8 and 71.3 mFl) analyzed 9 and 21 times over a one week period had relative errors of 4.5 and 2.6% respectively. All samples in the Georgia study were analyzed within two days of collection; North Carolina samples were analyzed within 24 hours of collection.

Electrode standardization of pH measurements was made relative to five buffer solutions with pH values between 4.00 and 9.18. pH adjustments were made when necessary by adding microliter quantities of 2N NaOH or 2N HCl. Field determinations of pH on North Carolina river water samples were made using short range pH paper.

The concentration of iron was adjusted in some solutions (Figure 9) by adding 20 microliter aliquots of 500 ppm iron stock solution ($FeCl_3$ in dilute HCl) to a 5 ml sample. The pH was adjusted after iron was added. Iron concentrations were calculated from the amount of iron added.

Total organic carbon was analyzed by the method of MacKinnon (1978).

Humic acid was extracted from a sediment sample from the Cape Fear River Estuary using the method of Cheshire, et. al. (1977). The sample was not desalted or purified.

Results

Dissolved silica

Dissolved silica in both study areas was too variable to be used as a tracer (Table 1). Dissolved silica in the Savannah River mixed conservatively with seawater ($r = -0.718$ and $P = 0.001$ for 30 data pairs) but that from the Ogeechee River did not ($r = 0.420$ and $P = 0.05$ for 28 data pairs) (Figures 2 and 3). The positive correlation coefficient for the Ogeechee River indicates that dissolved silica is increasing with salinity. In the North Carolina study area, dissolved silica differed significantly between the coastal plain and piedmont rivers, as in the Georgia area, however, during a short term variability study conducted for ten days in March of 1980 dissolved silica in the Cape Fear River varied by more than a factor of two between morning and afternoon samplings on the same day. Since the Cape Fear River is the major river in the area, this variability limits the usefulness of dissolved silica as a tracer. Coastal plain and piedmont rivers had large differences in silica concentrations, so use as a tracer during the winter months when biological activity is low may be possible.

Natural fluorescence

Natural fluorescence in both the Georgia rivers mixed conservatively with seawater (Figures 4 and 5) and the values for the two rivers differed by slightly more than the necessary factor of two making it a potential tracer. The correlation coefficient between salinity and natural fluorescence was -0.983 for 30 data pairs ($P > .001$) in the Savannah River and -0.996 for 28 data pairs ($P > .001$) in the Ogeechee River. Conservative behavior suggests that time variability was not a problem during the two day sampling time. According to Loder and Reichard (1980) any variation in the river end member will give apparent non-conservative mixing behavior. In the North Carolina study area, the difference between the natural fluorescence of coastal plain and piedmont rivers was also great enough to be useful as a tracer (Table 1), and short term variability in each river was small. Seawater from both study areas also had very low fluorescence values relative to the river waters. Natural fluorescence should therefore be a useful tracer to distinguish between coastal plain and piedmont river waters.

Because natural fluorescence can be used as a tracer in these study areas and perhaps also in other areas, other investigations were conducted to evaluate the method for tracer applications. The objective was to identify potential problems with the method before undertaking a more extensive use of fluorescence as a tracer. The following possibilities were considered:

1. Temperature dependence: The natural fluorescence of two samples and of the quinine standard (Figures 6 and 7) depended on the temperature at which the analyses were made. Fortunately, the maximum sensitivity in both cases occurred between 21 and 25°C. St. John (1973) attributes this effect at temperatures above room temperature to increasing efficiency of nonradiative deactivation (collisional quenching and vibrational deactivation) with increasing temperature. A competing process of delayed fluorescence becomes more important with decreasing temperature which may explain non-linear behavior. This temperature effect means that samples and standards should be near room temperature in order to achieve maximum sensitivity and precision, and all standards and samples should be at the same temperature to give comparable results.

2. pH dependence: Black and Christman (1963) found higher fluorescence in a sample of Suwannee River (Georgia) water at pH 11.0 than at pH 5.5, which may reflect changes in the protonation of humic acids. Dependence on pH was observed for a Black River (North Carolina) sample, however, insignificant effects were observed in a humic acid solution which contained approximately 80 mg/ℓ humic acids (Figure 8). In an earlier investigation, an excitation wavelength of 340 rather than 365 nm was used and a pH effect similar to that observed for the river water sample was observed for the same humic acid sample. This suggests that a pH effect may be observed with a filter fluorimeter which allows a broader range of energy to irradiate the sample. 340 nm is close to the excitation wavelength maximum for this humic acid sample, whereas for the river water samples the excitation wavelength maximum is 365 nm. Although pH effects could be significant in some areas, in the 62 North Carolina samples pH did not vary significantly from 6.6. pH was not monitored in the Georgia samples, however, the expected range of between 6 and 8 should cause a negligible effect relative to the changes caused by mixing with seawater.

3. Sample Storage Effect: The natural fluorescence of four samples increased between 5 and 25% with storage for two weeks (frozen or refrigerated and in glass or plastic bottles). Deionized water stored in similar conditions showed no fluorescence increase, so the increase is probably not a container effect. Samples had a constant fluorescence value for at least a month after this initial increase. Martin and Pierce (1971) also observed an increase in the concentration of humic acids after samples were stored frozen for two months, however, the increase was

close to the precision of the analysis.

4. Sensitivity: North Carolina river water was diluted with deionized water, artificial seawater and natural seawater to determine the lower detection limit. One part river water could be detected in 200 parts of natural seawater or in 500 parts of artificial seawater or deionized water. Scale expansion of 300x was required for this reading to be obtained. The detection limit for a tracer application is probably not instrumental, but rather would be set by the background Raman scattering of water (St. John, 1973) and the background natural fluorescence of seawater (Duursma, 1974).

5. Filtration Effect: Filtration of samples through a 0.45 micrometer pore size Millipore filter resulted in an increase of between 1 and 7% fluorescence for six North Carolina samples. Since no major changes were observed, filtration is not necessary.

6. Correlation with Total Organic Carbon: No correlation was observed between natural fluorescence (100, 78, 36, and 56 mFl) and total organic carbon (6.5, 13.5, 5.0, and 6.0 mgC/ℓ total organic carbon, respectively) for four Cape Fear River samples. This suggests that the fluorescing material was a major part of the organic material present.

7. Possible Interferences:

   a. Chlorophyll-a: A solution of 1.0 mg/ℓ pure chlorophyll-a from Sigma Chemical, and characterized by the spectrophotometric method of Strickland and Parsons (1972) was prepared in 90% water - 10% acetone. This solution gave no fluorescence reading at the wavelengths appropriate for measurement of natural fluorescence (365 and 460 nm compared with the 436 nm and greater than 660 nm maxima for chlorophyll-a). Acidified chlorophyll-a (pheophytin) also gave no signal at the natural fluorescence wavelength settings. The chlorophyll-a solution, when added to a river water sample, caused no fluorescence decrease other than by simple dilution of the river water, so absorption by chlorophyll-a is also negligible. Duursma (1965) reported that natural fluorescence did not correlate with chlorophyll, organic carbon, or organic nitrogen in the North Sea, which also suggests no analytical interferences from chlorophyll or total organic carbon.

b. Lignin sulfonates: Lignin sulfonate in water can be measured analytically by fluorescence (Christman and Minear, 1967). From the spectra provided, these compounds should not fluoresce significantly at the wavelengths used in the natural fluorescence measurements. Kraft mill effluent, unlike effluent from sulfite processing, is not significantly fluorescent (St. John, 1973). Neither kind of effluent should therefore affect analysis of natural fluorescence.

c. Petroleum: A mixture of approximately 80 mg/ℓ of 30 weight lubricating oil in deionized water had a fluorescence of between 150 and 300 mFl relative to the 73 mFl for the quinine standard. Similar high values were obtained for a mixed gasoline:oil (50:1) sample and a suspension of mixed gasoline and oil in water. In each some oil was clearly visible as a surface film or as a sheen on the glassware. These results indicate that natural fluorescence as a tracer is limited to areas which do not have a high input of oil.

d. Iron: Iron in mg/ℓ amounts can cause low results in the analysis of humic acids by spectrophotometric or fluorimetric methods (Brun and Milburn, 1977). This presumably results from complexation of iron by humic compounds. This was substantiated in this study for two North Carolina river water samples and for a humic acid sample (Figures 9 and 10). However, variation in iron concentration should not cause a problem in these North Carolina rivers with respect to using natural fluorescence as a tracer because the maximum iron concentration observed during a 15 year monthly sampling program was 0.94 mg/ℓ (Wilder and Slack, 1971). Average values reported in the Wilder and Slack (1971) study for the Cape Fear, Black and Northeast Cape Fear Rivers are 0.06, 0.21, and 0.25 mg/ℓ,, low enough to prevent significant variations in fluorescence. Brun and Milburn (1977), in analyzing for humic acids, eliminate iron interference by adding a tartrate-citrate complexing agent to complex the iron before analysis.

The advantages of using natural fluorescence as a tracer, even with the above complications, are that it is a rapid and inexpensive analysis which has good sensitivity and high specificity. Most compounds are not fluorescent. The probability of having more than one compound which both have the same excitation and emission spectra is low compared with a spectrophotometric method in which only one wavelength is used. Fluorometry has the additional advantage of scale expansion over several orders of magnitude compared with a usually much smaller range for spectrophotometry.

Conclusions

Natural fluorescence and salinity can distinguish between coastal plain and piedmont rivers as they mix with seawater in southeastern North Carolina and in northeastern Georgia. Using the matrix method of Zimmerman and Rommets (1974), the relative contribution from each source can be calculated. Natural fluorescence may also be applicable as a tracer in other areas if the limitations of the method are appreciated. This method of tracing individual river waters may prove to be most useful when used in conjunction with other tracers. For example, deuterium or oxygen-18 could be used for large scale information (Torgerson, 1979), with natural fluorescence providing better resolution on a small scale.

Acknowledgements

The authors would like to thank D. Menzel for critical comments. This research was supported by Department of Energy Contract EY-76-S-09-0889 to L. P. Atkinson and by a North Carolina University Marine Science Council grant to J. D. Willey.

References

Black, A. P. and Christman, R. F. 1963 Characteristics of colored surface waters. Journal of the American Water Works Association 53: 753-770.

Brun, G. L. and Milburn, D. L. D. 1977 Automated fluorometric determination of humic substances in natural waters. Analytical Letters 10(14): 1209-1219.

Cheshire, M. V., Berrow, M. L., Goodman, B. A., and Mundie, C. M. 1977 Metal distribution and nature of some Cu, Mn and V complexes in humic and fulvic acid fractions of soil matter. Geochimica et Cosmochimica Acta 41: 1134-1138.

Christman, R. F. and Minear, R. A. 1967 Fluorometric Detection of Lignin sulfonates. The Trend in Engineering 19(1): 3-7.

Duursma, E. K. 1961 Dissolved organic carbon, nitrogen and phosphorous in the sea. Netherlands Journal of Sea Research 1: 1-148.

Duursma, E. K. 1965 The dissolved organic constituents of sea water. In Chemical Oceanography, Volume 1 (Riley, J. P. and Skirrow, G., eds.) Academic Press, New York, pp. 433-477.

Duursma, E. K. 1974 The fluorescence of dissolved organic matter in the sea. In Optical Aspects of Oceanography (Jerlov, N. G. and Steeman—Neilsen, E., eds.) Academic Press, London, pp. 237-256.

Duursma, E. K. and Rommets, J. W. 1961 Interpretation mathematique de la fluorescence des eaux douces, saumatres et marines. Netherlands Journal of Sea Research 1 (3): 391-405.

Fanning, K. A. and Pilson, M. E. 1973a The lack of inorganic removal of dissolved silica during river-ocean mixing. Geochimica et Cosmochimica Acta 37: 2405-2415.

Fanning, K. A. and Pilson, M. E. 1973b On the spectrophotometric determination of dissolved silica in natural waters. Analytical Chemistry 45: 136-139.

Gardner, D. 1977 Nutrients as tracers of water mass structure in the coastal upwelling off northwest Africa. In A Voyage of Discovery (M. Angel, ed.) Pergamon Press, Oxford, England, pp. 305-326.

Hunt, D. J. E. 1978 Studies of the mixing of coastal waters in Liverpool Bay using dissolved silica as a tracer. Water Research 11(5): 465-470.

Kalle, K. 1949 Fluoreszenz und Gelbstoff im Bottnischen und Finnischen Meerbusen. Deutsche Hydrographische Zeitschrift 2 (4): 9-124.

Kalle, K. 1963 Uber das verhalten und die herkunft der un den Gewassern und in der atmosphare vorhandenen himmelblauen Fluoreszenz. Deutsche Hydrographische Zeitschrift 16(4): 153-166.

Loder, T. C. and Reichard, R. P. 1980 The dynamics of conservative mixing in estuaries. Estuaries, in press.

MacKinnon, M. D. 1978 A dry oxidation method for the analysis of the TOC in seawater. Marine Chemistry 7: 17-37.

Martin, D. F. and Pierce, R. H. 1971 A convenient method of analysis of humic acid in fresh water. Environmental Letters 1(1): 49-52.

Otto, L. 1967 Investigations on optical properties and water masses of the southern North Sea. Netherlands Journal of Sea Research 3(4): 532-551.

St. John, P. A. 1973 Luminescence techniques in water analysis. In Water and Water Pollution Handbook, Vol. 4 (L. L. Ciaccio, ed.) Marcel Dekker, Inc., New York, pp. 1687-1751.

Strickland, J. D. H. and Parson, T. R. 1972 A Practical Handbook of Seawater Analysis. Fisheries Research Board of Canada Bulletin 167, 310 p.

Torgerson, T. 1979 Isotopic composition of river runoff on the U. S. east coast: Evaluation of stable isotope versus salinity plots for coastal water mass identification. Journal of Geophysical Research 84(c7): 3773-3775.

Van Bennekom, A. J., Krijgsman-Van Hartingsveld, E., Van Der Veer, G. C. M., and Van Voorst, H. F. J. 1974 The seasonal cycles of reactive silicate and suspended diatoms in the Dutch Wadden Sea. Netherlands Journal of Sea Research 8(2-3): 174-207.

Wilder, H. B. and Slack, L. J. 1971 Summary of data on chemical quality of streams in North Carolina. U. S. Geological Survey Water-Supply Paper 1895-B, 236 p.

Zimmerman, J. T. F. and Rommets, J. W. 1974 Natural fluorescence as a tracer in the Dutch Wadden Sea and the adjacent North Sea. Netherlands Journal of Sea Research 8(2-3): 117-125.

Table 1. Average values ($\overline{X}$) for natural fluorescence (mFl) and for dissolved silica (µM) based on n samples for the various water types listed. The symbol σ indicates the standard deviation. The Georgia coastal water salinity was 30 $^o/_{oo}$; the North Carolina seawater salinity was 35 $^o/_{oo}$.

	Natural Fluorescence, mFl			Dissolved Silica µM		
	n	$\overline{X}$	σ	n	$\overline{X}$	σ
Savannah River	2	55	0	2	49	18
Ogeechee River	2	114	1	2	12	2
Georgia Coastal Water	3	2	4	3	7	5
Cape Fear River	19	37	4	19	42	26
Black River	11	71	8	10	5	4
Northeast Cape Fear River	19	75	11	15	9	9
North Carolina Seawater	2	1	1	6	1.0	0.4

Figure captions

Figure 1. Study area, including the fall line(--------) which separates the piedmont from the coastal plain region. The locations of the rivers investigated are shown.

Figure 2. Dissolved silica, μM, plotted versus salinity, parts per thousand, for water samples taken from the Savannah River Estuary. The line drawn is the least squares regression line.

Figure 3. Dissolved silica, μM, plotted versus salinity, parts per thousand, for water samples taken from the Ogeechee River Estuary. The line drawn is the least squares regression line.

Figure 4. Natural fluorescence, mFl, plotted versus salinity, parts per thousand, for water samples collected from the Savannah River Estuary. The line drawn is the least squares regression line.

Figure 5. Natural fluorescence, mFl, plotted versus salinity, parts per thousand, for water samples collected from the Ogeechee River Estuary. The line drawn is the least squares regression line.

Figure 6. Natural fluorescence, mFl, plotted versus temperature of analysis, ^{o}C, for a 0.1 mg/ℓ solution of quinine bisulfate in 0.01 N sulfuric acid.

Figure 7. Natural fluorescence, mFl, plotted versus temperature of analysis, ^{o}C, for two North Carolina river samples (indicated by X and □).

Figure 8. Natural fluorescence, mFl, plotted versus solution pH for an 80 mg/ℓ humic acid sample (Δ) and for one North Carolina river water sample (X).

Figure 9. Natural fluorescence, mFl, plotted versus concentration of iron, parts per million, for a humic acid sample (80 ppm humic acid). The solution pH was 8.2 ± 0.2, and the initial iron concentration was less than 1 mg/ℓ. A cloudy red precipitate became apparent after 60 mg/ℓ of iron had been added to the solution.

Figure 10. Natural fluorescence, mFl, plotted versus the concentration of iron, parts per million, in two North Carolina river water samples (indicated by X and ∇). The solution pH in each case was 6.9 ± 0.3, and the initial concentration of iron was less than 1 ppm. In one sample (X), a cloudy red precipitate appeared after addition of 20 ppm Fe; in the other sample (∇) this precipitate was observed after addition of only 8 ppm Fe.

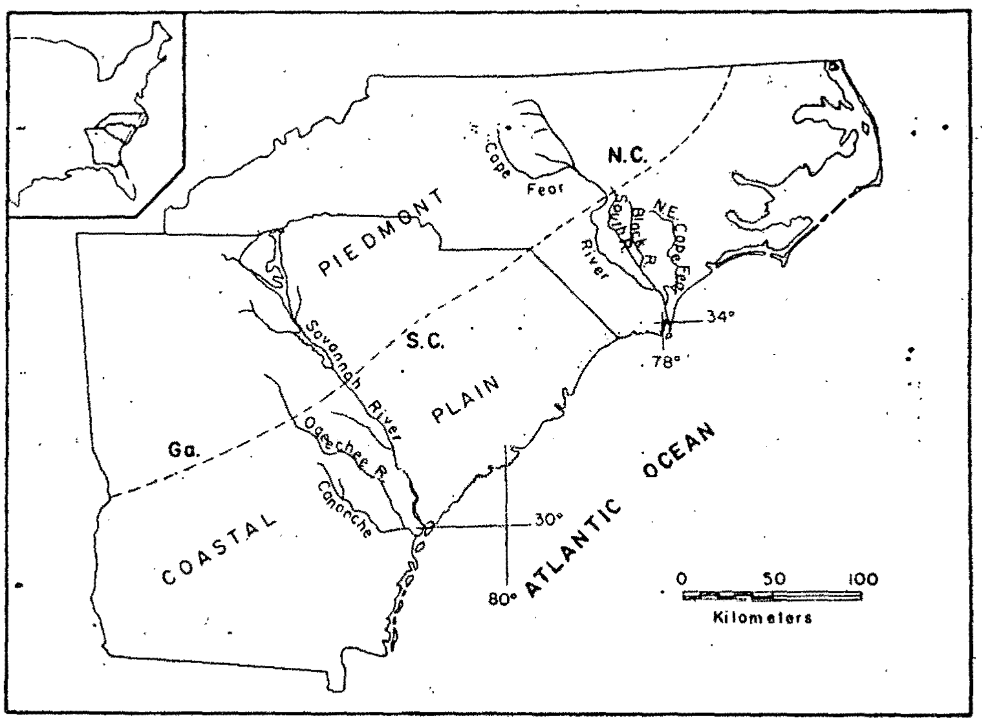
N.C.
Cape Fear
South R.
Black R.
NE Cape Fear
River
PIEDMONT
S.C.
PLAIN
Savannah River
Ogeechee R.
Canoochee
Ga.
COASTAL
ATLANTIC OCEAN
34°
78°
30°
80°
0 50 100
Kilometers

Figure 1

2

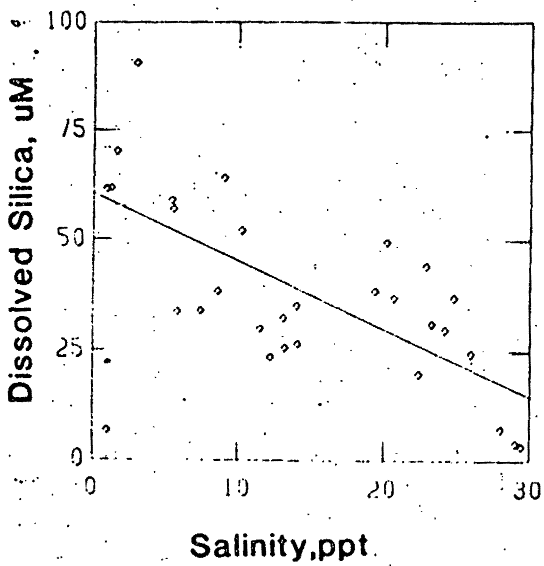
Dissolved Silica, uM
100
75
50
25
0
0
10
20
30
Salinity,ppt

3

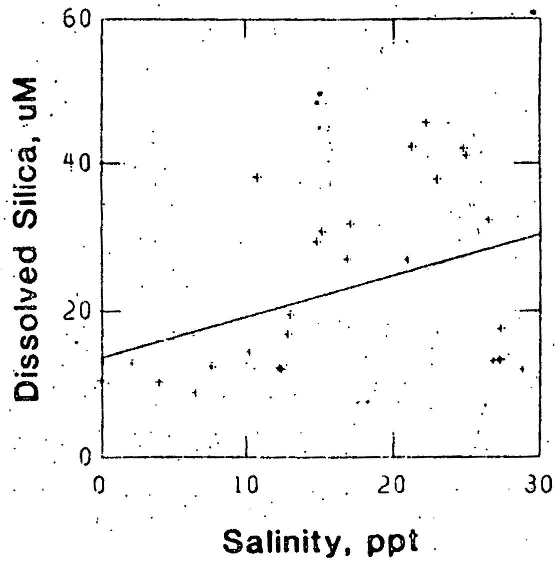
Dissolved Silica, uM
60
40
20
0
0
10
20
30
Salinity, ppt

5

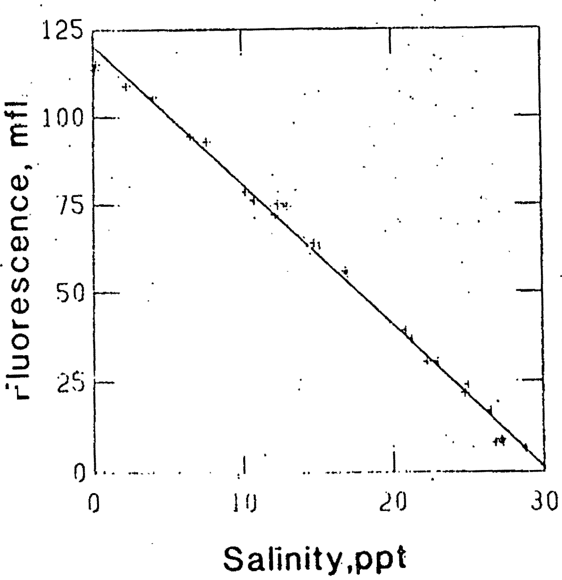
Fluorescence, mfl
125
100
75
50
25
0
0
10
20
30
Salinity,ppt

4

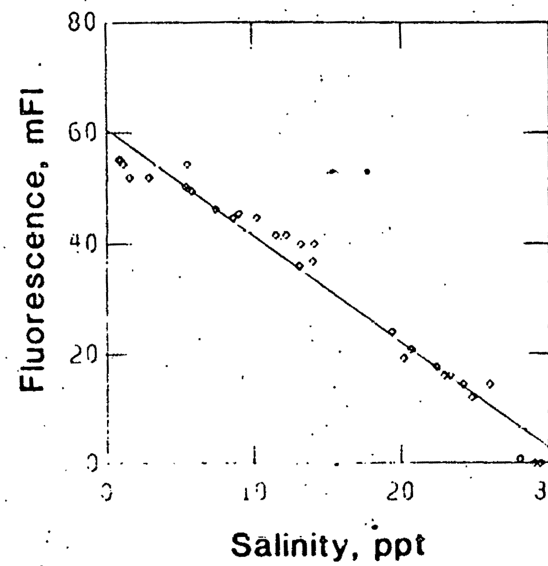
Fluorescence, mFl
80
60
40
20
0
0
10
20
30
Salinity, ppt

7

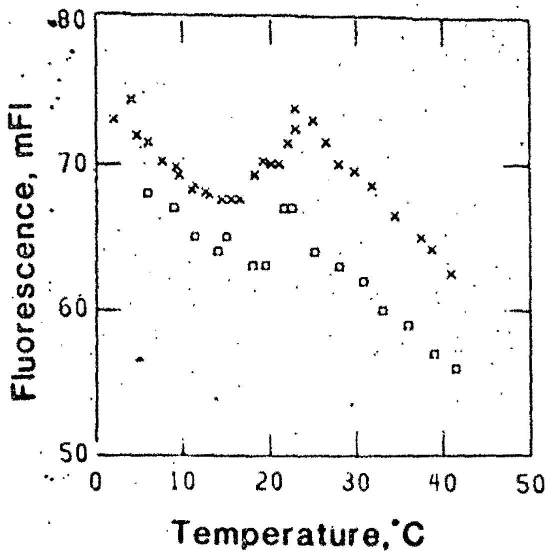

Fluorescence, mFI
80
70
60
50
0
10
20
30
40
50
Temperature, °C

6

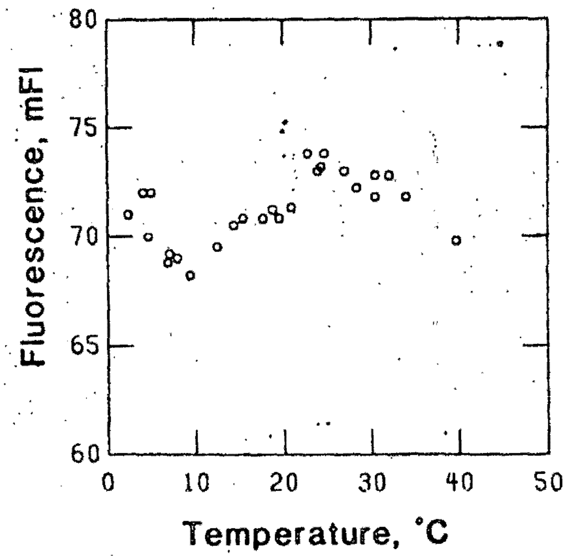

Fluorescence, mFI
80
75
70
65
60
0
10
20
30
40
50
Temperature, °C

8

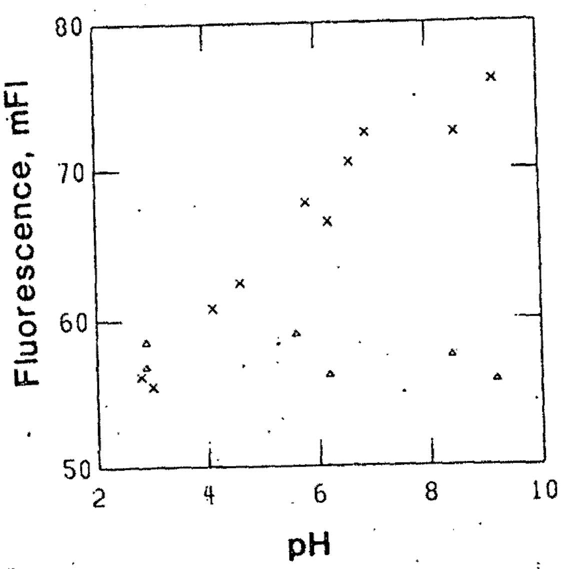

Fluorescence, mFI
80
70
60
50
2
4
6
8
10
pH

9

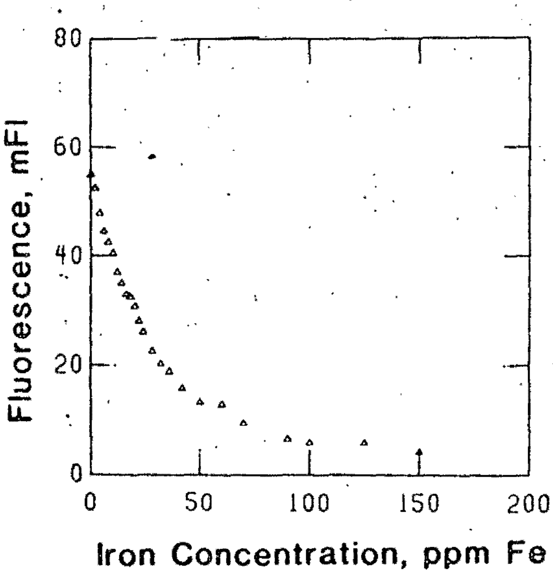
80
60
40
20
0
0
50
100
150
200
Fluorescence, mFI
Iron Concentration, ppm Fe

10

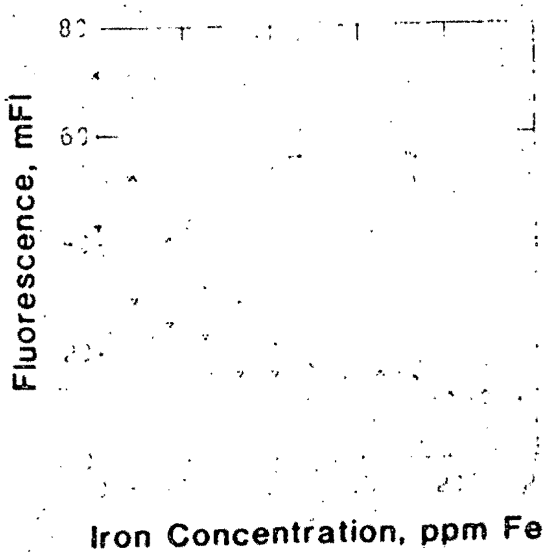
Fluorescence, mFI
Iron Concentration, ppm Fe

Figure 2

PLOT (18410009)
WILLEY
07/02/80 10:54:18

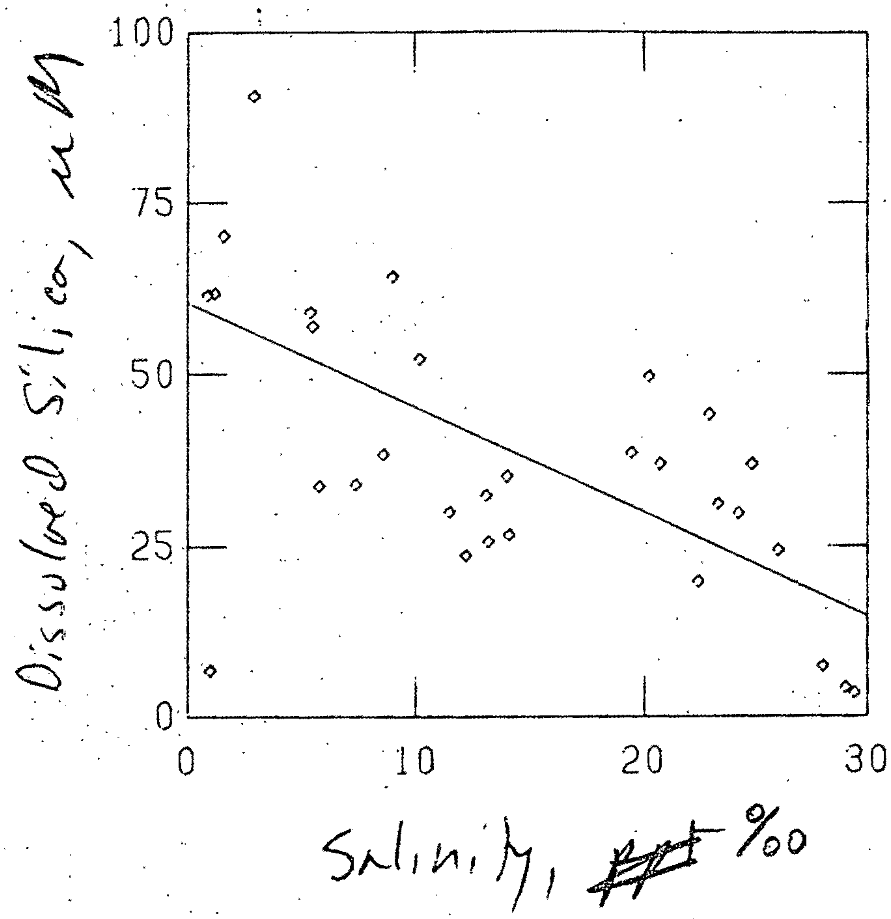

PLOT (18410009)
WILLEY
RECORDS PLOTTED = 320

PLOT (18411053)
WILLEY
07/02/80 11:03:29

Figure 3

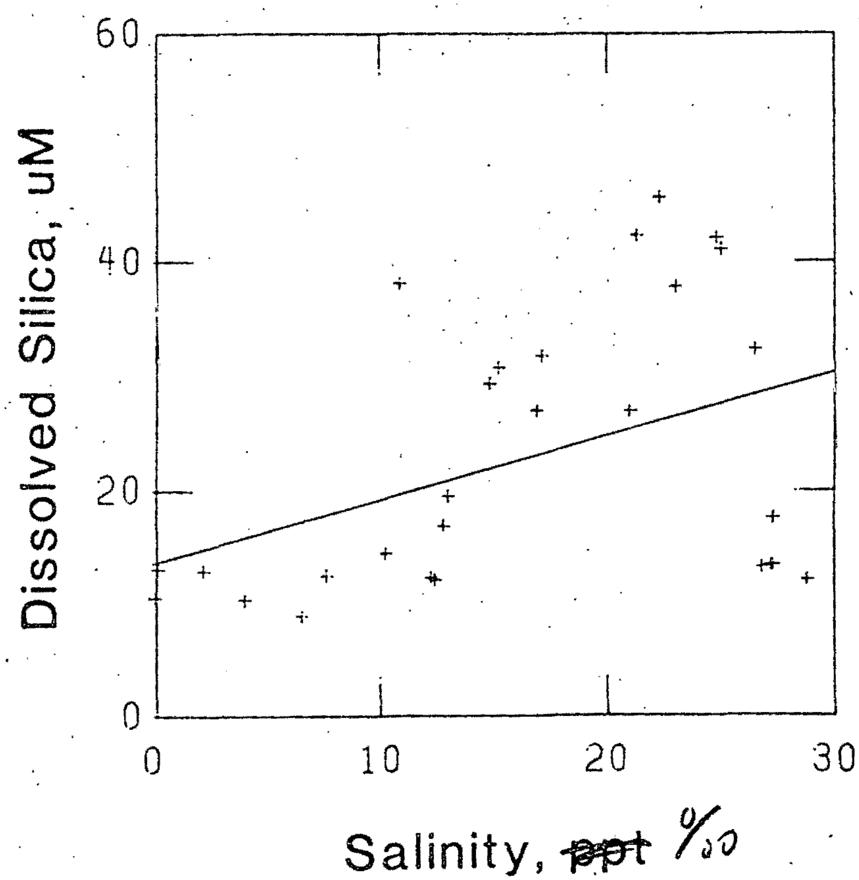

PLOT (18411053)
WILLEY

Figure 4

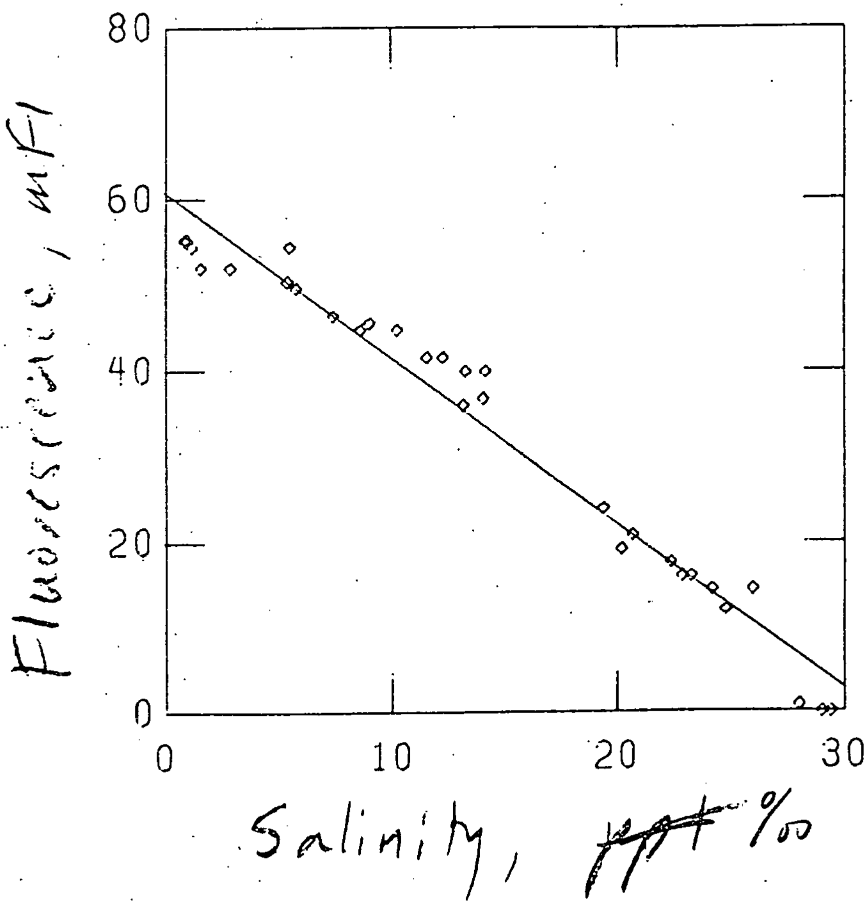

PLOT (18410059)
WILLEY
07/02/80 10:54:38

PLOT (18410059)
WILLEY
RECORDS PLOTTED = 296

Figure 5

PLOT (18411043)
WILLEY
07/02/80 11:03:41

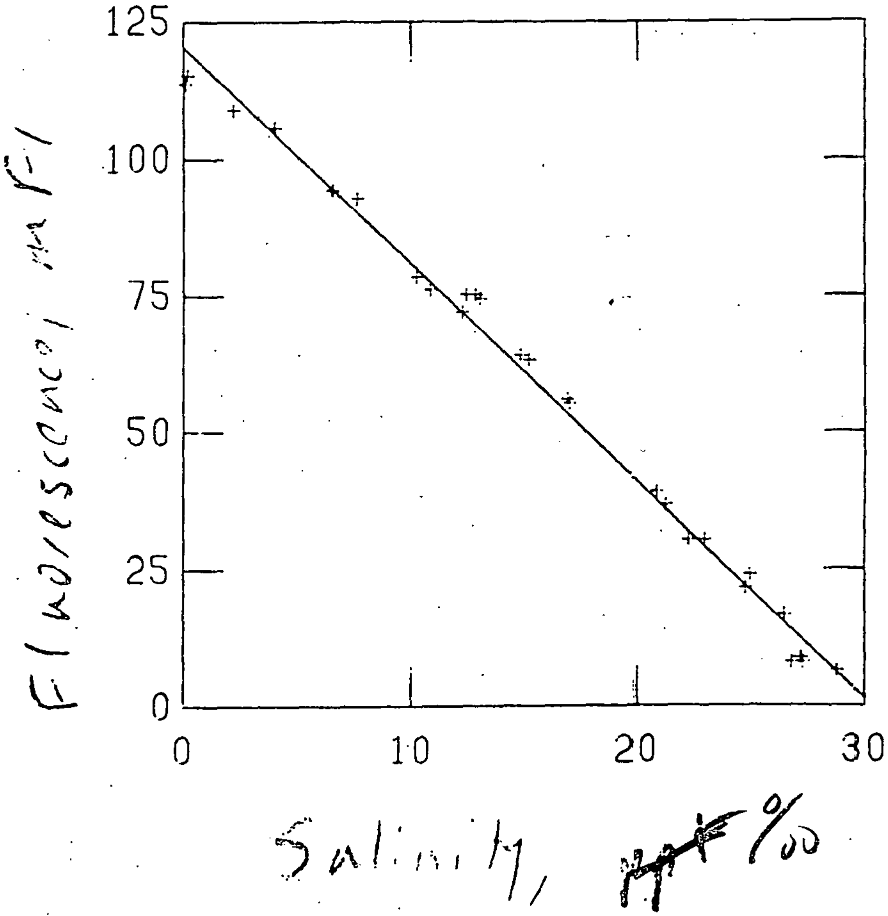

PLOT (18411043)
WILLEY

PLOT (17911070)
WILLEY
06/27/80 11:10:45

Figure 6

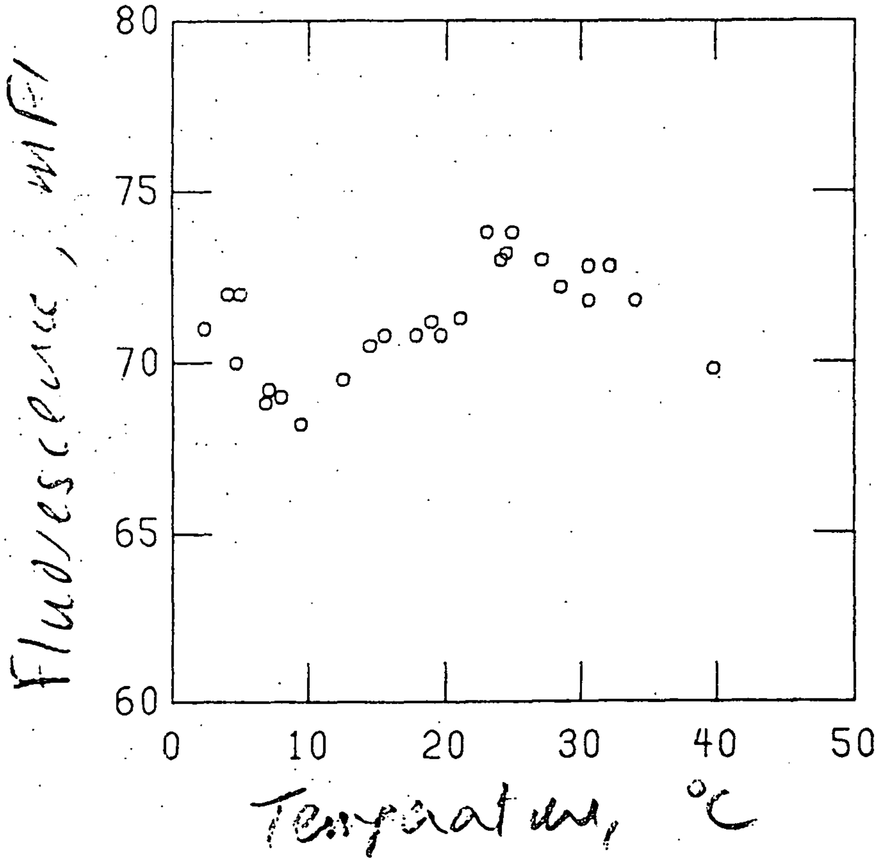

PLOT (17911070)
WILL

Figure 7

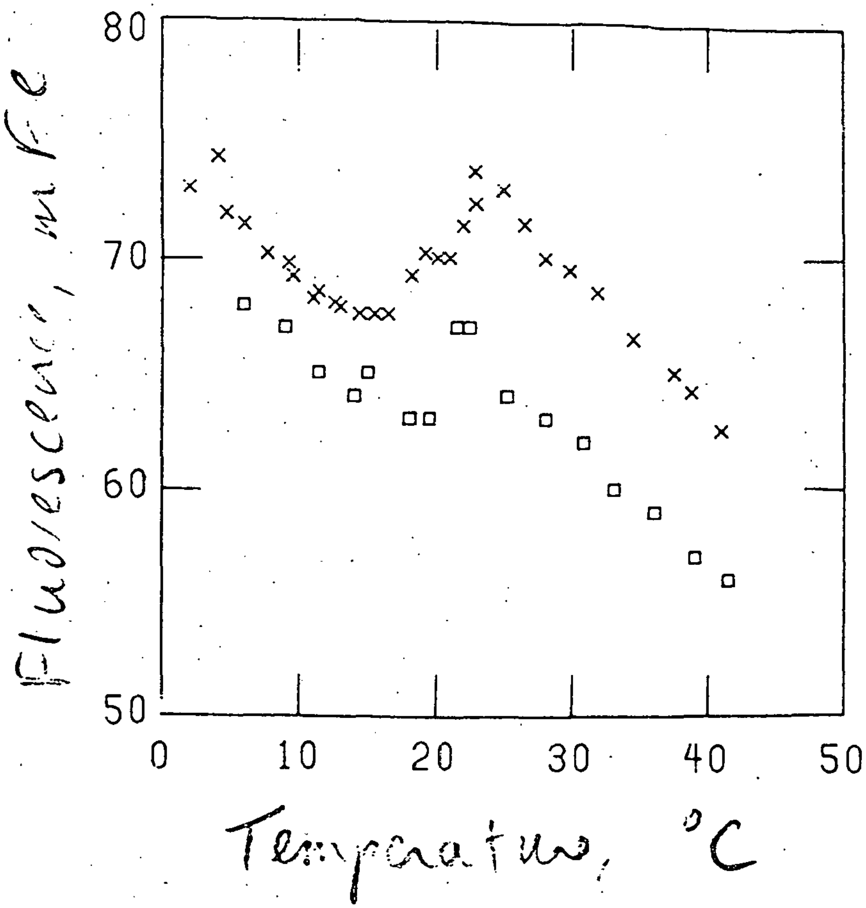

PLOT (18116152)
WILLEY
RECORDS PLOTTED = 312

WILLEY
07/01/80 18:09:42

Figure 8

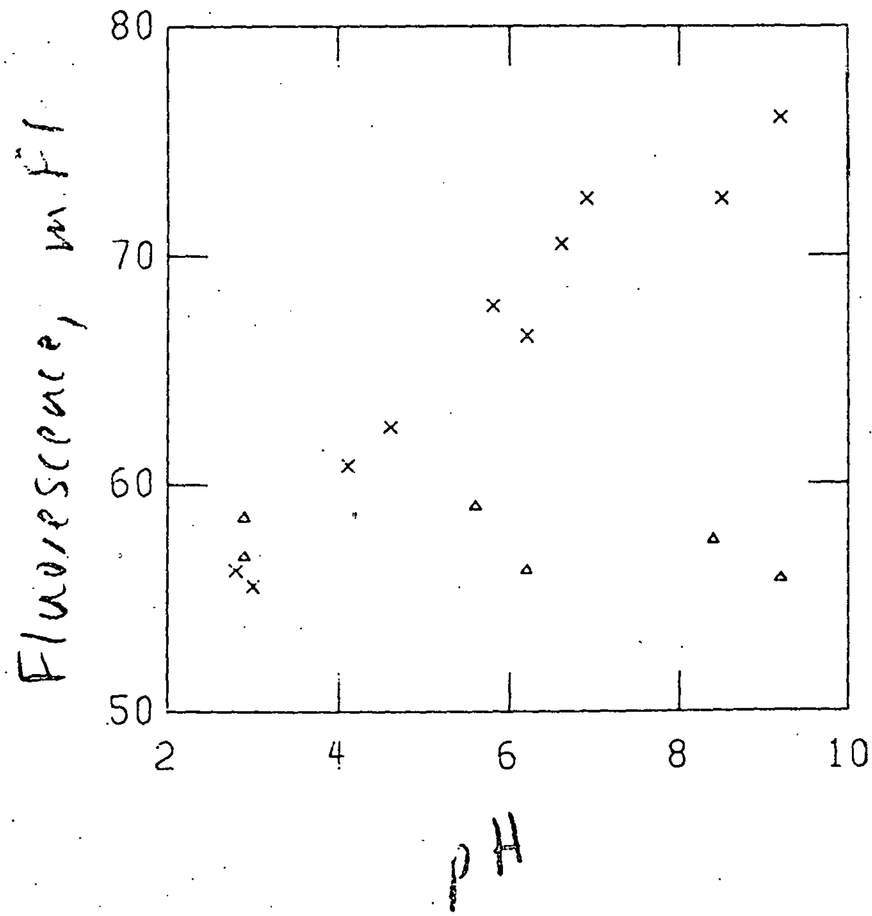

PLOT (18318015)
WILLEY
RECORDS PLOTTED = 295

PLOT (17817095)
WILLEY
06/26/80 17:44:45

Figure 9

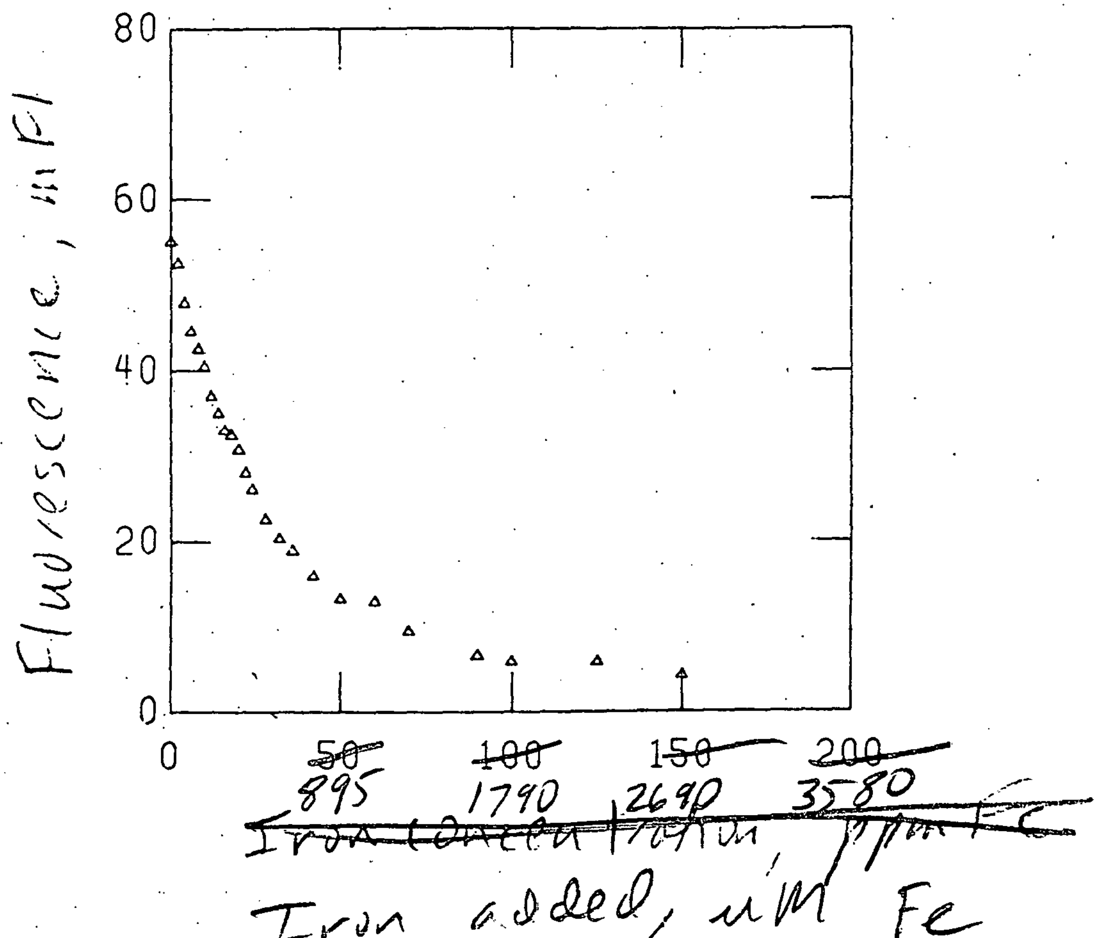

PLOT (17817095)
WILLEY
RECORDS PLOTTED = 286

Figure 10

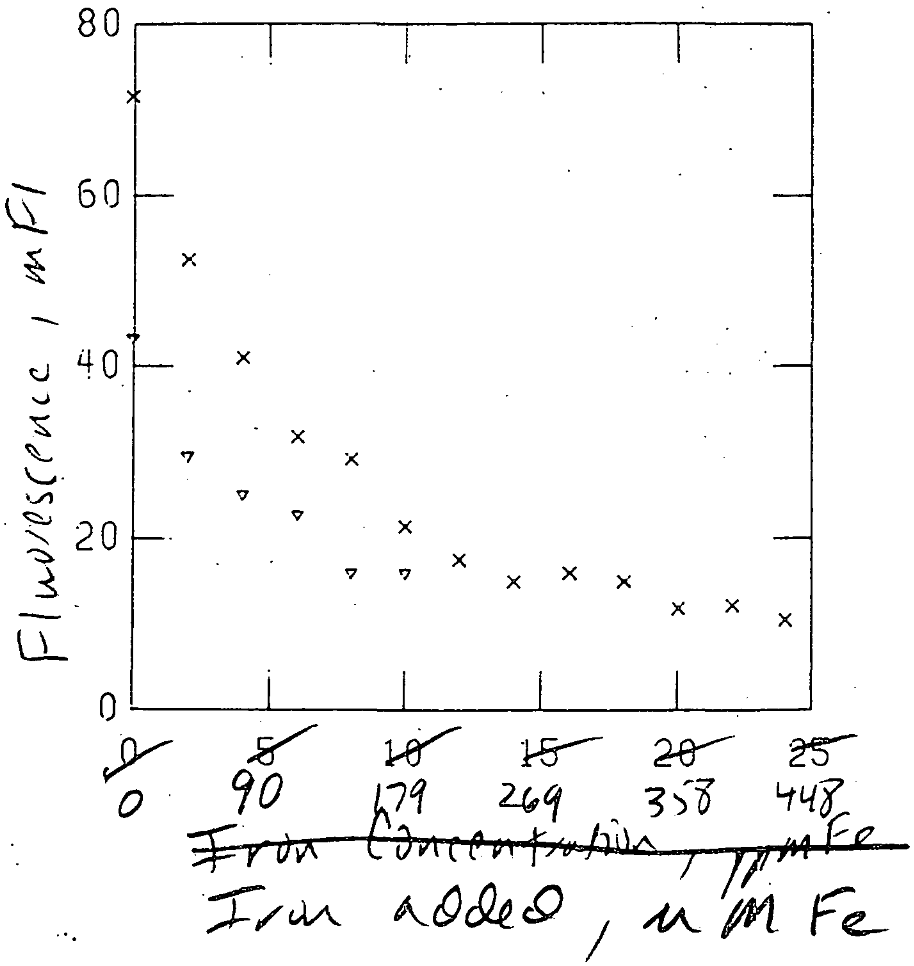

PLOT (18315079)
WILLEY
RECORDS PLOTTED = 297